Behavior of Standard AASHTO Type I Pretensioned High Performance Lightweight Concrete Beams with Fully Bonded ½-Inch Prestressing Strand

by

Daniel B. Thatcher, B.S.

Thesis

Presented to the Faculty of the Graduate School of

The University of Texas at Austin

in Partial Fulfillment

of the Requirements

for the Degree of

Master of Science in Engineering

The University of Texas at Austin

December 2000

Behavior of Standard AASHTO Type I Pretensioned High

Performance Lightweight Concrete Beams

with Fully Bonded ½-Inch Prestressing Strand

Approved by
Supervising Committee:

Ned H. Burns, Supervisor

John E. Breen, Supervisor

Dedication

To Kerry, for loving me constantly,

and to my parents, for all of their encouragement.

Acknowledgements

Abstract

Behavior of Standard AASHTO Type I Pretensioned High Performance Lightweight Concrete Beams with Fully Bonded ½-Inch Prestressing Strand

Daniel B. Thatcher, M.S.E.

The University of Texas at Austin, 2000

Supervisors: Ned H. Burns and John E. Breen

High performance lightweight concrete is desirable for use in Texas bridge girders to bring about significant reductions in the dead load of the structure. Concrete can be specified to have a unit weight of less than 120 lb/ft^3 (18.9 kN/m^3) with compressive strengths of 6000-8000 psi (41.4-55.2 MPa). Full-scale beam specimens were tested in order to determine the feasibility of their application in the field. The development length of the ½ in (12.7 mm) prestressing strands was measured, and an upper bound of 60 in (1524 mm) was determined. This indicated that the AASHTO specifications are conservative for both normal weight and lightweight concrete. The flexural behavior of the lightweight beams was similar to the behavior of the normal weight beam.

Table of Contents

List of Tables

List of Figures

Chapter 1: Introduction and Background

1.1 PRESTRESSED CONCRETE

Prestressed concrete is a modern building material that is seeing increased use and application in building and bridge design. Prestressing is a method of applying an initial stress level to a material prior to its being subjected to design loads and conditions. The fact that concrete is a strong material in compression, but is significantly weaker in tension, has led to the application of prestressing to concrete. This prestressing is accomplished by using high-strength steel strands in the concrete, in addition to typical reinforcing steel bars, and tensioning the strands during construction in such a way that an initial compression is applied to the concrete. When designed properly, this initial compression can minimize or even entirely eliminate the subsequent development of tension in the concrete when under applied load. The deflections of the prestressed concrete member can be specified and controlled, including a zero-deflection condition when under service load. Due to the prestressing, service load level crack widths can be controlled as well, thereby limiting the corrosion of the steel and lengthening the lifespan of the concrete [16]. The application of the prestressing can be carried out in several manners, including pretensioning and post-tensioning, which will not be discussed in detail here [11, 12, 14].

1.2 LIGHTWEIGHT CONCRETE MATERIAL

Concrete is composed of several components, including cement, water, admixtures, fine aggregates, and coarse aggregates. The use of lightweight coarse aggregates can lead to significant reductions in the self-weight of the concrete. Materials used as lightweight aggregate include slate, slag, palletized fly ash, and expanded clays and shales [14]. The clays and shales are mined from the ground and then placed in a kiln. As they are heated, gases are introduced and the materials expand into a hard, yet porous, material. The porosity (voids in the material) is the cause for its lighter weight relative to its volume, compared to concrete made with normal coarse aggregates consisting of gravel or crushed stone. The lightweight aggregate can weigh 40-50% less than normal coarse aggregate, and the hardened concrete using lightweight coarse aggregate can weigh less than 80% of concrete cast using normal weight coarse aggregate [8]. The typical unit weight of normal weight concrete is about 145 to 150 lb/ft^3 (22.8 to 23.6 kN/m^3). The unit weight of lightweight concrete is usually about 120 to 125 lb/ft^3 (18.9 to 19.6 kN/m^3), and can range as low as 90 lb/ft^3 (14.1 kN/m^3) [14].

The material properties of lightweight concrete compare favorably with those for normal weight concrete. The compressive strength can be the same as that of normal weight concrete, with careful proportioning of the different components in the mix design, and with careful attention to the water-cement ratio. The tensile strength, however, ranges between 80 to 100% of that of normal weight concrete. Additionally, the modulus of elasticity is somewhat lower than that of normal weight concrete. The creep and shrinkage of lightweight concrete are comparable to that of

normal weight concrete, and the same multipliers and coefficients in the code can be used for both [12, 17].

The use of lightweight concrete has been gaining popularity since 1955, particularly in California and Norway. Bridge girder and deck applications, as well as slabs in buildings, are common uses. Lightweight concrete is particularly useful in conditions where the dead load is the major component of the loading. Further uses and applications will be discussed later in this chapter.

1.3 CONCRETE STRENGTH

Concrete used in building practice today generally has a compressive strength ranging from 3500 to 12000 psi (24.1 to 82.7 MPa). These strengths can be split into two groups, normal strength and high strength, or high performance concrete. Following subsections deal with these types in greater detail.

1.3.1 Normal Strength

Normal strength concrete is generally defined as concrete with compressive strengths up to and including 6000 psi (41.4 MPa) [12]. The tensile strength of normal strength concrete is around 15% of the compressive strength [17]. Typical reinforced concrete will use a minimum of 3500 psi (24.1 MPa) concrete [11], and is in widespread use in the construction industry. Its uses range from foundations, pavements, and walkways to columns, storage tanks, and dams [17].

1.3.2 High Performance

High strength, or high performance, concrete is defined as concrete with strengths ranging from 8000 to 12,000 psi (55.2 to 82.7 MPa) [8]. Generally, high performance concrete refers to strengths greater than or equal to 8000 psi (55.2 MPa).

The higher strength is achieved through a mix design with a low water/cement ratio and admixtures [17]. The tensile strength of high performance concrete is an even lesser percentage of the compressive strength than normal strength concrete (around 10%). [17]

Prestressed concrete construction involves almost exclusive use of high performance concrete. In fact, commercial prestressing cable anchorages used in post-tensioned prestressed construction are designed for anchoring in high performance concrete [14]. The high performance concrete has a higher modulus of elasticity than normal lightweight concrete, which results in less elastic shortening of the concrete and thereby less loss of the initial prestress force. A lower rate of creep also contributes to less relaxation of the original prestress force. Additionally, high performance concrete has a higher tensile strength than normal strength concrete, which is useful in the high stress applications in which prestressed concrete is typically used.

High performance concrete is currently used in many building applications, from the columns of high-rise structures to the superstructures of modern bridges [17]. The higher durability of high performance concrete has made it particularly useful in the bridge industry, where the concrete is exposed to the environment.

1.4 USE OF HIGH PERFORMANCE LIGHTWEIGHT CONCRETE

The use of high performance lightweight concrete (HPLC) is most practical in applications where the dead load of the structure comprises the structure's major loading component. This is especially true for bridge girders, as well as for the double-tees often used in parking structure designs. The lighter unit weight of the HPLC, combined with the high strength, can lead to several advantages. First, for a

similarly sized section, a longer span can be employed than for a normal weight girder. Conversely, the size of the section can be reduced to span the same distance. However, since most bridge girders are constructed using AASHTO standard sections, the next smaller section may be too small to carry the desired loads. In this case, the spacing of the original girders may be increased if HPLC is employed. In some cases, the increased spacing may result in the use of one or two less girders than if normal weight concrete were used. The material savings for fewer girders must be balanced against the higher cost of the HPLC, and will vary depending on the specific job conditions [11].

An additional possible application of HPLC is in precast pretensioned deck panels. These panels comprise approximately half the thickness of the deck to be placed, and are positioned on top of the girders, spanning the spaces between them. The panels act as formwork, and are left in place when the rest of the deck is placed on top of them to form a composite member. This eliminates the difficulty and cost of getting underneath the bridge in order to remove typical wooden formwork; the precast prestressed panel is serving as a stay-in-place form to support cast-in-place concrete.

1.5 BACKGROUND

The material under investigation in this thesis is prestressed lightweight concrete. The area of emphasis is the behavior of prestressed lightweight concrete under load, particularly its flexural behavior. The transfer length of the pretensioned strands in prestressed lightweight beams was tested and reported by Kolozs [10]. A portion of the testing of the development length of the lightweight beams was also reported by Kolozs [10], and is completed in this thesis. Additionally, strains,

deflections, strand elongation, crack patterns, cracking and ultimate loads and moments, and failure types are reported here.

1.5.1 Lightweight Concrete Background

The fundamentals of lightweight concrete as a construction material were presented in the previous sections of this chapter. The focus of this study is the behavior of lightweight concrete beams loaded to flexural failure. This behavior, in the areas discussed in the previous sections, is compared to the behavior of a normal weight beam loaded under similar conditions. Of particular interest is the actual development length of the prestressing strands in the lightweight concrete material, compared to normal weight concrete. Several equations exist in the literature for calculation of the theoretical development length; however, these were developed for normal weight concrete. This study will investigate the applicability of the AASHTO minimum development length equation for use with lightweight concrete.

Additional details of the actual mix-design of the lightweight concrete used to construct the beams, as well as a more detailed discussion of the material properties of lightweight concrete, are beyond the scope of this thesis; however, such details are found in the work by Heffington [8].

1.5.2 Deck Panels Background

The use of precast prestressed deck panels in bridge construction was introduced in previous sections of this chapter. Due to TxDOT's interest in the subject, deck panels composed of lightweight concrete were used in two of the lightweight beams' decks. The construction of the decks is treated in greater detail in Chapter 2. The key area of study of precast prestressed deck panels centers on the issue of composite action between the precast beam, precast panels, and cast-in-place

6

deck. Barnoff performed a study on this topic and determined that full composite action was developed in cases of normal weight deck panel use [3]. The results of this study, with respect to composite action using lightweight concrete, will be discussed in Chapters 3 and 4.

1.5.3 Development Length Background

All concrete, whether normal weight or lightweight, is strongest when used in compression. Concrete's strength in tension is significantly lower than its compressive strength. In order to use concrete in applications other than direct compression, a method of tensile resistance must be introduced in flexural members. This has led to the development of reinforced concrete, where steel bars are placed in the tension regions of the concrete member in order to resist the tensile forces after the concrete has cracked.

In pretensioned concrete members, in addition to standard reinforcing bars, high strength prestressing strands are placed in the formwork prior to casting the beams. These strands are stressed to a high tensile stress prior to casting the concrete. After the beams have been cast and the concrete allowed to gain strength, the strands are released and the tension force in the strands is transferred to the concrete as a compressive force. In order for the force-transfer to occur, a level of bond must exist between the concrete and the prestressing steel. Bond occurs over the length of the strand, and therefore a minimum length of strand must be bonded in order to fully develop the forces at transfer in a pretensioned prestressed concrete beam. This length is called the transfer length.

When a prestressed concrete beam is subject to loads, the tension zone of the concrete must first develop enough stress to overcome the precompression that was

added by the prestress force designed for the member. Beyond that level of stress, and up to the capacity of the beam, the length of bond required to fully develop the tensile resistance of the strands is called the flexural bond length. The sum of the transfer length and the flexural bond length is the development length of the beam.

Several equations for calculating the theoretical development length of normal weight concrete exist in the literature, and were reviewed by Kolozs [8]. These equations are shown in Table 1.1, along with the name of their developers. The scope of this thesis is limited to the experimental verification of the applicability of the AASHTO-calculated minimum development length for lightweight concrete.

Table 1.1 Development Length Equations

Author	Development Length Equation
ACI 318 / AASHTO [2,1]	$L_d = \left(f_{ps} - \dfrac{2}{3} f_{se} \right)$
Zia & Mostafa [18]	$L_d = L_t + 1.25(f_{pu} - f_{se})d_b$
Buckner (FHWA) [5]	$L_d = L_t + \lambda(f_{ps} - f_{se})d_b$
Mitchell [13]	$L_d = L_t + (f_{ps} - f_{se})d_b \sqrt{\dfrac{4.5}{f'_c}}$

1.6 LITERATURE REVIEW

Detailed literature investigations on the subjects of high-strength lightweight concrete, prestressed lightweight concrete, deck panels, transfer length, and development length were performed by Heffington and Kolozs [8, 10]. This thesis

follows closely upon the completion of their theses, and no significant pertinent papers were found in the short period between their searches and the author's.

1.7 SCOPE OF PROJECT

This thesis presents a discussion of the results from The University of Texas at Austin Center for Transportation Research (CTR) Project 0-1852, sponsored by the Texas Department of Transportation (TxDOT) and the Federal Highway Administration (FHWA). The project focuses on the potential use of prestressed high performance lightweight concrete in bridge girders, and examines the use of lightweight prestressed panels as bridge deck formwork. The six tasks of the project were:

Task 1.) Literature Search

Task 2.) Past Use of Lightweight Concrete Mix Designs

Task 3.) Development of Lightweight Concrete Mix Designs

Task 4.) Materials Research and Testing

Task 5.) Full-Scale Testing of Type A Beams with Decks

Task 6.) Prestress Loss and Evaluation of Beam Behavior, Handling of

Beams, and Final Report

Tasks 1, 2, and 3 were performed previously and reported by Heffington [8]. Task 4 and a portion of Tasks 5 and 6 were performed and reported by Kolozs [10]. This thesis covers the completion of Tasks 5 and 6. Major topics of discussion are presented in the following section.

1.8 ORGANIZATION OF THESIS

This thesis is organized into five chapters. The first chapter introduces the subject matter of the thesis. Background information on lightweight concrete and high performance concrete is presented, as well as current and potential uses of HPLC. The concept of the development length of prestressing strands in concrete is discussed, and a review of current relevant technical literature on lightweight concrete, development length, and deck panels is mentioned. The scope of the project is discussed, and the organization of the thesis is presented.

The second chapter details the test set-up and procedure. The origin and make-up of the test specimens is discussed, as well as the variables under examination. The equipment used to test the specimens is described, and its application to the test specimens themselves is detailed. The actual testing procedure is also outlined.

The third chapter presents test results from the six tests on the 8000 psi beams carried out by the author. The results are then discussed.

The fourth chapter presents test results from all twelve tests, including the six performed by Kolozs and the six carried out by the author. The results are then compared and discussed.

The fifth chapter of this thesis presents a summary of all the test results and the conclusions reached. Based on this summary, recommendations for Code use and application in the field are presented. Finally, areas for future study are suggested.

Chapter 2: Testing

Since the test procedures used are basically the same as reported by Kolozs [10], the subject matter of this chapter is presented in a somewhat abbreviated form.

2.1 INTRODUCTION

This chapter covers the development of the specimens for testing, the test geometry and set-up, and the actual testing procedure followed for each test. The testing program included five lightweight beams and one normal weight beam to be used as a control specimen. Each test will be referred to in the manner presented in Figure 2.1.
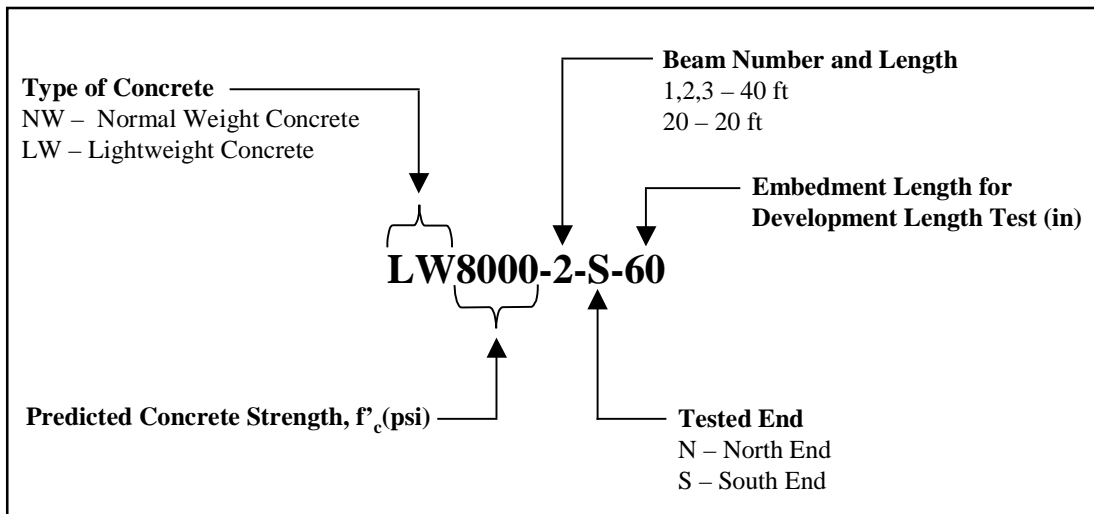
Figure 2.1 Beam Nomenclature

The first two letters of the nomenclature indicate whether the beam is composed of normal weight (NW) or lightweight (LW) concrete. The next number

indicates the specified design strength of the concrete beam, 6000 or 8000 psi (41.4 or 55.2 MPa). The number following the dash indicates which beam of that particular strength it is, as specified by the preceding indicator. Next, the end of the beam tested is indicated by N (for north) or S (for south). The ends of the beam were labeled in the casting yard and kept consistent throughout the testing process. The final number in the nomenclature indicates the development length tested on that end of the specimen. For example, the nomenclature listed in Figure 2.1 indicates that the test was performed with an embedment length of 60 in (1524 mm) on the south end of the second lightweight beam with specified design strength of 8000 psi (55.2 MPa).

The full nomenclature will not be used at all times throughout this thesis. When a particular beam is referenced, with both ends included, the nomenclature will leave off the development length and beam end indicators. Additionally, if a group of beams is referred to, only the first term will be presented (e.g. LW8000 to refer to all of the 8000 psi (55.2 MPa) lightweight beams).

2.2 TEST SPECIMENS

The complete testing program involved a total of twelve tests on six beams, with each beam undergoing two separate tests. Kolozs tested the first three beams and reported the results [10]. The results from the last three beams tested by the author are reported in this thesis. The beams were all cast at Heldenfels Prestressing Plant in San Marcos, Texas. They were cast in groups of three over six days, with strand release occurring the day after casting. All cross-section details were the same for each beam; the only variable consisted of the concrete mix specified. One normal weight beam and two lightweight beams were cast the first day, all with a 28-day specified compressive strength of 6000 psi (41.4 MPa). Two days after the strand

release, three lightweight beams with a 28-day specified compressive strength of 8000 psi (55.2 MPa) were cast. Following instrumentation and testing of the transfer length of each of the beams, they were transported to Ferguson Structural Engineering Laboratory (FSEL) at the J.J. Pickle Research Campus of The University of Texas at Austin. For more details of the mix designs and the casting of the beams, see Heffington [8].

2.2.1 Concrete Mix

The concrete mixes used in casting the six test beams were developed by Heffington and Kolozs, and were reported in detail by Heffington [8]. Three mixes were developed: a normal weight mix with a 28-day nominal compressive strength of 6000 psi (41.4 MPa), a lightweight mix with a 28-day nominal compressive strength of 6000 psi (41.4 MPa), and a lightweight mix with a 28-day nominal compressive strength of 8000 psi (55.2 MPa). The resulting properties for each can be seen in Table 2.1.

Table 2.1 Concrete Properties

| Beam ID | Compressive Strength (f'$_c$), psi / (MPa) | | Unit Weight |
	1-day	Long Term	lb/ft^3 / (kN/m^3)
NW6000	3,490 (24.1)	5,500 (37.9)	149 (23.4)
LW6000	4,900 (33.8)	8,130 (56.1)	118 (18.5)
LW8000	5,560 (38.3)	7,850 (54.1)	122 (19.2)

The long-term strength of the normal weight mix was a bit short of the specified strength. The long-term strength of the lightweight 6000 psi (41.4 MPa) mix was around 8000 psi (55.2 MPa), significantly higher than the specified strength.

13

The long-term strength of the 8000-psi (55.2 MPa) mix was actually slightly less than the specified strength. These results were examined and discussed by Heffington [8].

2.2.1.1 Normal Weight Aggregate

The aggregate used in the normal weight mix was comprised of ¾ in (19.05 mm) Hard Rock Coarse aggregate readily available in the Austin, Texas region. It resulted in an equilibrium concrete weight at 28-days of approximately 145 lb/ft^3 (222.8 kN/m^3).

2.2.1.2 Lightweight Aggregate

The aggregate used in the lightweight mix was comprised of a ¾ in (19.05 mm) Lightweight Coarse aggregate called Clodine, obtained from Texas Industries (TxI). Clodine aggregate is an expanded clay. It resulted in an equilibrium concrete weight at 28-days of approximately 118 to 122 lb/ft^3 (18.5 to 19.2 kN/m^3) [8].

2.2.1.3 Other Components

The concrete mixes developed by Heffington and Kolozs consisted of water, sand, cement, fly ash, retarder, and superplasticizer, in addition to the aggregate discussed previously. The amounts of each component for the three mixes are shown in Table 2.2.

Table 2.2 Mix Designs

Material	NW6000	LW6000	LW8000
Water	250	222	247
Cement (Type III)	517	504	671
Fly Ash	0	168	316
3/4 in Hard Rock Coarse Aggregate	1869	0	0
3/4 in Lightweight Coarse Aggregate	0	1264	1123
Sand	1355	1149	1029
Retarder	12	12	12
Superplasticizer	20.4	34	54

Notes:
1) Quantities in lbs and oz
2) Quantities per yd^3

2.2.2 Cross-Section Details

The cross sections of all of the test beams were the same, with an area of 276 in^2 (1780.6 cm^2). The beams were I-shaped sections 28 in (711.2 mm) deep, with a larger bottom flange region than top flange region. Exact dimensions are shown in Figure 2.2. The prestressing strands and pattern were the same in each test beam, as were the reinforcing details (see Sections 2.2.3 and 2.2.4).
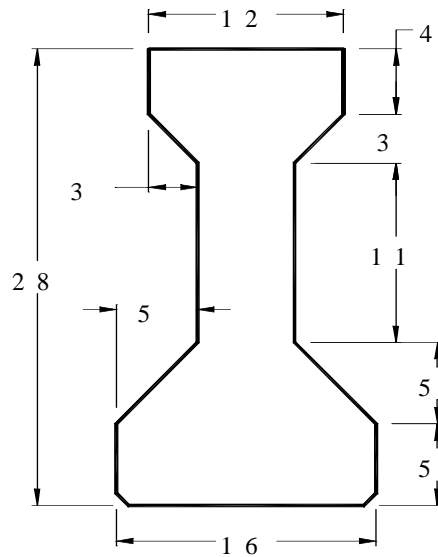
Figure 2.2 Beam Dimensions

2.2.3 Prestressing Strands

The prestressing strands used in the test beams were ½ in (12.7 mm) diameter, low relaxation, ASTM A416, Grade 270 ksi (1861.6 kN/m^3) 7-wire strands. The ultimate stress was reported on the mill certificates as 270 ksi (1861.6 kN/m^3), with an elastic modulus of 28,000 ksi (193,054.4 MPa). The strands were supplied by American Spring Wire Corporation.

Twelve strands were placed in each test beam in a 2 in (50.8 mm) grid pattern. Two strands were located in the top flange to ensure compression in that region, and ten in the bottom flange. The bottom flange strands were placed in two rows, to allow a larger moment arm to develop. The strand layout can be seen Figure 2.3.

16
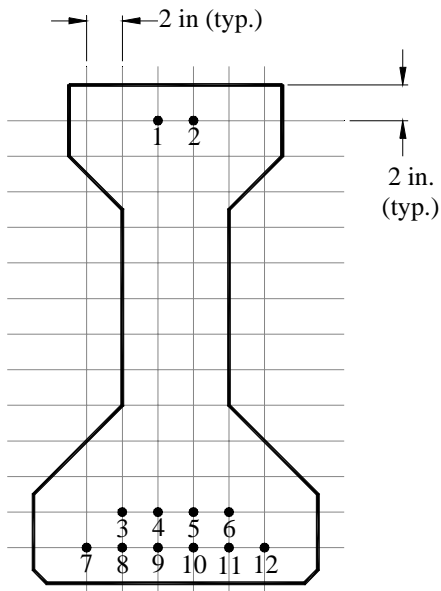
Figure 2.3 Strand Layout

2.2.4 Reinforcement

The non-prestressed reinforcement used in the test beams was Grade 60 steel, and was supplied by Border Steel. The yield stress was reported on the mill certificates as 66 ksi (455.1 MPa), with an ultimate stress of 100 ksi (689.5 MPa).

The flexural reinforcement was placed in patterns used in similar tests and satisfactory to TxDOT requirements. The shear reinforcement placed in the beams exceeded shear reinforcement typical for similarly sized beams, in order to ensure that the beams would not undergo sudden shear failure during testing due to the short shear spans of the tests. Shear failure of the beams would not have allowed effective determination of the development lengths; thus a flexural failure was ensured by the amount of shear reinforcement used. The layout of the reinforcement is shown in Figures 2.4 and 2.5.

17

REINFORCEMENT DETAIL 1 (40' GIRDERS)

TOP FLANGE

BOTTOM FLANGE

AASHTO TYPE I BEAM

ELEVATION
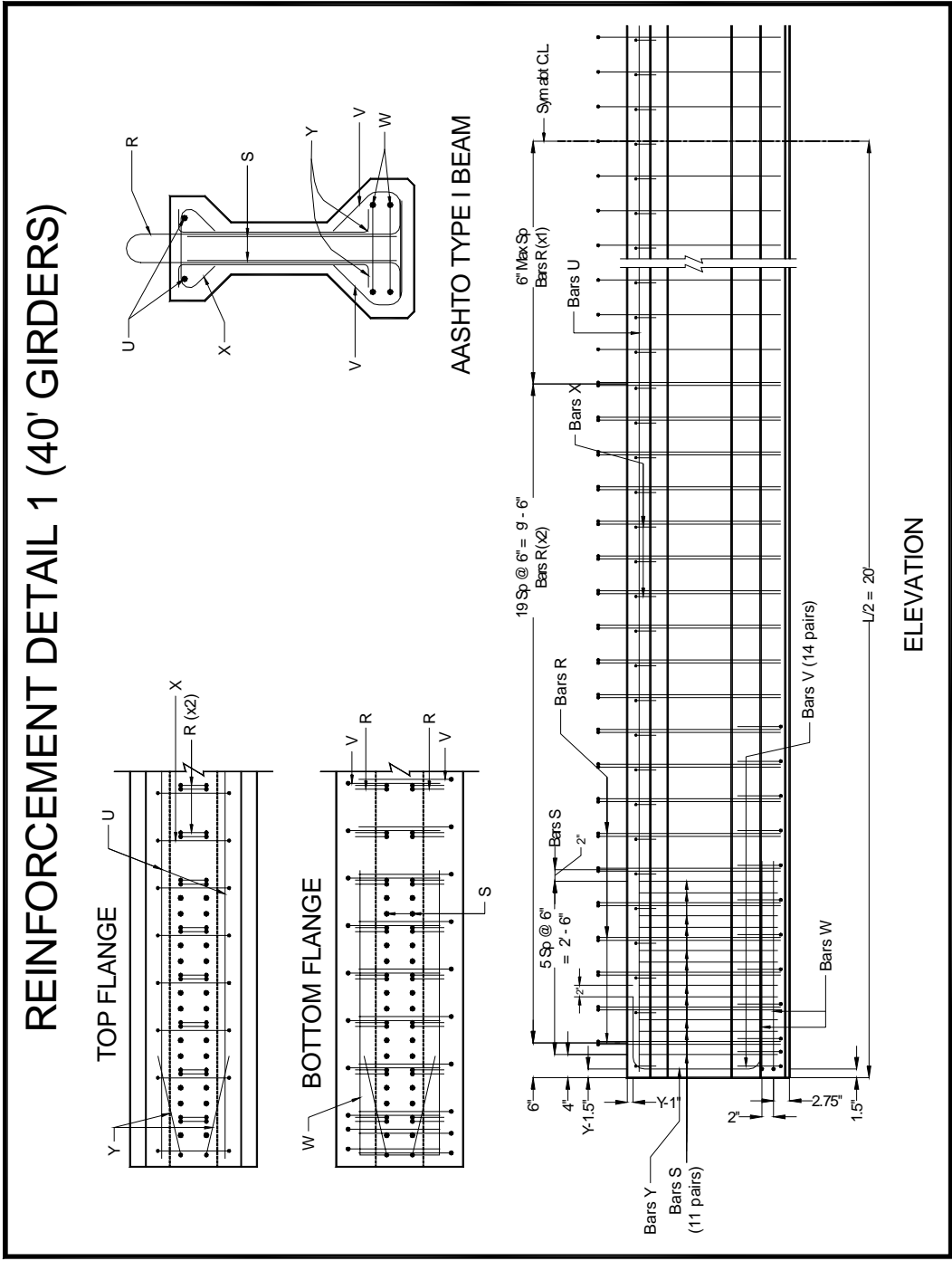
Figure 2.4 Test Beam Reinforcement Details

18

REINFORCING BAR DETAILS

BARS Y (# 6)

1'-10"

1'-0.5"

BARS X (# 3)

3.625"

9"

BARS W (# 5)

10"

3'

30.75" = Min Lap

BARS U (# 5)

Beam Length minus 3"

BARS S (# 5)

2'

BARS R (# 4)

3.25"

2'-7"

4"

BARS V (# 4)

6.25"

11.625"

3.125"
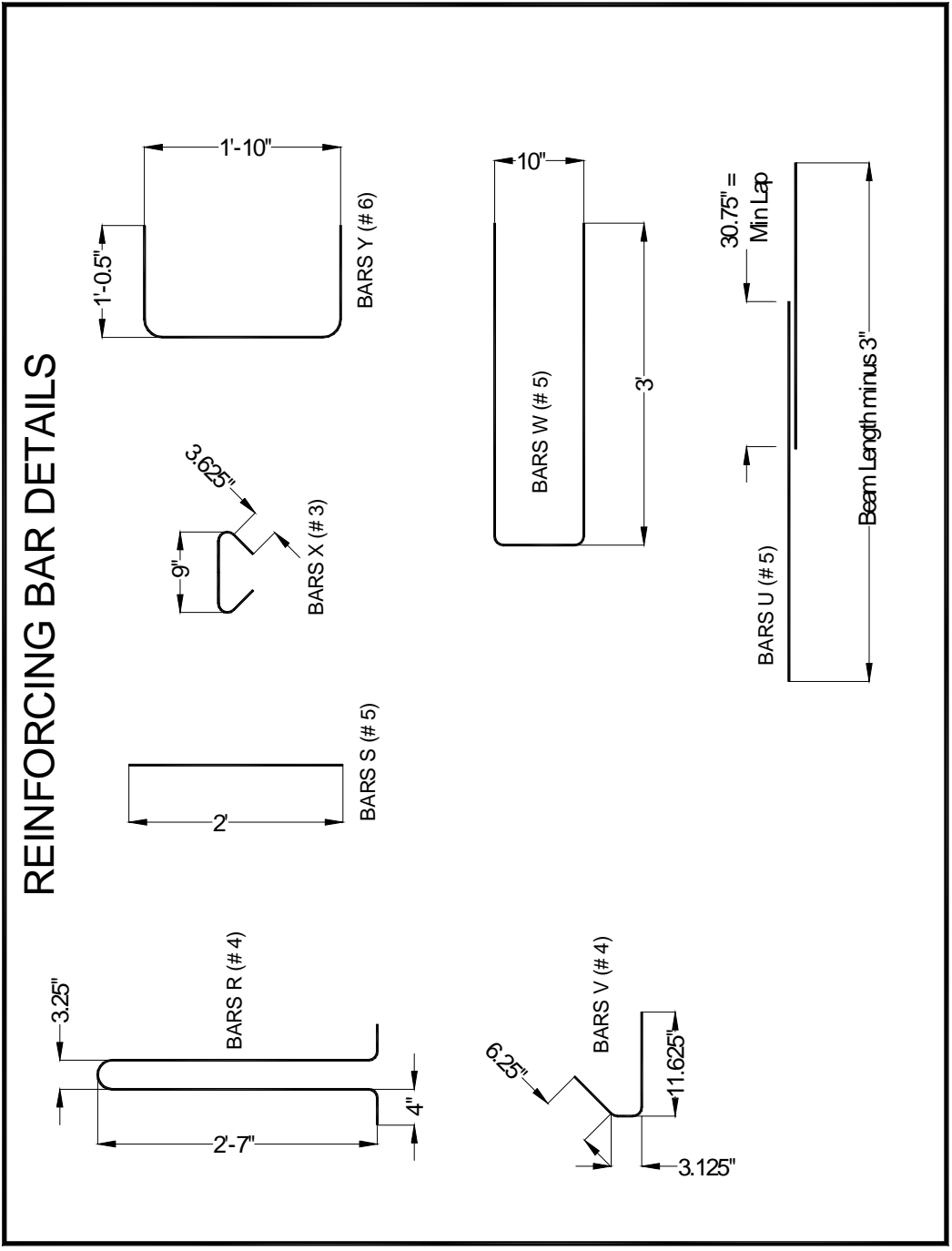
Figure 2.5 Reinforcement Bar Details

2.2.5 Deck & Panels

Each test beam was tested as a composite section that was constructed by placing a concrete slab, or deck, on top of the beam after it was brought into FSEL. The deck components were varied from test to test, but the dimensions were held constant. The reinforcement was designed using AASHTO specifications [1], and the placement is shown in Figure 2.6.
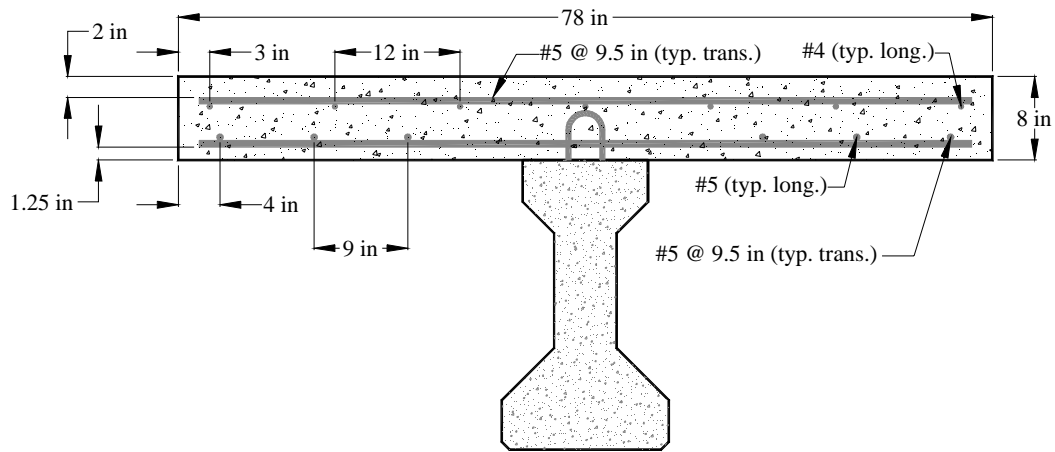
Figure 2.6 Concrete Deck Details without Panels

A normal weight concrete deck, a combination deck with lightweight panels and normal weight concrete, and a completely lightweight deck were built. The decks were each cast 8 in (203.2 mm) deep and 6 ft 6 in (2.0 m) wide. The deck variations can be seen in Table 2.3.

20

Table 2.3 Test Beam Concrete and Deck Type

Beam ID	Length	Beam Concrete	Deck Concrete	Lightweight Deck Panels
NW6000-1	40-ft	NW 6000-psi	NW 5000-psi	No
LW6000-1	40-ft	LW 6000-psi	NW 5000-psi	No
LW6000-2	40-ft	LW 6000-psi	NW 5000-psi	Yes
LW8000-1	40-ft	LW 8000-psi	NW 5000-psi	No
LW8000-2	40-ft	LW 8000-psi	NW 5000-psi	Yes
LW8000-3	40-ft	LW 8000-psi	LW 5000-psi	No

Notes:
1 ft = 0.305 m
1 psi = 6.895 kPa
LW = Lightweight
NW = Normal Weight

The decks were all built in FSEL. The formwork consisted entirely of wood, and was oiled before placement of the reinforcement to ease its removal upon curing of the concrete. The concrete was placed using an overhead bucket, was vibrated, and then finished with a screed, followed by bullfloats. Trowels were not used because the finish of the deck was not critical to the test procedure. The decks were allowed to cure for four days before formwork removal, and the beams did not undergo testing until the decks had reached their specified strength according to cylinder compression tests.

The panels used in two of the decks were cast at the Austin Prestressed Concrete Plant in Austin, Texas, using a mix design developed by Heffington and Kolozs. They were shipped to FSEL and placed in the deck formwork using an overhead crane. The panels were placed on a ½ in (12.7 mm) thick by 1 in (25.4 mm) wide strip of fiberboard on the top edges of the beam. This allowed the greatest area of contact between the beam and the deck in order to develop full composite action,

21

as shown in Figure 2.7. The reinforcement was slightly different in the decks with panels, and is shown in Figure 2.8.
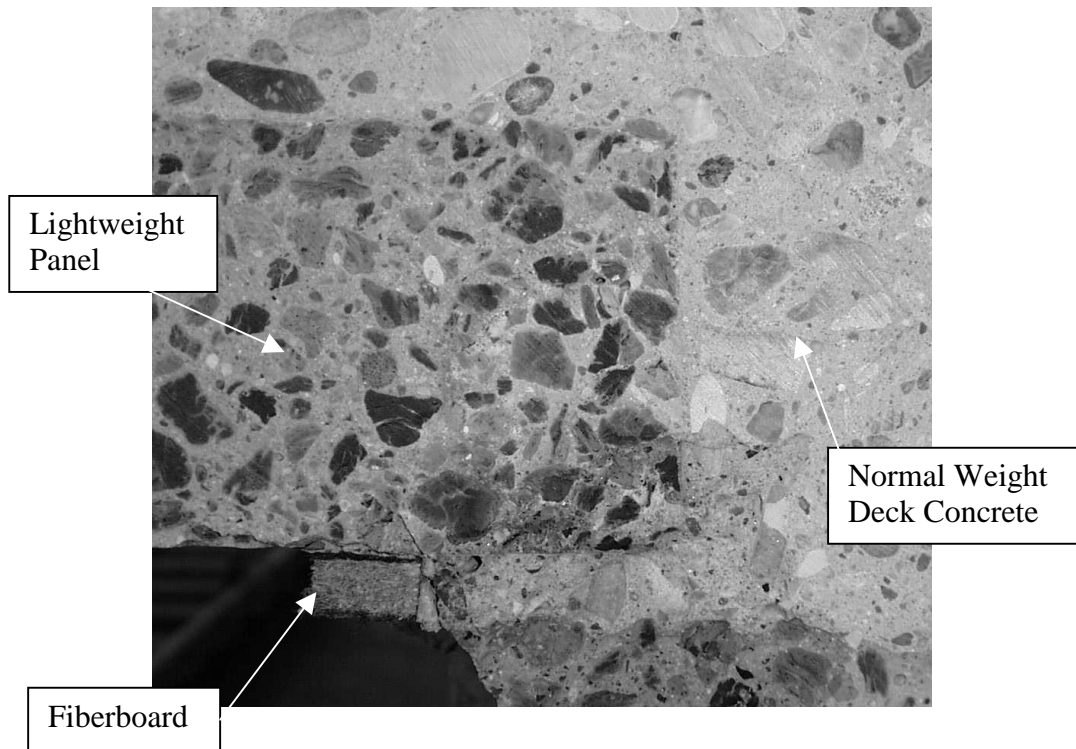
Figure 2.7 Deck Panel on Fiberboard

Top Mat Reinforcment
Same as Normal Weight Deck

Ø 3/8 in strand

3 in

4 in

Lightweight Concrete Panels

Fiberboard Insert
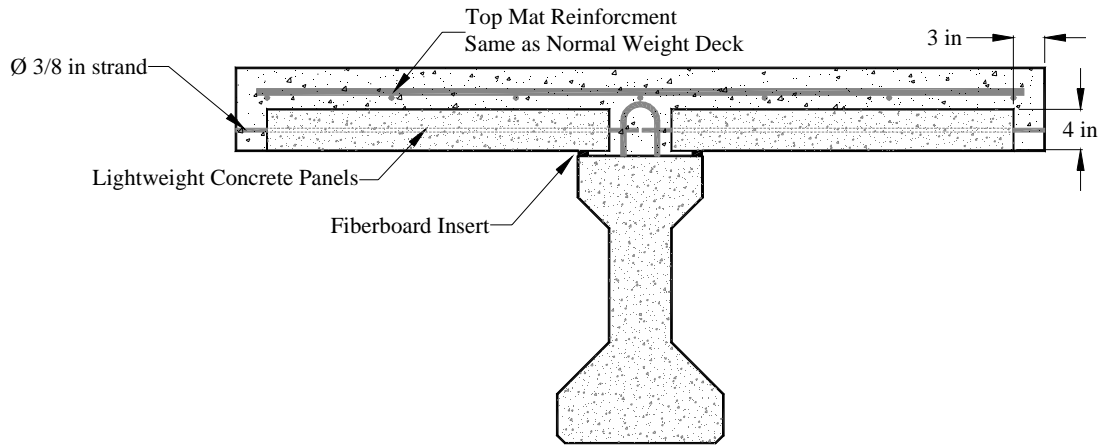
Figure 2.8 Concrete Deck Details with Panels

2.3 TEST SET-UP

2.3.1 General Layout

Each test beam was brought into FSEL using an overhead crane and placed on 11 in x 20 in x 3 in (279.4 mm x 508 mm x 76.2 mm) thick reinforced elastomeric bearing pads on top of 3 ft (0.9 m) high reinforced concrete blocks. The centerline of the bearing pad was lined up with a line 6 in (152.4 mm) in from the end of the beam, as shown in Figure 2.9. The centerline of the opposing pad was lined up with a point 24 ft 6 in (7.5 m) from the end of the beam. The beam was then tested over a 24 ft (7.3 m) span length, leaving a length of the beam 15 ft 6 in (4.7 m) long cantilevered and relatively unaffected by the test. Following a test, the geometry was reversed and the other end of the beam was tested. Using this approach, each beam could be tested twice, and the limited number of beams cast for the project was able to produce twice the results. This approach had been used with success on previous projects at FSEL for TxDOT and was therefore used again here.

23
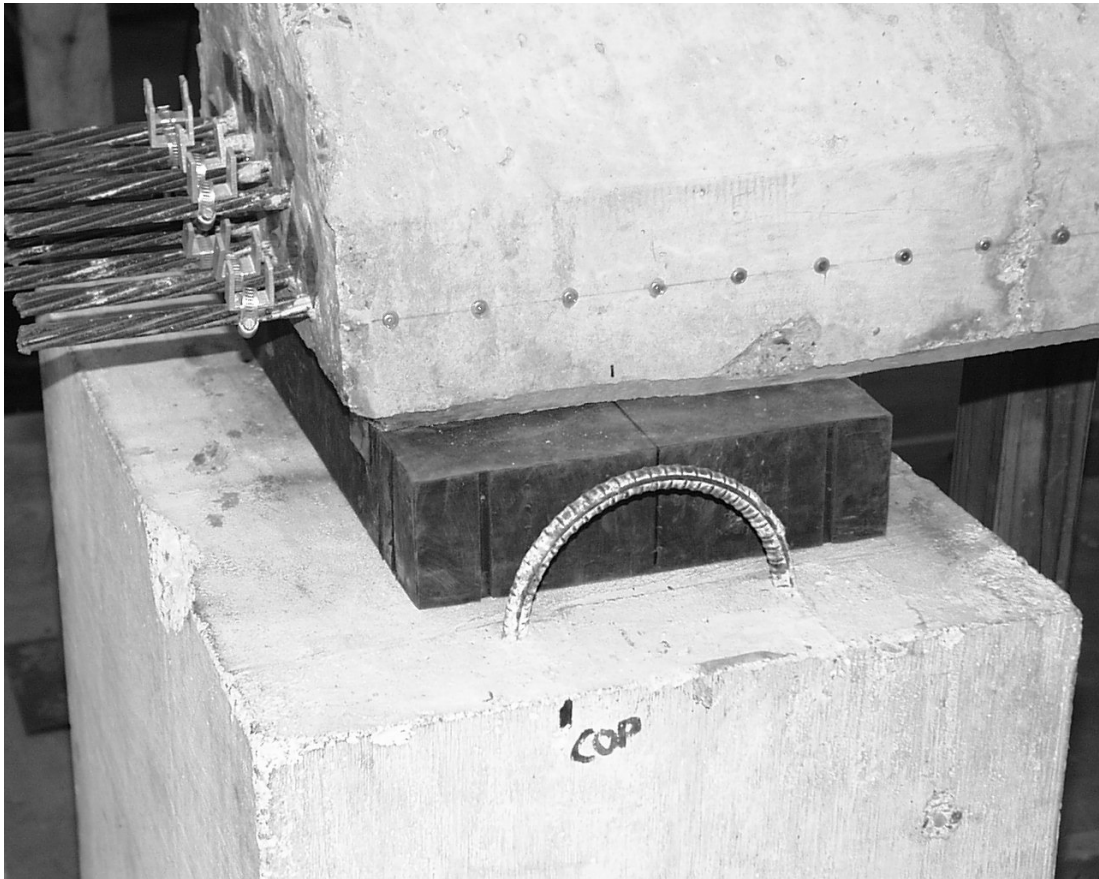
Figure 2.9 Beam on Pad and Concrete Block

2.3.2 Loading Apparatus

When the formwork from the deck was removed and the deck concrete was cured sufficiently to have gained its desired strength, the load frame was brought into place. The load frame consisted of a four-column frame supporting a load actuator on a steel I-beam, as shown in Figure 2.10.

.
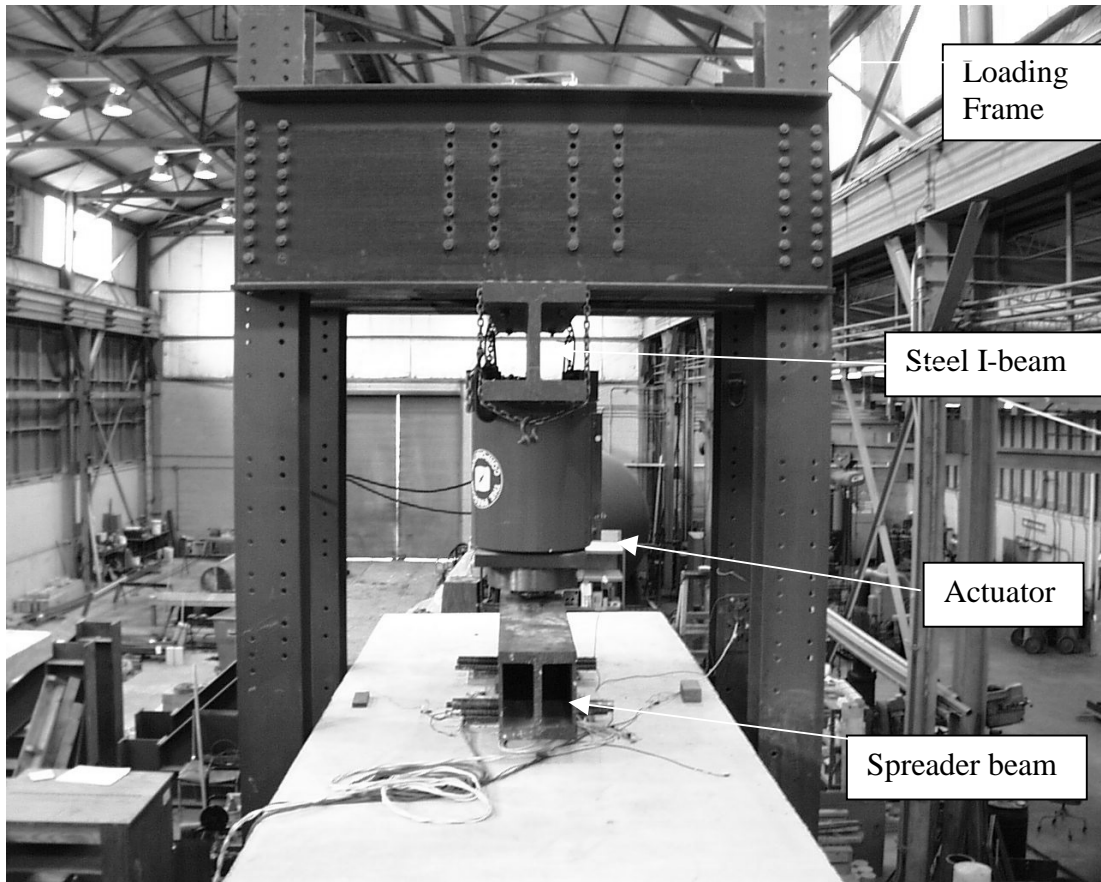
Figure 2.10 Load Frame and Actuator

The I-beam allowed the actuator to be moved longitudinally along the beam. The load was transferred from the load actuator into a spreader beam placed on top of two 2.5 in (63.5 mm) diameter steel roller supports. The rollers sat on two steel loading pads and were free to roll, thereby preventing the transfer of any horizontal shear into the test beam. The steel pads were hydrostoned to the top of the deck to prevent excess movement. The frame itself was firmly bolted down to a structural floor in order to prevent additional excess movement during testing. The spreader beam, rollers, and steel pads are shown in Figure 2.11.

25
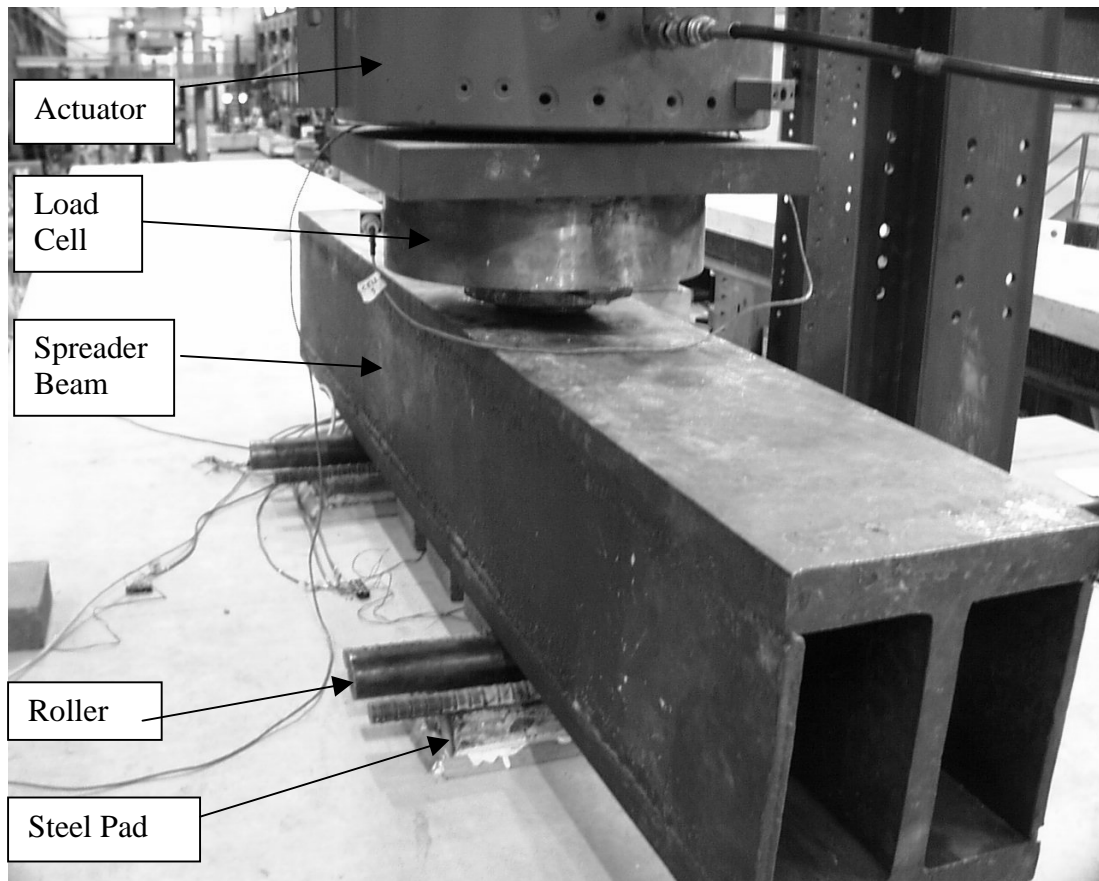
Figure 2.11 Spreader Beam, Rollers, and Loading Pads

The load was applied to the test beam at two contact points. Due to the geometry of the setup, it was possible to position the actuator at a point along the spreader beam such that the two loads applied to the beam through the loading pads would create a constant moment region in the test beam directly underneath the loading pads. The exact point for the actuator on the spreader beam varied for the different development lengths being tested, as well as the concrete deck composition. The loading pads were placed such that the first loading pad was a distance from the end of the beam equal to the development length being tested. This configuration is

shown in Figure 2.12. The variation of the embedment lengths and the actuator load points on the spreader beam are listed in Table 2.4.

ELEVATION

NOTE: ↧   LINEAR POTENTIOMETER AND
                DIRECTION OF MEASURE
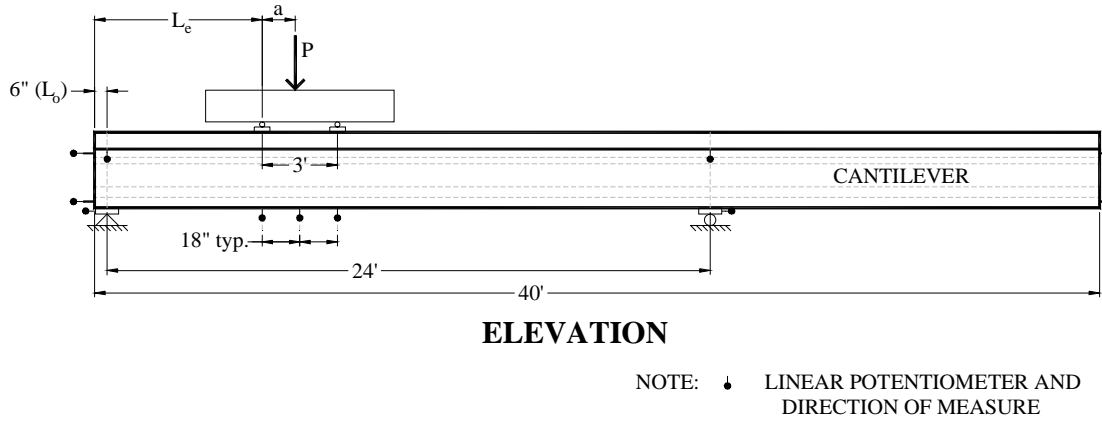
Figure 2.12 Test Set-up Geometry

Table 2.4 Test Configurations

Beam ID	Embedment Length,* in / (mm)	a* in / (mm)	Lightweight Deck Panels
NW6000-1-N-80	80 (2,032)	10.8 (274)	No
NW6000-1-S-60	60 (1,524)	9.18 (233)	No
LW6000-1-N-80	80 (2,032)	10.60 (269)	No
LW6000-1-S-70	70 (1,778)	9.12 (232)	No
LW6000-2-N-70	70 (1,778)	9.12 (232)	Yes
LW6000-2-S-60	60 (1,524)	7.68 (195)	Yes
LW8000-1-N-80	80 (2,032)	10.60 (269)	No
LW8000-1-S-70	70 (1,778)	9.12 (232)	No
LW8000-2-N-70	70 (1,778)	9.12 (232)	Yes
LW8000-2-S-60	60 (1,524)	7.68 (195)	Yes
LW8000-3-N-70	70 (1,778)	9.20 (234)	LW deck
LW8000-3-S-60	60 (1,524)	7.62 (194)	LW deck

* see Figure 2.12 for dimensions "a" and "L_e"

The embedment lengths for each test were chosen in such a way as to develop the greatest amount of meaningful information with the limited number of tests available. The predicted development length per AASHTO [1] was calculated as 82 in (2.1 m) for the normal weight beam. It was determined that the first test should occur at an embedment length of 80 in (2.0 m), since previous experience had indicated that the AASHTO development length was conservative. The shortest embedment length that could be tested and still produce a flexural failure and not risk

a sudden shear failure was 60 in (1.5 m). The normal weight beam was then tested at both 80 and 60 inches (2.0 and 1.5 m). The subsequent lightweight beams were then tested at 60, 70, and 80 in (1.5, 1.8, and 2.0 m), in order to observe whether a bond failure occurred and if any strands slipped.

2.3.3 Instrumentation

The instrumentation used in this test procedure was electronic, with selected manual measurements made to check the accuracy of the electronic results. All of the data-collecting instruments were attached by wires to a bridge box, from which cables carried the information into the data acquisition device. This device was connected to a computer running a program that managed the data. The types of measurement devices and instrumentation are described in the following sections.

2.3.3.1 Load Measurement

The measurement of the amount of load applied to the beam was carried out in both manual and electronic form. A pressure gauge was attached to the hydraulic pump operating the actuator, as shown in Figure 2.13. A reading of this gauge was taken manually at each load increment during the test procedure. This was compared to the measurement taken by the load cell attached to the actuator and wired into the data acquisition system. The load cell data was taken and recorded continuously throughout the test procedure.

29

Figure 2.13 Hydraulic Pump and Pressure Gauge

2.3.3.2 Beam Displacement Measurement

The vertical displacement of the beam was taken at three points below the beam. The first point was located at a distance from the end of the beam equal to the development length being tested. The second point was 18 in (457.2 mm) beyond the first, and the third was at a point 36 in (0.9 m) beyond the first, directly beneath the second loading pad. The displacement was measured using 6 in (152.4 mm) linear potentiometers placed in a frame and wired to the data acquisition system, as shown

in Figure 2.14. A glass slide was attached to the bottom of the beam at the point where the potentiometer came into contact with the beam to ensure a smooth, consistent testing surface.
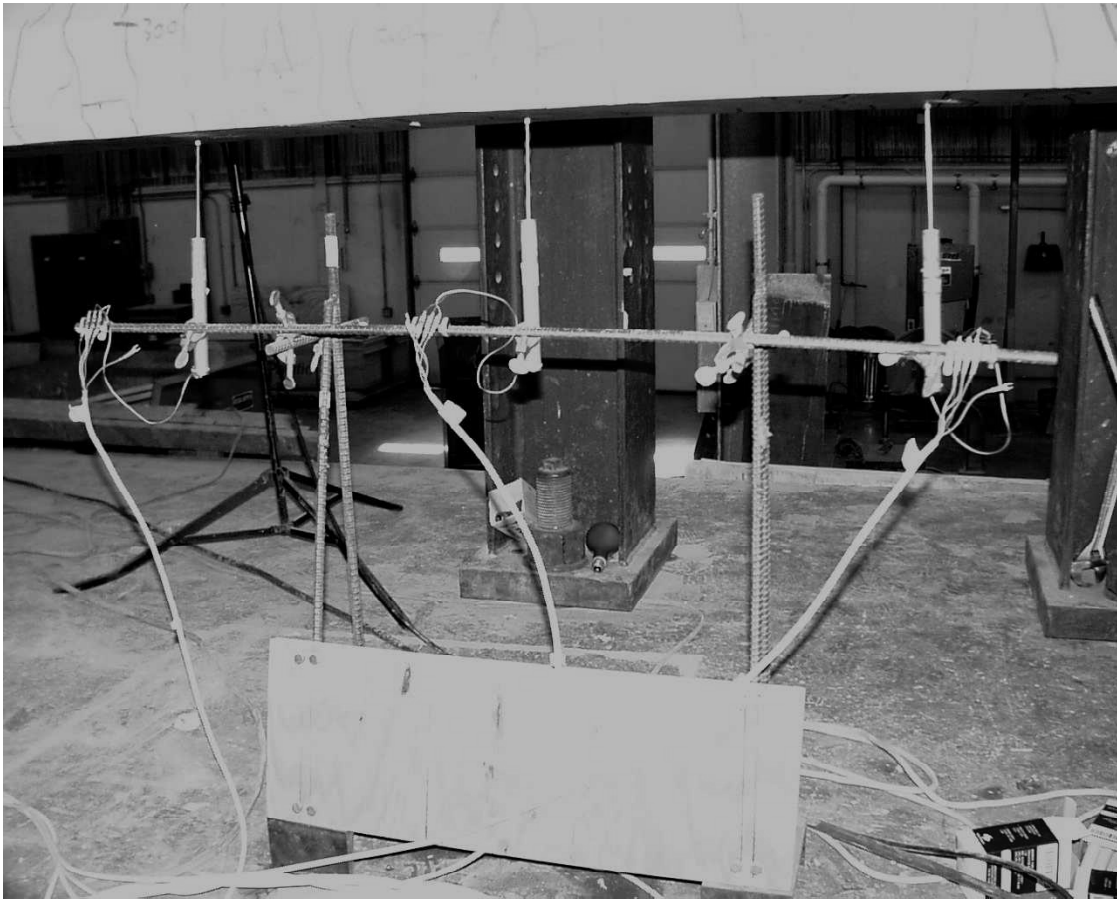
Figure 2.14 Vertical Displacement Potentiometers

As a manual backup to this system, a ruler was attached to the side of the beam directly above the location of the second potentiometer. A piano wire was stretched along the beam from support to support, and attached at a level equivalent to the centroid of the cross section. Thus, as the beam deflected and rotated at the supports, the vertical position of the piano wire attachment points remained constant.

31

A reference measurement was taken on the ruler before the test began, and then manual measurements of where the wire crossed the ruler were taken at each load increment during the test procedure, similar to the readings of the pressure gauge previously mentioned.

2.3.3.3 Support Displacement Measurement

The displacement of the support was taken using several types of linear potentiometers at different points. The horizontal displacement of the bearing pad was measured using 2 in (50.8 mm) potentiometers placed in a block support and wired to the data acquisition system. These are shown in Figure 2.15. A glass slide was attached to the beam at the point where the potentiometer came into contact with the beam to ensure a smooth, consistent testing surface. The vertical displacement of the support was measured using 5 in (127 mm) string potentiometers attached to the bottom of the deck and to the concrete support block, as shown in Figure 2.16. The same arrangement was used at each support location of the beam during a test.
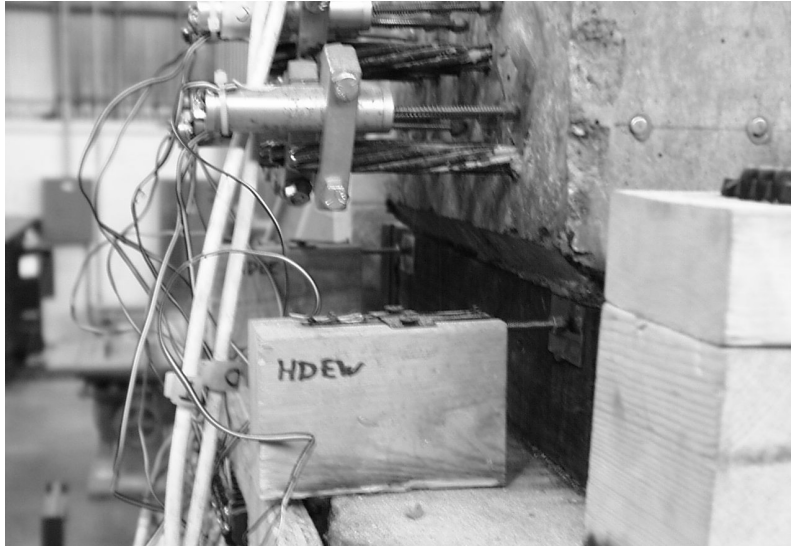
Figure 2.15 Horizontal Support Displacement Potentiometer

String
Pot
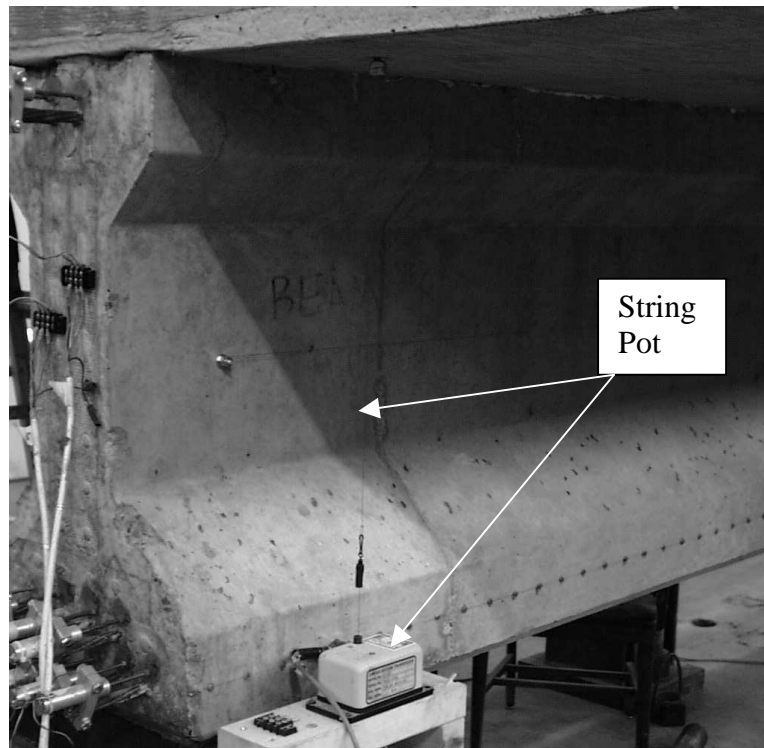
Figure 2.16 Vertical Support Displacement Potentiometer

2.3.3.4 Strand Slip Measurement

The measurement of the slip, or bond failure, of the prestressing strands was a critical part of the test procedure, since the slip of a strand would be an indication of a limit on the development length of the beam. The measurements were taken on each strand using a 2 in (50.8 mm) linear potentiometer that was attached to the strands using a bracket system as shown in Figure 2.17.
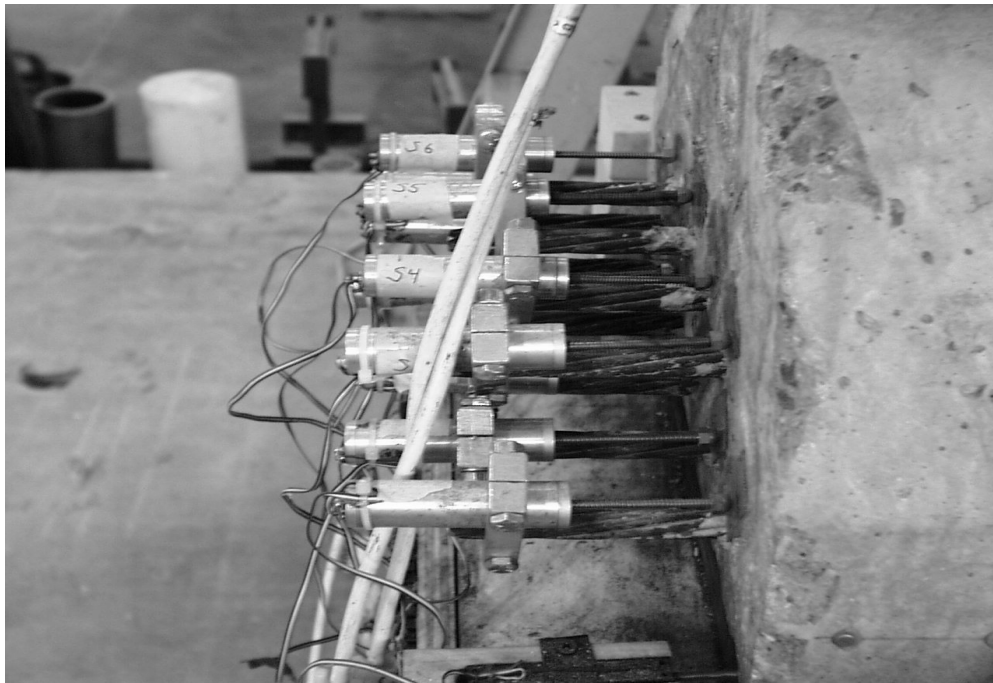
Figure 2.17 Strand Slip Measurement

A glass slide was attached to the beam at the point where the potentiometer came into contact with the beam to ensure a smooth, consistent testing surface. The potentiometers and brackets were adjusted such that each was free to move any distance in or out relative to the others, allowing complete measurement of the

potential slip of the strand. They were then wired into the data acquisition system. The wiring is shown in Figure 2.18.
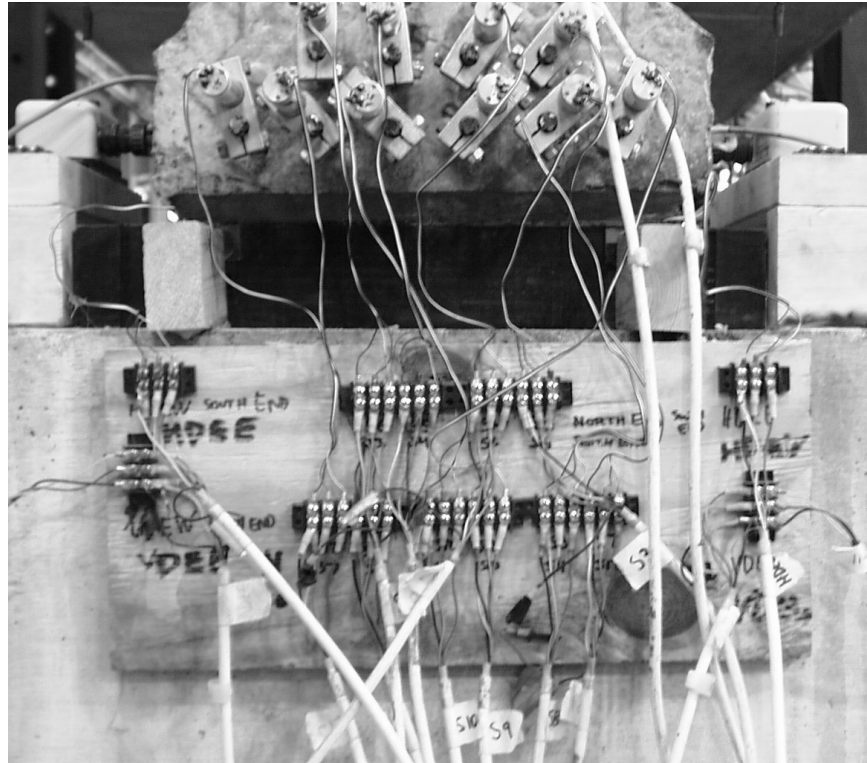
Figure 2.18 Strand Potentiometer Wiring

2.3.3.5 Strain Measurement

The top fiber strain of the concrete deck was measured using eight strain gauges placed in the arrangement shown in Figure 2.19. Prior to placing the strain gauges, the surface of the deck concrete was carefully prepared. The gauging area was first ground down to exposed aggregate, and then treated with several chemicals before a layer of epoxy was placed. After allowing the epoxy to set for a day, the epoxy was treated with chemicals and then the gauge was attached, using the same

epoxy. It was held down using a typical brick. Between the gauge and the brick, however, a soft pad was placed to prevent damage to the gauge. These pads are visible in Figure 2.20. The gauges were then wired and connected to the data acquisition system.
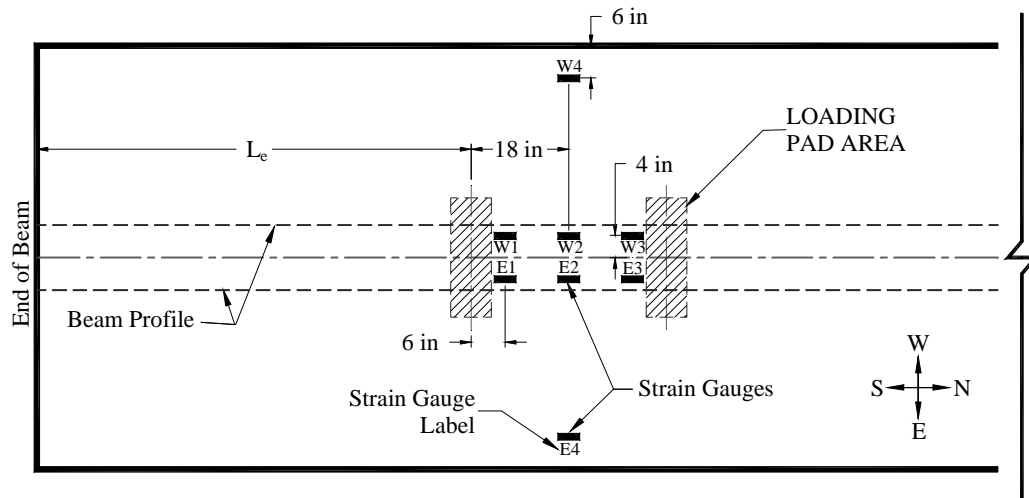
Figure 2.19 Strain Gauge Locations
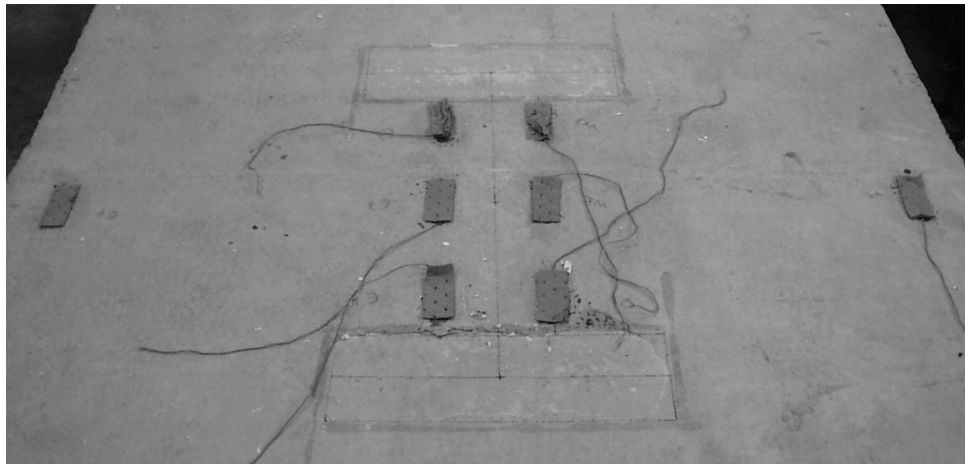
Figure 2.20 Strain Gauge Locations and Pads

2.3.3.6 Crack Measurement

The sizes of the largest cracks were measured at the ultimate stage of loading during the test procedure. This was done manually, using a crack width indicator.

2.3.4 Data Acquisition Equipment

The data acquisition system consisted of bridge boxes, wires, cables, and a computer system to handle the data, as shown in Figures 2.21 and 2.22. The computer ran an Excel program called Measure that managed the data acquisition. The system took data readings from all potentiometers and strain gauges every 5 seconds during loading. The data were taken every 10 seconds while load application was paused and cracks were marked. Following the test, the data were reduced for some calculations to the key points corresponding with the load increments and any significant events that occurred. The full data set was used for certain calculations as well.
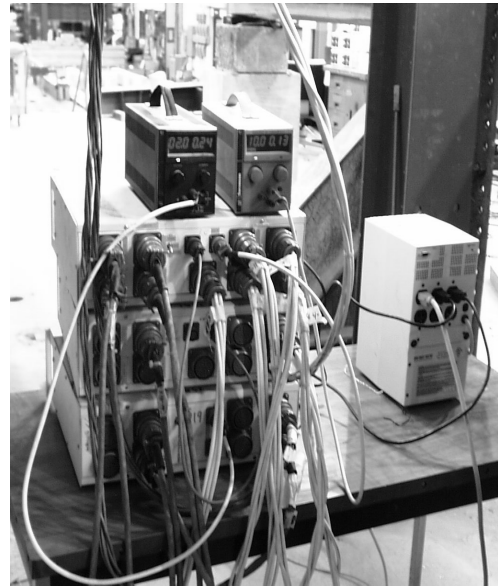
Figure 2.21 Data Acquisition System

Figure 2.22 Data Acquisition Computer

38

2.4 TEST PROCEDURE

2.4.1 Loading

The test procedure consisted of several loading stages. The loading took place in approximately 30 kip (133.4 kN) increments until first cracking occurred. The cracking load was noted, and then the loading continued in 30 kip increments. At each load increment, manual readings of the pressure gauge and the vertical displacement of the beam were made, and cracks were marked. Continuously updated graphs of the strand slip, the load versus concrete deck strain, and the load versus vertical displacement of the beam were monitored throughout the entire test procedure. After the failure limit was reached, the beam was unloaded and final measurements were taken to observe the inelastic effects on the beam.

2.4.2 Cracking

At each load increment, time was taken to mark all of the cracks visible on the beam at that stage. Flexural cracks and shear cracks were marked in separate colors. At high loads, where flexural-shear cracks develop, the cracks were all marked in the flexural crack color. After marking all of the cracks, pictures were taken of the current crack pattern. Pictures were also taken following any significant events. At the failure limit, the widths of the largest cracks were measured and noted.

2.4.3 Failure Limit

The failure limit was slightly different for each test. Careful attention was given to the strain in the top fiber of the deck concrete and the vertical displacement of the beam. Crushing failure of the deck concrete was the desired failure limit, but several of the tests were halted short of that mark due to safety concerns over high strains and/or limiting deflections.

Chapter 3: 8000 psi Beam Test Results

3.1 INTRODUCTION

This chapter covers the testing of the nominal 8000 psi (55.2 MPa) beam series carried out by the author. The test results covering multiple categories of behavior are presented, and the results are discussed.

3.2 TEST RESULTS

This section covers the results from the testing of the 8000 psi (55.2 MPa) beam series. The material properties of the individual beams, decks, and panels are presented, followed by the results from the tests. The categories of behavior reported include initial stiffness, cracking and ultimate moment and load, strand elongation, maximum strain and displacement, crack patterns, strand slip, and failure types. A plot of the applied moment versus displacement of all six tests is shown in Figure 3.1. This figure is shown to provide an overall perspective of the test results before the details are given. The curves show that the behavior of the three beams during the six tests was very similar, and the stiffnesses and moments achieved show good correlation of the data.
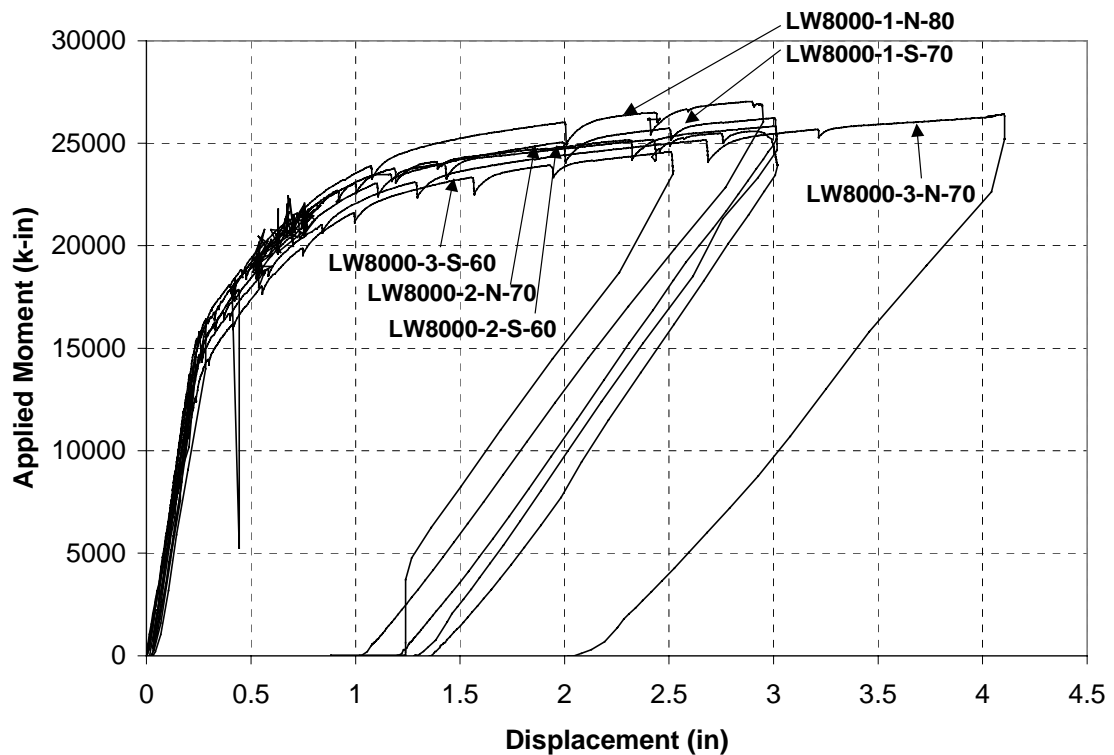
Figure 3.1 Initial Results

3.2.1 Beam Properties

The beams tested in this portion of the project were all nominal 8000 psi (55.2 MPa) compressive strength lightweight concrete, and their properties are shown in Table 3.1. The first had a normal weight cast-in-place concrete deck, the second a combined deck of lightweight concrete panels and normal weight cast-in-place concrete, and the third a cast-in-place lightweight concrete deck. The actual strength of the first of the three pretensioned beams at the time of testing was well below the specified 8000 psi (55.2 MPa) strength, the actual strength of the second was slightly below the specified 8000 psi (55.2 MPa) strength, while the third had an actual strength just above 8000 psi (55.2 MPa). The moduli of elasticity of the three beams

42

were relatively similar, with the second and third having roughly the same modulus, and the first having a lower modulus, corresponding to its lower strength.

The strengths of the normal weight concrete deck and the normal weight concrete used in the composite deck with lightweight concrete panels were very similar, and close to the specified 5000 psi (34.5 MPa) strength. The lightweight concrete used for the third deck was specified to be 5000 psi (34.5 MPa) strength, but when tested was above 7000 psi (48.3 MPa). The moduli of elasticity of the first two normal weight cast-in-place concrete decks were similar, while the modulus of the third deck with the lightweight concrete was significantly less than the other decks, but similar to that of the lightweight beams. The lightweight panels had achieved a strength of approximately 7000 psi (48.3 MPa) when the beam was tested, with a modulus similar to that of the full-depth lightweight deck. The properties of the pretensioned beam concrete mixes were discussed in greater detail by Heffington [8].

Table 3.1 Beam Properties

Beam	Le	Beam Concrete Strength (psi)	Beam Modulus (ksi)	Deck Concrete Strength (psi)	Deck Modulus (ksi)	Panels	Panel Concrete Strength (psi)	Panel Modulus (ksi)
LW8000-1 N	80 in	6848	2576	5112	4803	No		
LW8000-1 S	70 in	6848	2576	5112	4803	No		
LW8000-2 N	70 in	7847	3141	5182	4453	Yes	7321	2680
LW8000-2 S	60 in	7847	3141	5182	4453	Yes	7321	2680
LW8000-3 N	70 in	8013	3104	7011	2511	No		
LW8000-3 S	60 in	8013	3104	7011	2511	No		

The unit weights (lb/ft) of the composite concrete beams used in this testing procedure varied according to the amount of lightweight concrete in the composite beam. Figure 3.2 shows the unit weights of three normal weight beams with varying deck components, and three lightweight beams with varying deck components. The

43

composition of each beam is indicated by the figure above each column, with white used to indicate normal weight concrete and black used to indicate lightweight concrete. This group of tests comprised the three lightweight beam combinations, with the normal weight combinations presented for comparison. The reduction in weight due to the lightweight concrete can be particularly significant when dealing with long spans, where the savings in dead load allow the use of smaller sections or less beams in a particular bridge design.
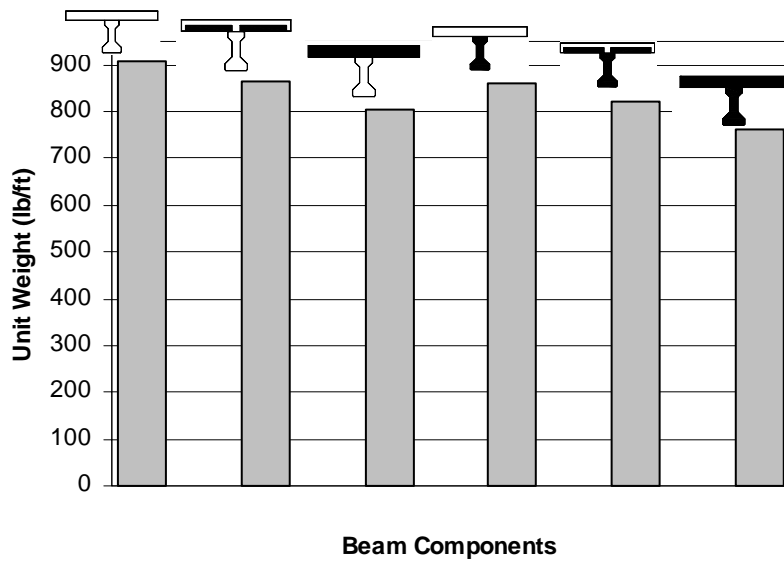
Figure 3.2 Unit Weight

The six tests took place at three different embedment lengths, in order to determine the development length of the beams experimentally. These embedment lengths ranged from 80 in to 60 in, with each of the three beams having a 70 in length test, in order to allow correlation of the test data.

3.2.2 Initial Stiffness

The initial stiffnesses of the beams during each test are presented in this subsection. The stiffnesses calculated from the geometry of the cross section and the modulus of elasticity of the concrete are shown in Table 3.2 and Figure 3.3, as well as the stiffnesses observed during the testing of the beams. The elastic modulus affects the amount of deflection relative to the amount of load applied. As the modulus is decreased, the deflection due to applied force increases. Due to lightweight concrete's lower modulus of elasticity compared to that of normal weight concrete's, the amount of lightweight concrete in the composite beam under consideration should affect the initial stiffness. The lightweight concrete used in this test procedure had a modulus of elasticity approximately half that of normal weight concrete [8]. The composite beams tested had varying components of lightweight concrete. All had lightweight concrete pretensioned girders, while the amount of lightweight concrete in the deck varied. This is shown by the figures above each column in Figure 3.3, with lightweight concrete indicated by the black portions of the cross section.

Table 3.2 Initial Stiffness

Beam ID	Modulus of Elasticity (ksi)			Moment of Inertia (in^4) Transformed to E_{beam}	Calculated Stiffness (k-in^2)	Measured Stiffness (k-in^2)
	E_{beam}	E_{Deck}	E_{Panel}			
LW8000-1-N-80	2576	4803		125,979	3.25E+08	1.26E+09
LW8000-1-S-70	2576	4803		125,979	3.25E+08	1.22E+09
LW8000-2-N-70	3141	4453	2680	112,019	3.52E+08	---
LW8000-2-S-60	3141	4453	2680	112,019	3.52E+08	8.32E+08
LW8000-3-N-70	3104	2511		99,147	3.08E+08	1.03E+09
LW8000-3-S-60	3104	2511		99,147	3.08E+08	8.03E+08

Figure 3.3 Initial Stiffness

The results of the testing indicate that the expectation of slightly lower initial stiffness for increased percentage of lightweight concrete components in the cross section was generally true. However, the relative affect was small when considering the magnitude of the values. For the tests on LW8000-1, the lower modulus of elasticity colors the data. If the modulus of this beam had been 3100 ksi like the other beams, the calculated stiffness would have increased to 3.66×10^8 k-in^2, a value slightly higher than the other beams. During the testing of the beams, the measured stiffnesses were higher than the calculated values, but agreed with the predicted trend of decreasing stiffness for increased lightweight concrete components. It should be emphasized that while this trend is true, the actual decrease in stiffness is only on the order of 16%.

46

3.2.3 Cracking and Ultimate Moment and Load

The cracking and ultimate moments are shown in Figure 3.4. The ratio of the ultimate to the cracking moment is shown above the column for each test. The ultimate moments are relatively the same for all of the tests, as was expected due to the similarity in the beams being tested. The cracking moments show some significant differences. This is likely largely due to the difficulty in observing the exact onset of flexural cracking in the beam during testing.
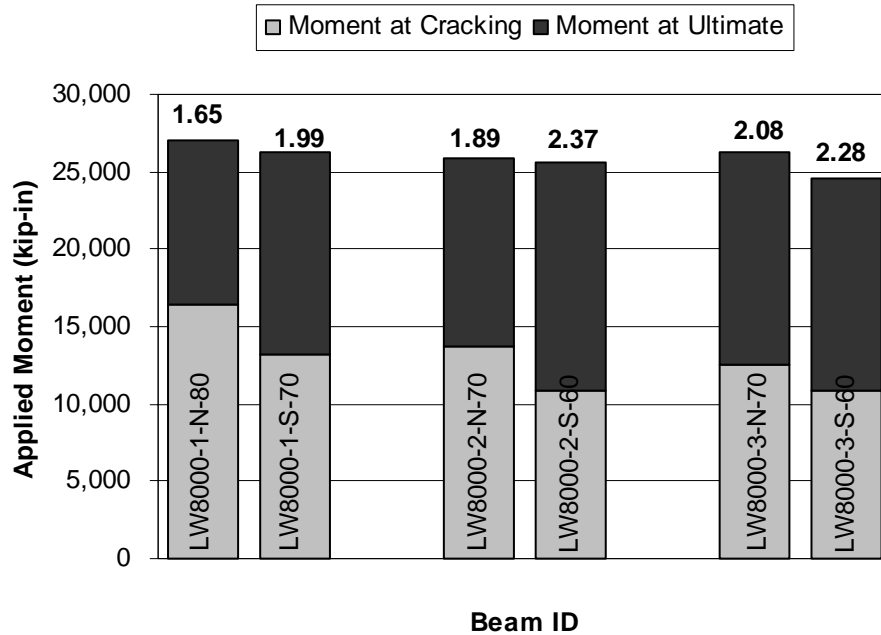
Note: Ratio of ultimate to cracking moment is shown above each test

Figure 3.4 Cracking and Ultimate Moments

The cracking and ultimate loads are shown in Figure 3.5, and are grouped according to the embedment length tested, since this affected the amount of moment developed in the beam. The cracking loads were similar within embedment length groups, and show good correlation of the test data. The ultimate loads are also shown

in Figure 3.5, as well as the ratio of the ultimate to the cracking load, which is shown above the column for each test. Within groups, the ultimate loads and the ratios are similar, with some slightly higher than others due to the subjective decision of when to stop the test and declare an ultimate condition.
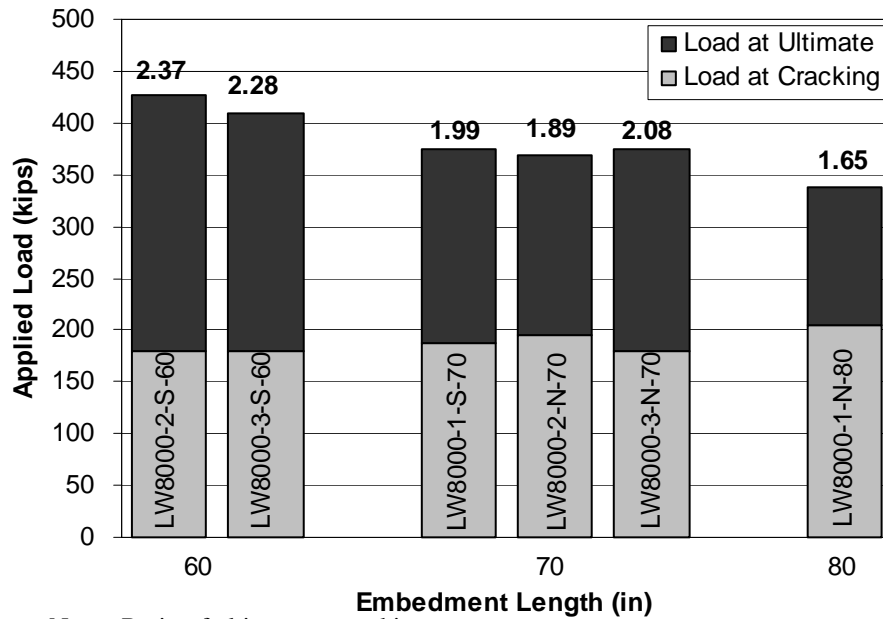
Note: Ratio of ultimate to cracking
moment is shown above each test

Figure 3.5 Cracking and Ultimate Loads

3.2.4 Strand Elongation

The elongation of the strands at ultimate is presented in this subsection. The strand elongation was calculated for the bottom layer of strands in the beams. The values were obtained assuming a linear strain distribution in the composite beams. The depth of the cracking in the deck was observed visually, and the maximum strains in the deck above the web due to the load were measured. The strain in the steel was then calculated from the deck strain and the geometry of the cross section.

48

This was added to the strain already present in the strands due to prestressing and subsequent losses. From this final strain in the steel strands, the elongation was calculated. The results are given in Table 3.3 and shown in Figure 3.6. The data of LW8000-2-N-70 is incomplete, due to problems with the strain gages during that particular test.

Table 3.3 Strand Elongation

Beam ID	L_e in (mm)	Depth of Cracking at Ultimate, in / (mm)	Maximum Concrete Strain measured, microstrain	Strand Elongation (%)
LW8000-1-N	80 (2,032)	2.9 (74)	3,650	4.9
LW8000-1-S	70 (1,778)	2.5 (64)	2,732	4.4
LW8000-2-N	70 (1,778)	2.5 (64)	---	---
LW8000-2-S	60 (1,524)	2.5 (64)	3,061	4.8
LW8000-3-N	70 (1,778)	2 (51)	3,711	7.1
LW8000-3-S	60 (1,524)	2.5 (64)	3,646	5.6
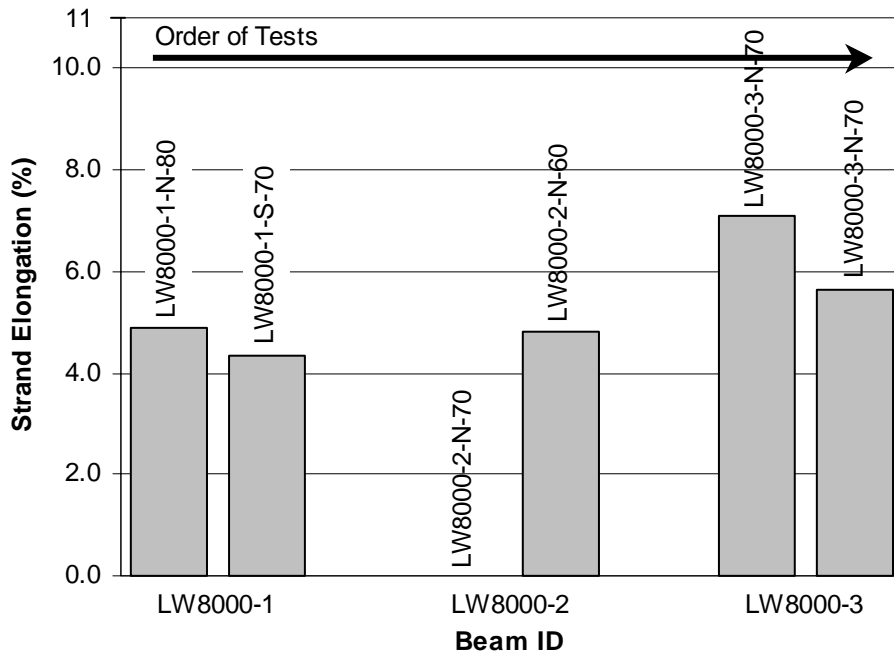
Figure 3.6 Strand Elongation

The order of the tests is indicated in Figure 3.6 to show that the strand elongations increased as the author pushed the last tests further than previous ones.

Yielding of the strands will occur at around 1% elongation, and the percentage strain in the strands at ultimate for each of the tests was substantially higher than that value. Between 1% and 4% elongation, the individual strand will undergo an increase in load of 2.3 kips. The large yielding of the strands at ultimate is an indication that the flexural ultimate load was actually reached, since after yielding of the strands, further increases in strain occur without significant increases in stress, or load level. None of the strands failed during the testing of the beams.

50

3.2.5 Maximum Strain and Displacement

The average measured strains and maximum deflections are given in Table 3.4. Due to shear lag across the deck, the average of the strain gage readings was used. The data of LW8000-2-N-70 is incomplete, due to problems with the strain gages during that particular test. The maximum deflections were taken at the midpoint of the constant moment region in the beam.

Table 3.4 Strains and Deflections

Beam	Le	Maximum Load (kips)	Average Strain (microstrain)	Maximum Deflection (in)
LW8000-1 N	80 in	335	2695	2.9
LW8000-1 S	70 in	375	1984	3.0
LW8000-2 N	70 in	365	---	3.0
LW8000-2 S	60 in	425	2208	2.9
LW8000-3 N	70 in	375	3400	4.0
LW8000-3 S	60 in	410	2590	2.5

A plot of the applied moment vs. average microstrain across the top of the deck for each test is shown in Figure 3.7. The curves show similar behavior from all six tests. A plot of the applied load vs. average microstrain across the top of the deck for each test is shown in Figure 3.8. The curves for tests of the same embedment length show similar behavior. Individual plots of the applied load vs. microstrain readings for each test are displayed in Appendix D. Due to shear lag, the microstrain measurements varied across the top of the deck. Generally, the readings from the gauges located at the outer edges of the slab showed lower strains than those located above the web of the beam.
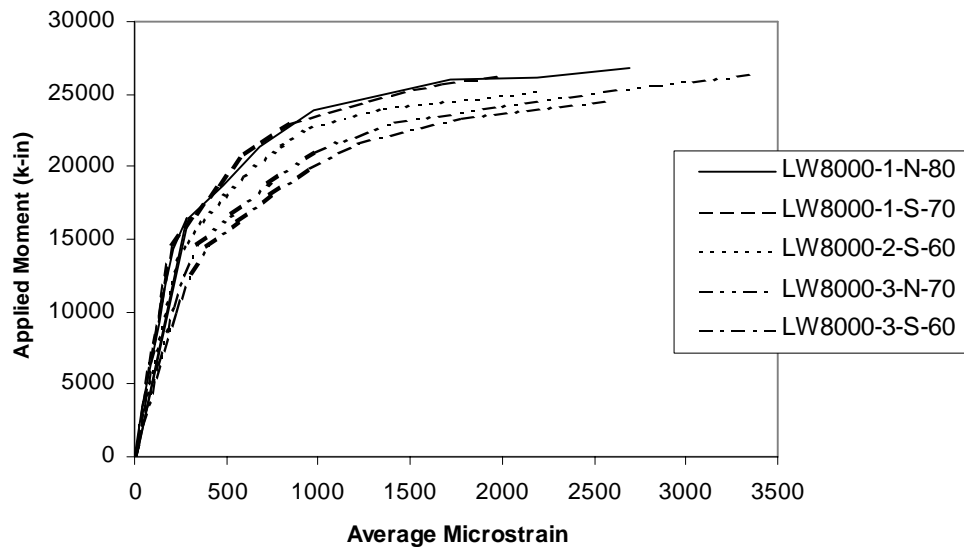
Figure 3.7 Applied Moment vs. Average Microstrain
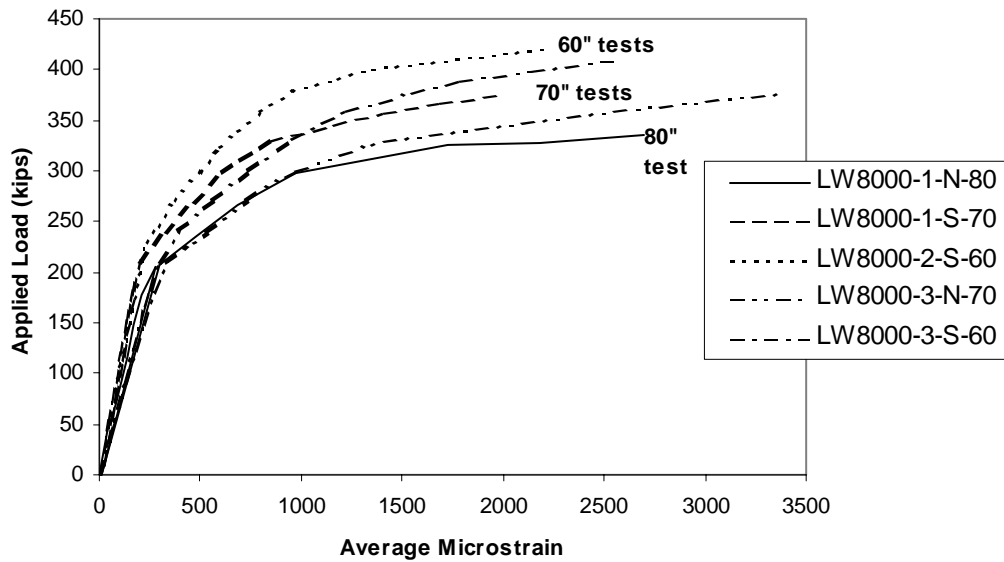
Figure 3.8 Applied Load vs. Average Microstrain

The ultimate deflections are shown in Figure 3.9. The deflections achieved were similar for all tests, since a deflection of approximately 3 in (76.2 mm) was used

as one of the criteria for stopping the test procedure. The test on LW8000-3-N-70 was pushed to a further limit to observe deck crushing and load pickup at high levels of strain. The load increase was insignificant, but the increase in strain caused the beam to deflect 4 in (101.6 mm), which is shown in Figure 3.10. The test on LW8000-3-S-60 was stopped due to high strains at the top of the composite deck.
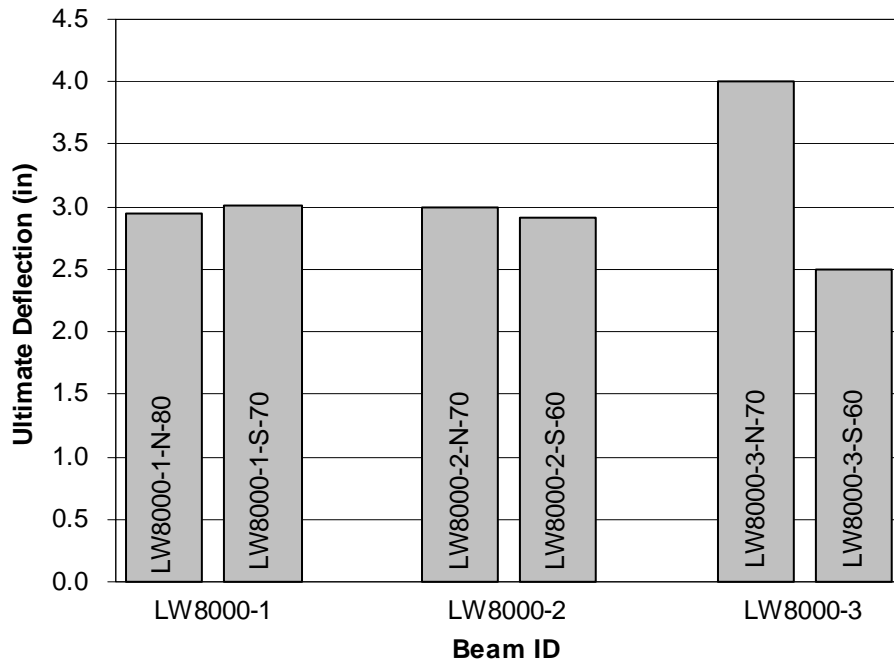
Figure 3.9 Ultimate Deflections
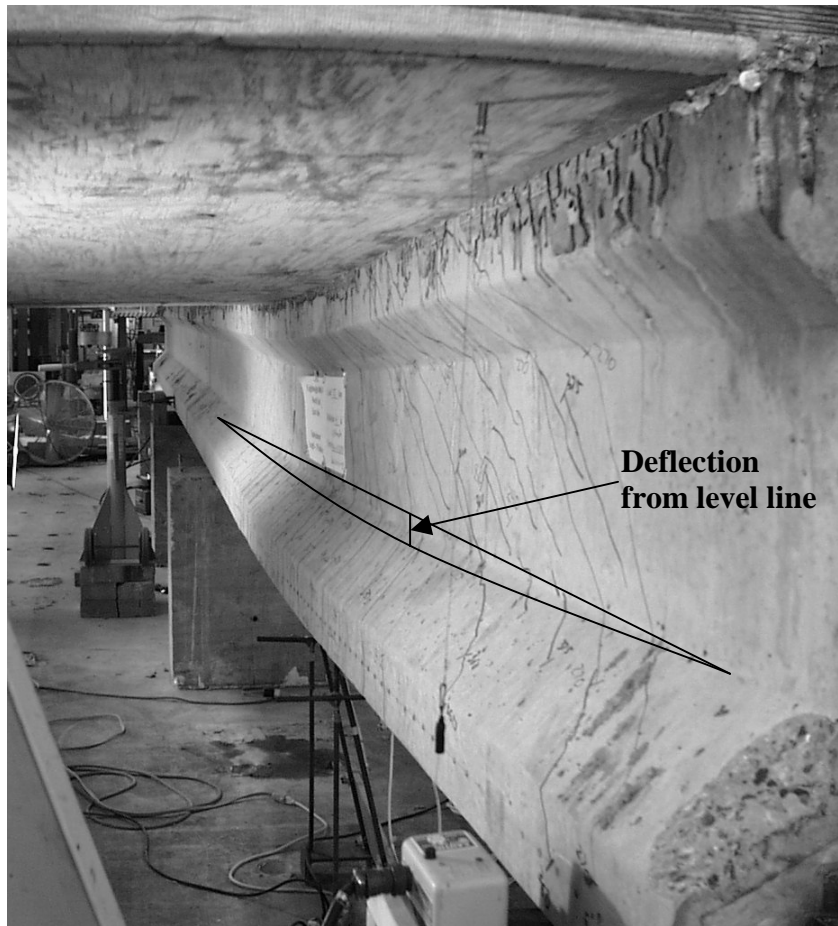
Figure 3.10 LW8000-3-N-70 Deflection

3.2.6 Crack Patterns

The crack patterns developed during each test are presented in this subsection. The results from each individual beam will not be presented here, due to the uniformity of the crack formation in the beams during each of the tests. Rather, this section gives a general presentation of the resulting crack patterns.

The cracks were marked on the beams with colored markers at each load increment until ultimate. One color was used for flexural cracks, while another was

used for shear cracks. The crack patterns were divided into three distinct regions, or zones. Zone 1 extended from the end of the beam to the first loading point, a distance equal to the embedment length of the test. This zone was dominated by shear cracks. The shear cracks formed in the web, and extended at approximately 45 degree angles in both directions as the load increased. These cracks formed and then propagated all the way down to the support point of the beam at the bearing pad. Some flexural cracks formed in this zone as well. The flexural cracks formed at the bottom of the beam and extended up at a slight inclination as the load increased. Zone 1 is shown in Figure 3.11.
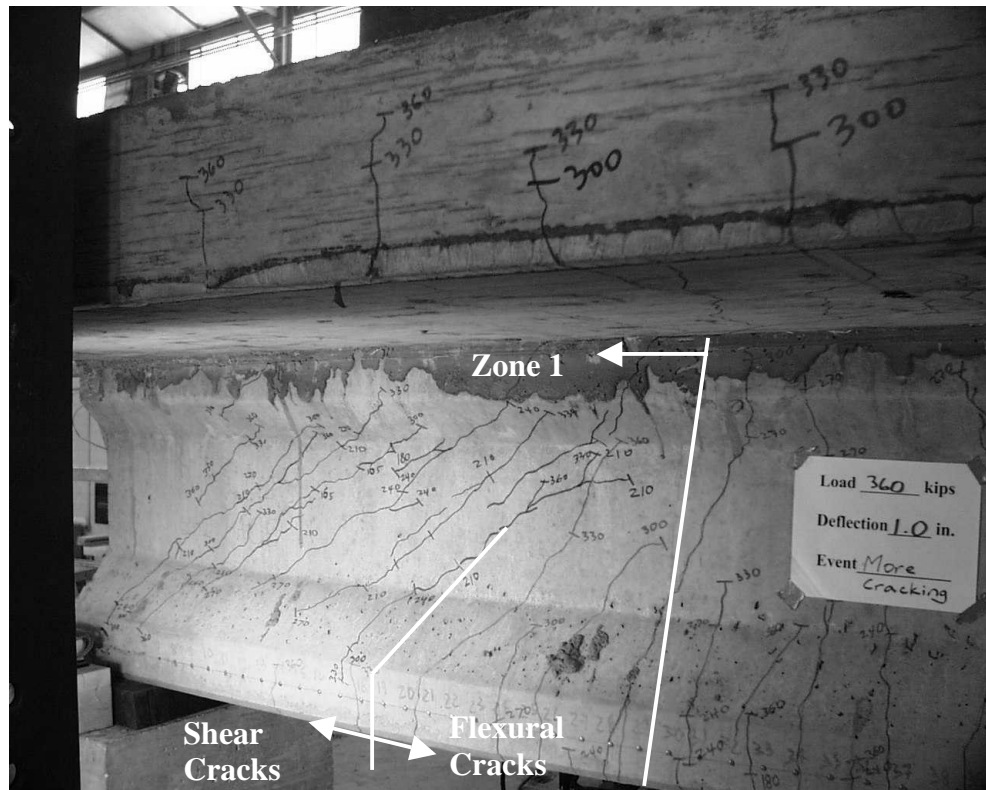
Figure 3.11 Zone 1 Cracking

Zone 2 extended from the end of Zone 1 to the second loading point, a distance equal to 36 in (914.4 mm). This zone was dominated by flexural cracks, and was the essentially constant moment region developed beneath the loading points. The flexural cracks formed at the bottom of the beam and extended up until they reached the neutral axis depth at each loading. These cracks lengthened as the load increased, and the number of them increased with load as well. The flexural cracks extended nearly vertically, with those at the edge of the zone showing a slight inclination. Zone 2 cracking is shown in Figure 3.12.
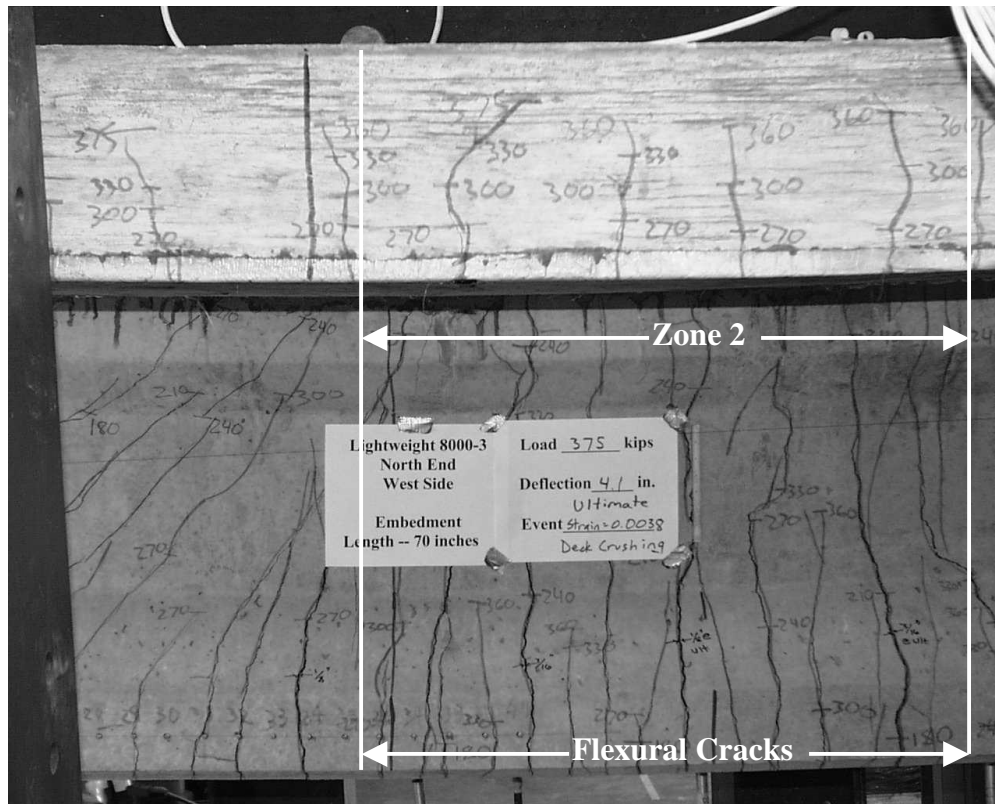
Figure 3.12 Zone 2 Cracking

Zone 3 extended from the end of Zone 2 to the other support point of the beam. Zone 3 was dominated by shear cracks. The shear cracks formed in the web and extended at approximately 45 degree angles in both directions as the load increased. These cracks extended from the bottom of the beam up to the deck of the composite beam and into the deck for some cracks. The shear cracks in this zone did not form gradually, however. During each successive load increment, another crack or two would spring forth with an audible pop, a slight distance further down the beam than the previous one. Some flexural cracks formed in Zone 3 as well, in the area closest to Zone 2. The flexural cracks formed at the bottom of the beam and extended up at a slight inclination as the load increased. Zone 3 is shown in Figure 3.13.
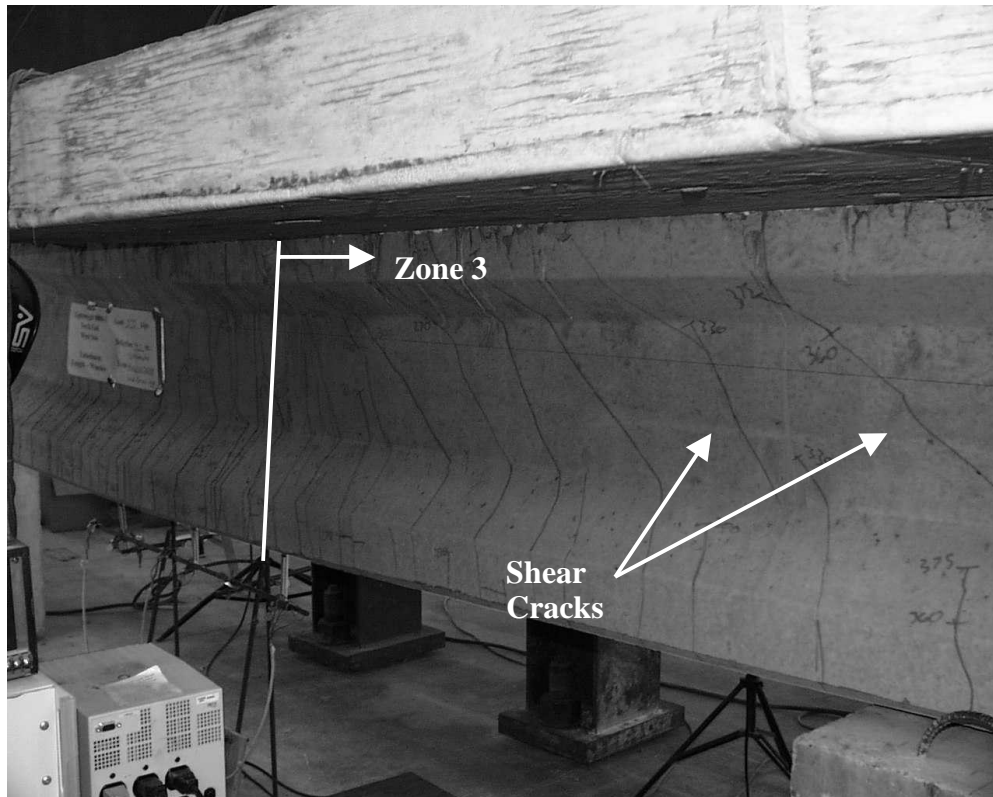
Figure 3.13 Zone 3 Cracking

3.2.7 Strand Slip

Strand end measurements taken during testing indicated that no strand slips occurred in the 8000 psi (55.2 MPa) beam series. For each of the tests, the measured slip was less than 0.01 in (0.25 mm), which can be attributed to electronic noise in the data acquisition equipment. A slip of a strand would have indicated a bond failure, which would have established that the development length required was greater than the embedment length being tested. However, since none of the strands slipped, their full strength was developed. Clearly, the development length is some distance less than the minimum embedment length tested of 60 in.. The results are shown in Table 3.5.

Table 3.5 Strand Slip

Beam ID	Embedment Length, in / (mm)	Maximum Strand Slip, in / (mm)
LW8000-1-N-80	80 (2,032)	< 0.01 < (0.25)
LW8000-1-S-70	70 (1,778)	< 0.01 < (0.25)
LW8000-2-N-70	70 (1,778)	< 0.01 < (0.25)
LW8000-2-S-60	60 (1,524)	< 0.01 < (0.25)
LW8000-3-N-70	70 (1,778)	< 0.01 < (0.25)
LW8000-3-S-60	60 (1,524)	< 0.01 < (0.25)

3.2.8 Failure Types

Several types of failure were observed during the testing of the 8000 psi (55.2 MPa) beams, and are presented in this subsection. They are listed in Table 3.6. All of the beams were tested to some form of flexural failure. However, the exact manifestation of the failure varied for each beam and each test. The failure state was limited to a flexural one by the design of the beam, which included heavy shear reinforcement to ensure such a failure, as discussed previously in Section 2.2.4. The criterion for a flexural failure varied somewhat for each test, but was generally one of high deflection or strain in the beam at ultimate load.

Table 3.6 Types of Failure

Beam ID	Type of Failure
LW8000-1-N-80	Flexural Failure
LW8000-1-S-70	Flexural Failure
LW8000-2-N-70	Flexural Failure, V-Crack, Spalling at Support in Beam Flange
LW8000-2-S-60	Flexural Failure, Complete Deck Crack, V-Crack, Spalling at Support in Beam Flange
LW8000-3-N-70	Flexural Failure, Deck Cracking Initiation
LW8000-3-S-60	Flexural Failure, Complete Deck Crack, Spalling at Support in Beam Flange

The first beam tested was constructed with a normal weight concrete deck. The two tests performed on this beam resulted in typical flexural failures, with large strains and deflections, as discussed in previous subsections. The second beam tested was constructed with lightweight deck panels and normal weight concrete for the

remainder of the deck. The two tests performed on this beam exhibited flexural failure characteristics like the first beam, with the addition of two other types of secondary failure. A crack formed in the deck at a level equal to the top of the lightweight panels in the deck that, instead of continuing vertically up the deck, veered off to either side in a V-shape, as seen in Figure 3.14. A type of hinging action at that point in the deck likely caused this crack formation. No steel was placed to interconnect the panels. Thus, when the load on the deck began to cause significant deflection, the panels began to rotate with respect to one another. The crack then tended to spread laterally as the beam deflected.
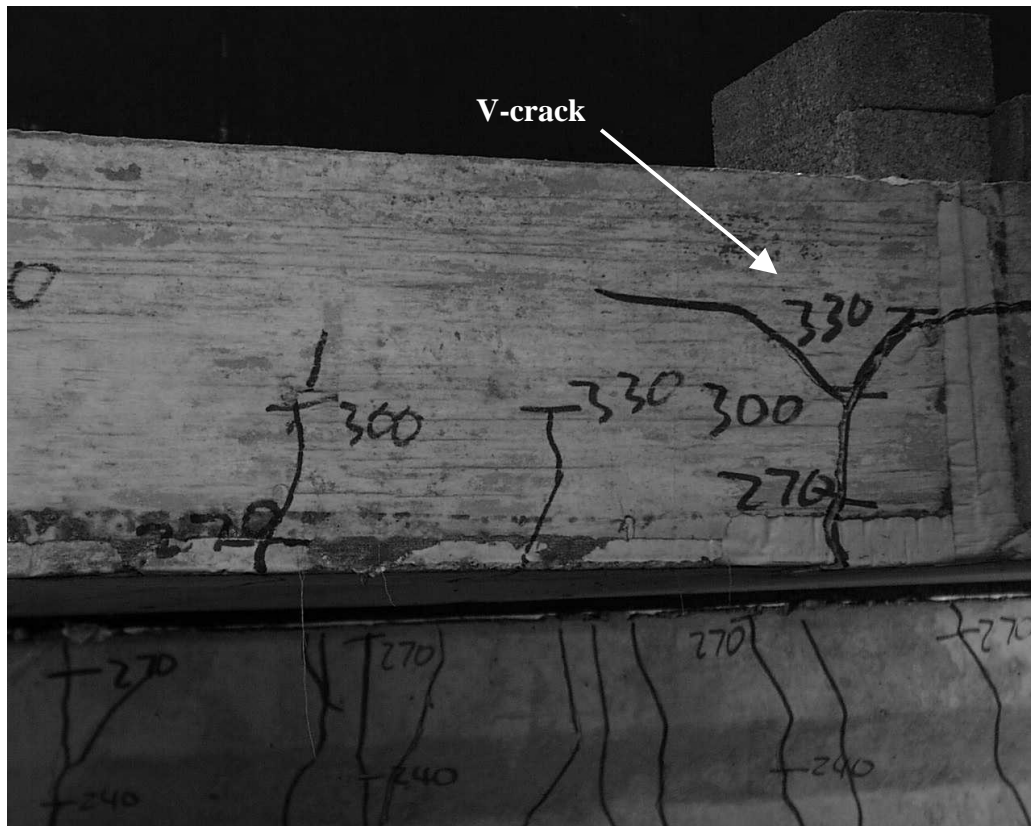
Figure 3.14 V-crack in Deck

Another form of failure that occurred in several of the tests was a spalling of the concrete that occurred on one side at the end of the beam at loads near ultimate. This spalling will be discussed in the following subsection in more detail.

The final three tests were pushed a bit further than the previous three, due to confidence in obtaining meaningful data while maintaining safety during the testing, as the author's experience increased. These tests achieved cracking in the deck due to compressive stresses at the end of the test. Two of the tests reached a point where deck crushing occurred, as seen in Figure 3.15. This is referred to later as "complete deck crack."

Figure 3.15 Deck Crushing

3.2.9 Support Spalling

Three of the six tests had support spalling prior to ultimate. This condition was not considered to be an ultimate condition, since the ultimate load of the beam was not affected by the formation of the spall. The spalls were very similar in appearance in all three tests, and occurred on only one side of the beam in each case. They are shown in Figures 3.16, 3.17, and 3.18.
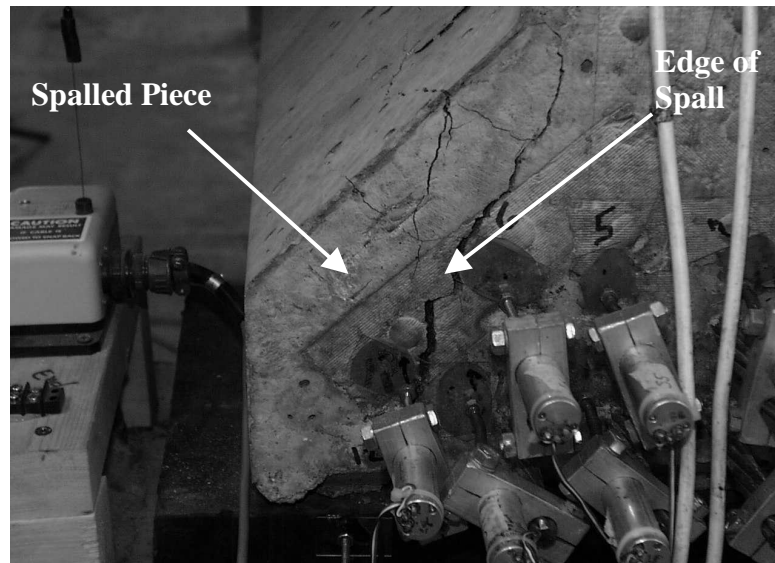
Figure 3.16 Support Spall at End (LW8000-2-N-70)
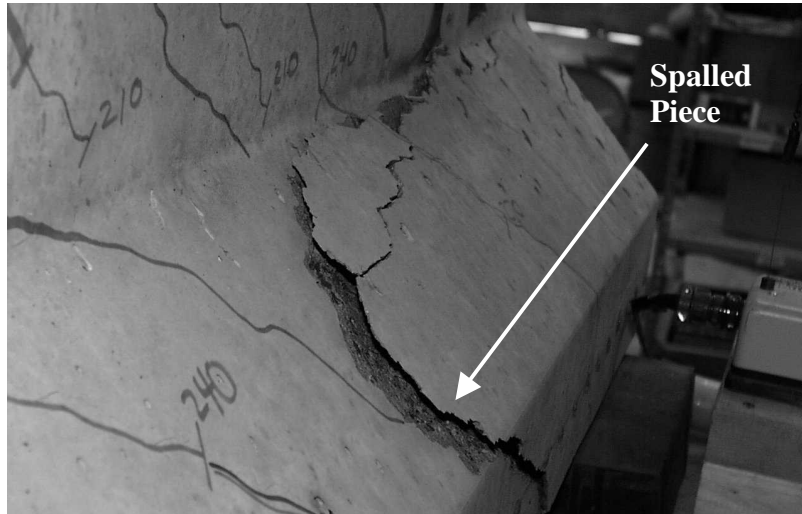
Figure 3.17 Support Spalling (LW8000-2-N-70)
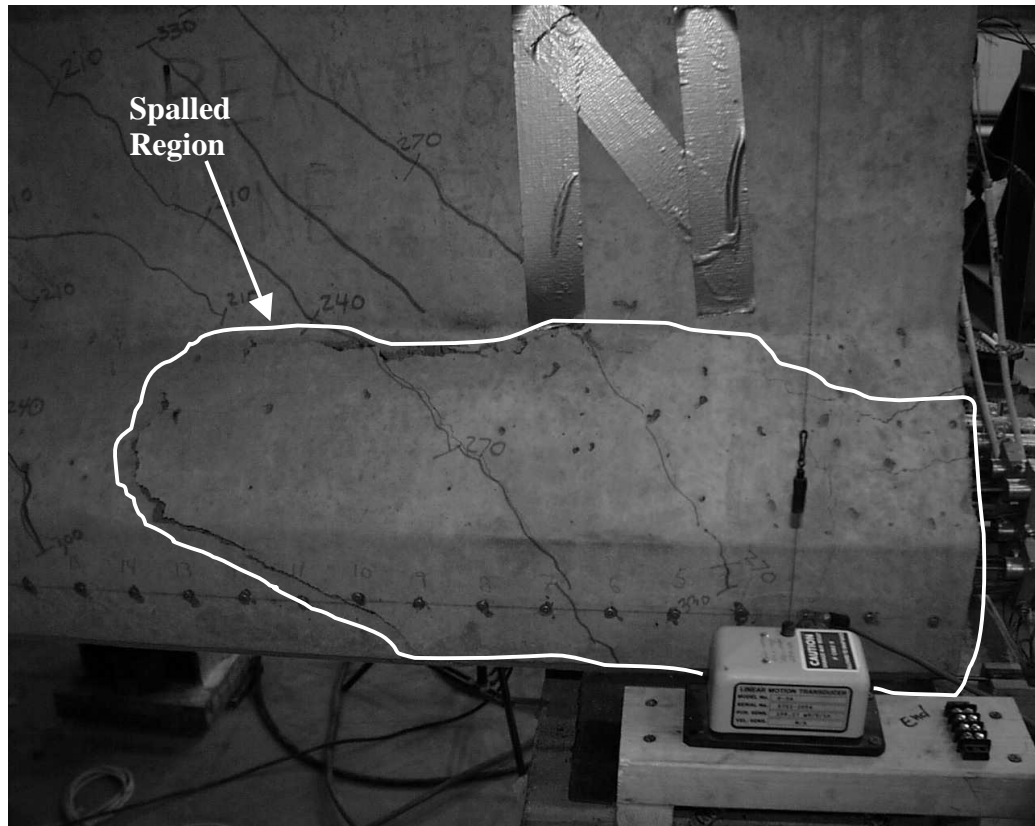
Figure 3.18 Support Spalling Area (LW8000-2-N-70)

The load at which the spall occurred is shown in Figure 3.19 as a ratio of the spalling load relative to the cracking load. For LW8000-2-N-70 and LW8000-3-S-60, the spall occurred at 92% and 98%, respectively, of the ultimate load during the test. For LW8000-2-S-60, the spall occurred at 75% of the ultimate load during the test, but the ultimate load was not affected by the formation of the spall. The occurrence of the spall in each case was at a load level more than twice the service load level if dead load is taken equal to live load, and more than three times the service load level if dead is taken equal to twice live, which is more common for bridge applications. This indicates that the spalling is not a service level occurrence, but rather an ultimate level occurrence. An explanation of the formation of the support spalls is discussed in the following section.
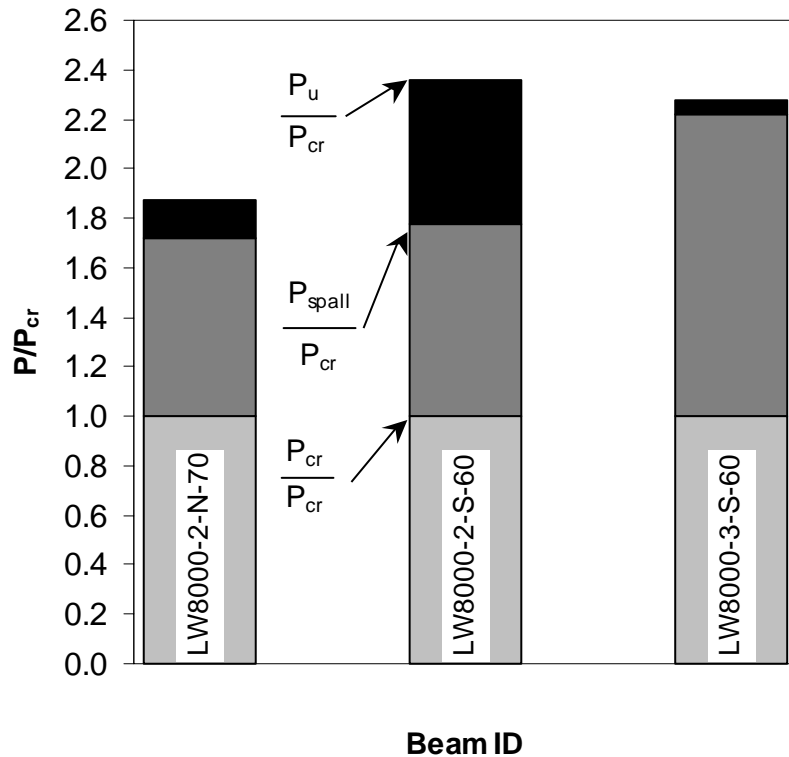
Figure 3.19 Support Spalling Loads

3.3 DISCUSSION

This section presents a discussion of the results of the 8000 psi (55.2 MPa) beam tests. The test results are discussed, a theory for the formation of the support spalls is introduced, and behavior observed with the use of the lightweight panels is discussed.

3.3.1 Test Results

This subsection compares the results obtained from the testing of the 8000 psi (55.2 MPa) beams.

3.3.1.1 Moment Comparison

This subsection compares the theoretical calculated moments with those obtained during the testing of the beams. Three methods of calculation were used, the AASHTO Standard Method, the Whitney Stress Block method, and the Stress Block Factors Method [6]. A factor of $\phi = 1.0$ was used in each method. All of these methods are based on the assumption of strain compatibility and give virtually identical results for these beams. The results of these calculations are shown in Table 3.7, along with the ultimate moment achieved by the beams during testing. The ultimate-to-calculated moment ratios are shown as well, and demonstrate substantial correlation.

Table 3.7 Moment Comparison

Beam ID	AASHTO Standard, k-in (kN-mm)	Whitney Stress Block, k-in (kN-mm)	Stress Block Factors, k-in (kN-mm)	Ultimate Moment, k-in (kN-mm)	Ultimate / Calculated
LW8000-1-N-80	14,743 (2,601)	14,800 (2,611)	14,820 (2,614)	17,900 (123,421)	1.21
LW8000-1-S-70	14,743 (2,601)	14,800 (2,611)	14,820 (2,614)	18,200 (125,489)	1.23
LW8000-2-N-70	14,758 (2,603)	14,810 (2,612)	14,830 (2,616)	17,900 (123,421)	1.21
LW8000-2-S-60	14,758 (2,603)	14,810 (2,612)	14,830 (2,616)	18,400 (126,868)	1.24
LW8000-3-N-70	14,964 (2,640)	15,050 (2,655)	15,060 (2,657)	18,100 (124,800)	1.20
LW8000-3-S-60	14,964 (2,640)	15,050 (2,655)	15,060 (2,657)	17,600 (121,352)	1.17
Averages	**14,822 (2,615)**	**14,887 (2,626)**	**14,903 (2,620)**	**18,017 (2,900)**	**1.21**

Standard Deviation   0.02

The ultimate moment achieved by the beams exceeded the theoretical calculated moment by an average of 21%. The reason for this difference is due to the conservative nature of the design theory and possibly a higher ultimate stress in the strand than the reported 270 ksi. The low standard deviation reveals that the method is consistent in its conservative level, and that the data is tightly clustered.

3.3.1.2 Displacement Comparison

This subsection compares the deflections of the beams during all six tests. The plots of applied moment versus load are shown in Figure 3.20, with all six tests plotted together in order to show direct comparisons. The figure shows that the

ultimate deflection for all of the tests was very similar, except for LW8000-3-N-70, which was intentionally pushed further in order to observe additional crushing behavior in the deck. The ultimate moment, as reported in Table 3.7, is the actual moment applied to the beam minus the moment due to pretensioning the beam.
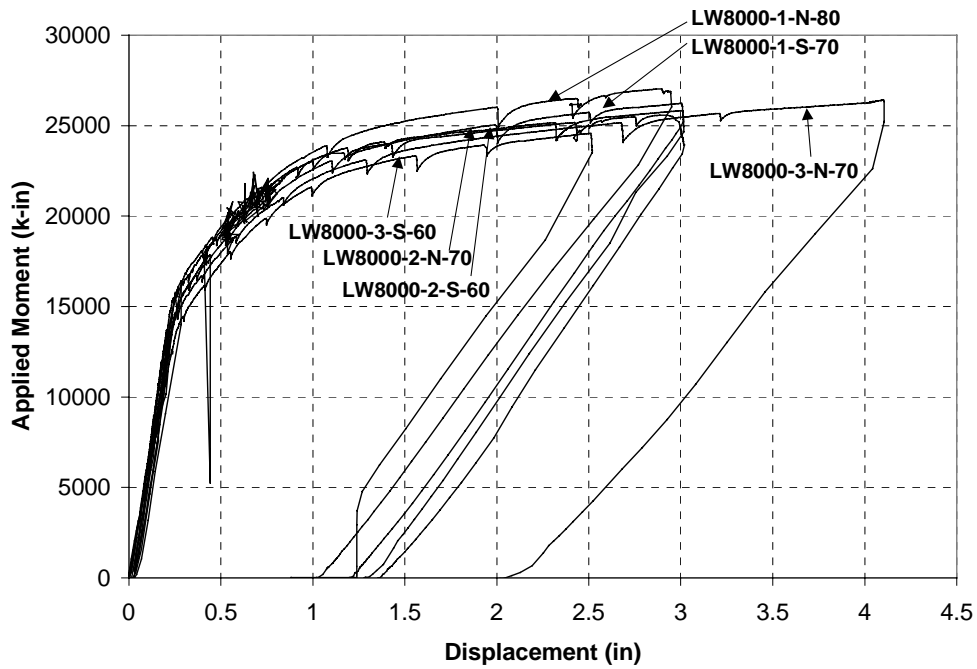
Figure 3.20 Displacement Comparison (Moment)

The plots of applied load versus deflection for all six tests are shown in Figure 3.21. Individual plots of the load versus deflection for each test are displayed in Appendix C. Tests of the same embedment length showed similar behavior. While there was no comparison to be made for the 80 in (2032 mm) test, and its total load was lower due to the shear span length, its deflection path was similar to the other tests. The three 70 in (1778 mm) tests show very similar behavior within that group, as do the two 60 in (1524 mm) tests.
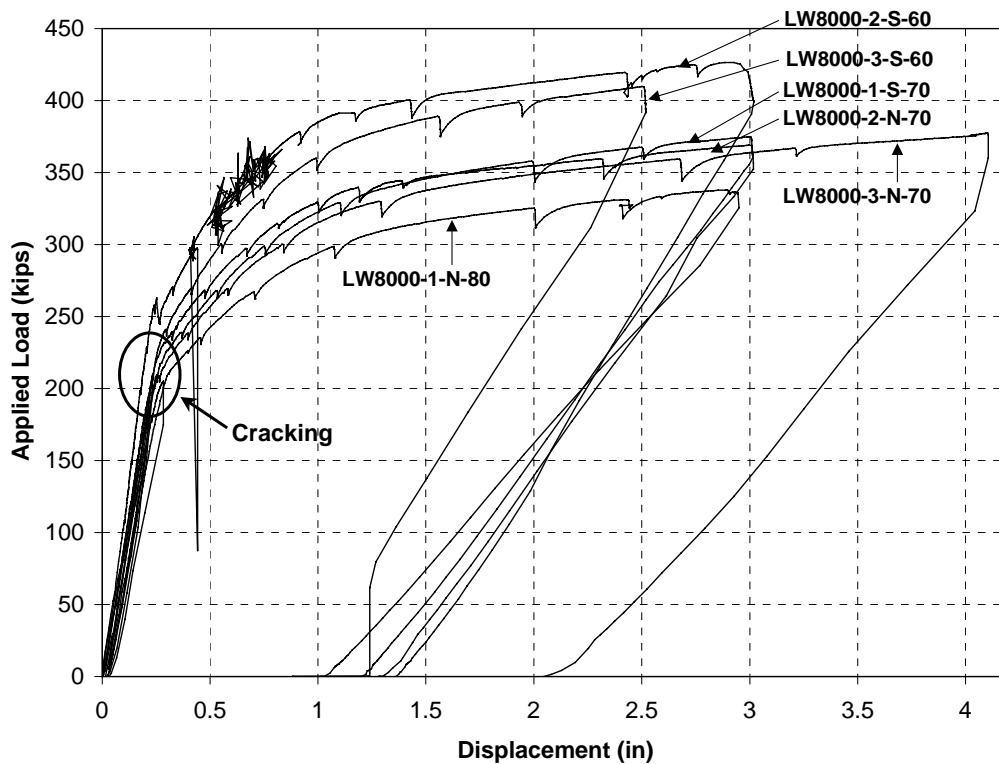
Figure 3.21 Displacement Comparison (Load)

3.3.1.3 Development Length Comparison

This subsection compares the tested embedment lengths with the calculated development lengths of the beams. The development lengths were calculated using several different methods. The results from these calculations are shown in Table 3.8, as well as the results of the development length testing. In every case, the calculated development length exceeded the actual development length of the beam. This was verified by testing each beam at a specified embedment length. The equation proposed by Mitchell [13] came the closest to the actual range of the development length, which was experimentally determined to be less than 60 in (1524 mm). It

should be noted that all of the methods shown were developed for normal weight concrete. The test results show that the equations are also valid for lightweight concrete. The Mitchell equation may come the closest, because it takes into account the square root of the compressive strength of the concrete. This has the same effect as taking into account the actual modulus of elasticity of the concrete, since an approximation of the modulus of elasticity is often calculated using a constant times the square root of the compressive strength.

Table 3.8 Development Length Comparison

Author	Development Length Equation	L_d LW8000 in / (mm)
ACI 318 / AASHTO [2,1]	$L_d = \left(f_{ps} - \dfrac{2}{3} f_{se} \right)$	86 (2,193)
Zia & Mostafa [18]	$L_d = L_t + 1.25(f_{pu} - f_{se})d_b$	92 (2,344)
Buckner (FHWA) [5]	$L_d = L_t + \lambda(f_{ps} - f_{se})d_b$	102 (2,601)
Mitchell [13]	$L_d = L_t + (f_{ps} - f_{se})d_b \sqrt{\dfrac{4.5}{f'_c}}$	68 (1,724)
Actual L_d	Determined from testing	< 60 < (1,524)

3.3.2 Support Spalling

This subsection discusses the support spalling that occurred during three of the 8000 psi (55.2 MPa) beam tests. The explanation for the formation of the support spalls is a topic for further study beyond this thesis. No clear correlation between

69

these local failure occurrences was found, and the ultimate load for the beam was not affected. No spalls occurred during the two tests of the lightweight beam with a normal weight deck. Spalls did occur during both tests on the lightweight beam with lightweight deck panels and a normal weight topping deck, but a spall occurred during only one of the tests on the lightweight beam with the full-depth lightweight deck. Therefore, no direct correlation between lightweight concrete decks and the formation of the spalls can be drawn. Kolozs presented a possible explanation for the formation of the spalls:

> "Due to the lower tensile strength of the lightweight concrete, it was theorized that the distributed load applied by the bearing pad put the flange of the beam into deep beam bending. Also, due to the curvature of the beam, the beam had to bear on less area as the load increased and therefore more stress was concentrated in a smaller area of the beam flange. The failure looked very similar to a split cylinder test. Once the stress exceeded the rupture stress, a crack was initiated and as the stress redistributed, it exceeded the cracking strength of the concrete and the crack unzipped along the length of the concrete in the flange of the support." [10]

If this theory were completely true, the spalling would have been expected to occur on all of the lightweight beam tests. Since this was not the case, an additional modification to the theory is presented here. It was possible that some longitudinal rotation, or torsion, developed as the beam deflected such large amounts. Whether it was due to an initial eccentricity in the load or merely due to the deflection of the beam is not critical. Due to this rotation, the bearing area of the end of the beam was decreased even more and the tensile stresses increased beyond the capacity of the lightweight concrete. This would account for the spalling that occurred in some of the tests and not in others, and always on only one side of the beam. Additionally, local imperfections in the bottom of the beam "as built" could account for the formation of the spalls. Again, further study of this matter is required before a

definitive answer can be provided, but the ultimate capacity of the composite beam was not affected by the local concrete spalling at the support.

3.3.3 Lightweight Deck Panels

This section discusses the use of the lightweight deck panels during this project. The panels presented no difficulty when placing them in the formwork. On a construction site, the panels will negate the need for such formwork. However, since only one beam was being tested at a time, formwork was needed in this study to support the panels' outside edges. The panels fit together well, and were easily managed by an overhead crane with one set of hands to direct the final placement.

During the testing, the panels behaved very well. Although the initial stiffness of the composite beam was lower, this was due to the use of lightweight concrete in the panels, and not the presence of the panels themselves. The full depth lightweight concrete deck exhibited an even lower initial stiffness than the deck with panels. The panels introduced a new form of crack propagation with the V-cracks discussed previously and shown in Figure 3.11. However, these cracks did not affect the ultimate strength of the beam. The spalling at the support occurred during both tests of the beam with the lightweight panels; however, the panels are not believed to be the cause of the spalling, as discussed previously.

Chapter 4: 6000 psi and 8000 psi Beam Test Results

4.1 INTRODUCTION

This chapter covers the testing of the nominal 6000 psi (41.4 MPa) beam series carried out by Kolozs [10], and the testing of the nominal 8000 psi (55.2 MPa) beam series carried out by the author. For the sake of comparison, many of the results from the 8000 psi (55.2 MPa) beam testing presented in Chapter 3 are reproduced in this chapter. Test results covering multiple categories of behavior are presented and compared, and the results are discussed.

4.2 TEST RESULTS

This section covers the results from the testing of both the 6000 psi (41.4 MPa) and 8000 psi (55.2 MPa) beam series. The material properties of the individual beams, decks, and panels are presented, followed by the results from the tests. The categories of behavior reported include initial stiffness, cracking and ultimate moment and load, strand elongation, maximum strain and displacement, crack patterns, strand slip, and failure types. A plot of the applied moment versus displacement of all six tests carried out by the author is shown in Figure 4.1, and a plot of the applied moment versus displacement of all six tests carried out by Kolozs is shown in Figure 4.2. These figures are shown to provide an overall perspective of the test results before the details are given. The curves show that the behavior of the six beams during the twelve tests was very similar, and the stiffnesses and moments achieved show good correlation of the data.
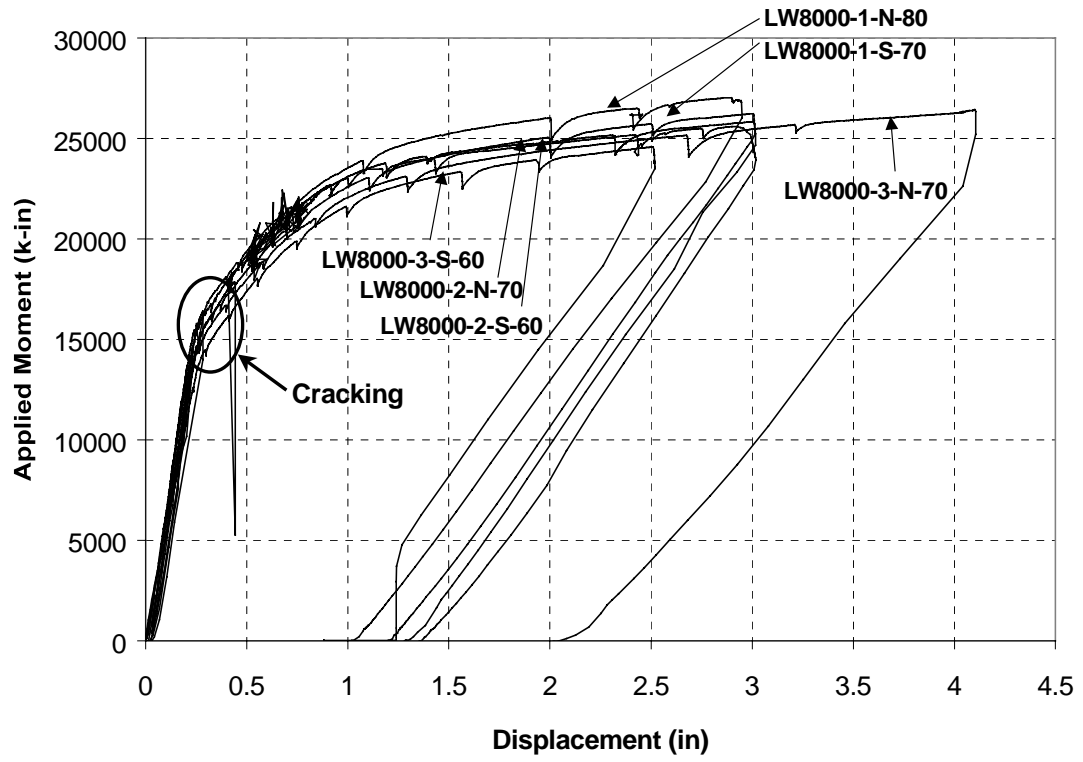
Figure 4.1 Initial Results - Thatcher

73
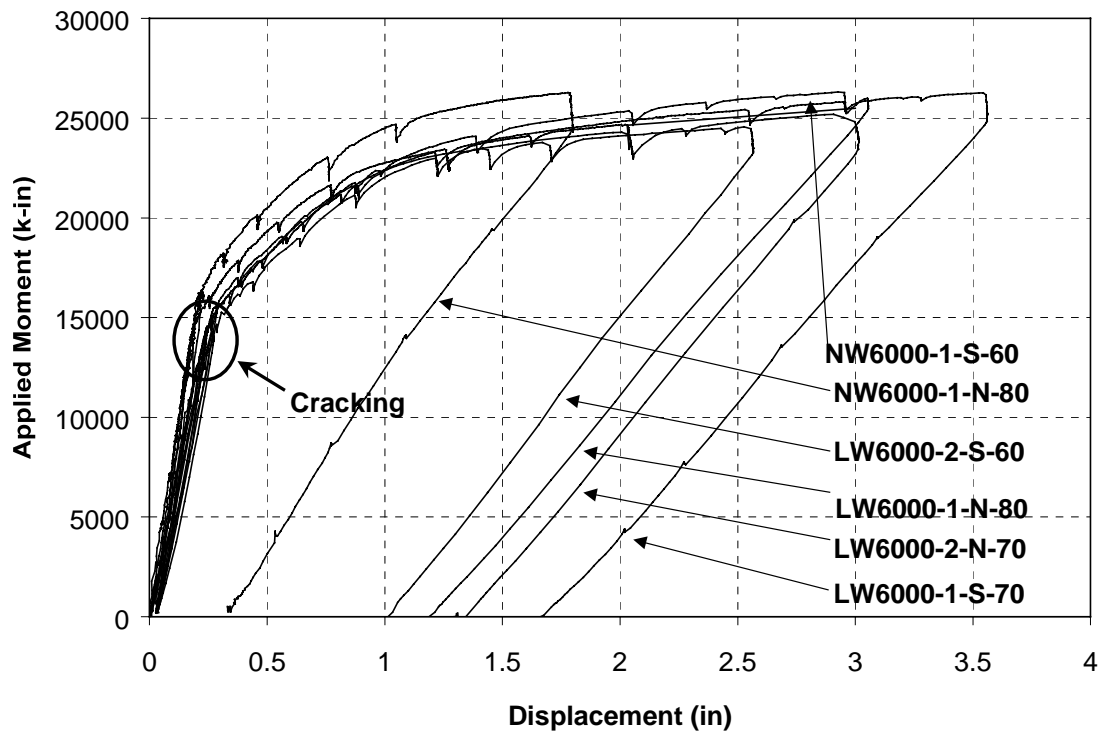
Figure 4.2 Initial Results - Kolozs

4.2.1 Beam Properties

The beams tested consisted of nominal 6000 psi (41.4 MPa) compressive strength normal weight concrete, nominal 6000 psi (41.4 MPa) compressive strength lightweight concrete, and nominal 8000 psi (55.2 MPa) compressive strength lightweight concrete. The beam properties are shown in Table 4.1. The normal weight beam had a normal weight cast-in-place concrete deck. Of the 6000 psi (41.4 MPa) lightweight concrete beams, the first had a normal weight cast-in-place concrete deck, and the second a combined deck of lightweight concrete panels and normal weight cast-in-place concrete. Of the 8000 psi (55.2 MPa) beams, the first had a normal weight cast-in-place concrete deck, the second a combined deck of

74

lightweight concrete panels and normal weight cast-in-place concrete, and the third a cast-in-place lightweight concrete deck.

Table 4.1 Beam Properties

Beam	Le	Beam Concrete Strength (psi)	Beam Modulus (ksi)	Deck Strength (psi)	Deck Modulus (ksi)	Panels	Panel Strength (psi)	Panel Modulus (ksi)
NW6000-1-N	80 in	6607	5742	5399	5335	No		
NW6000-1-S	60 in	6772	5335	5679	5076	No		
LW6000-1 N	80 in	8126	3253	5285	5335	No		
LW6000-1 S	70 in	8030	3253	5285	5335	No		
LW6000-2 N	70 in	8030	3253	4551	4486	Yes	7235	2539
LW6000-2 S	60 in	8030	3253	4551	4486	Yes	7235	2539
LW8000-1 N	80 in	6848	2576	5112	4803	No		
LW8000-1 S	70 in	6848	2576	5112	4803	No		
LW8000-2 N	70 in	7847	3141	5182	4453	Yes	7321	2680
LW8000-2 S	60 in	7847	3141	5182	4453	Yes	7321	2680
LW8000-3 N	70 in	8013	3104	7011	2511	No		
LW8000-3 S	60 in	8013	3104	7011	2511	No		

The actual strength of the normal weight pretensioned beam at the time of testing was well above (10%) the specified 6000 psi (41.4 MPa). The actual strength of the two lightweight 6000 psi (41.4 MPa) beams at the time of testing was significantly higher than the specified strength. The strength was above 8000 psi (55.2 MPa), an increase of 33%. The actual strength of the first of the three 8000 psi (55.2 MPa) beams at the time of testing was well below the specified 8000 psi (55.2 MPa) strength, the actual strength of the second was slightly below the specified 8000 psi (55.2 MPa) strength, while the third beam had an actual strength just above 8000 psi (55.2 MPa). These strengths are discussed in greater detail by Heffington [8].

The modulus of elasticity of the normal weight beam was significantly higher than the moduli of the lightweight beams, by about 100%. This was to be expected,

and was predicted in Section 1.2. The moduli of the 6000 psi (41.4 MPa) beams were determined to be approximately the same. The moduli of elasticity of the three 8000 psi (55.2 MPa) beams were relatively similar, with the second and third having roughly the same modulus, and the first having a lower modulus, corresponding to its lower strength. Overall, the moduli of elasticity of the lightweight beams were very similar, with the exception of the first 8000 psi (55.2 MPa) beam, which had a lower compressive strength.

The strengths of the normal weight concrete decks were very similar, as well as the normal weight concrete used in LW8000-2 with the panels, and were close to the specified 5000 psi (34.5 MPa) strength. The strength of the normal weight concrete deck on LW6000-2 was a bit lower than the other decks. The lightweight concrete used for the deck on LW8000-3 was specified to be 5000 psi (34.5 MPa) strength, but when tested was up to 7000 psi (48.3 MPa).

The moduli of elasticity of the normal weight cast-in-place concrete decks were similar in both the 6000 psi (41.4 MPa) beams and the 8000 psi (55.2 MPa) beams, while the modulus of the deck concrete on LW6000-2 was lower, and the modulus of the lightweight concrete cast-in-place deck on LW8000-3 was significantly less than the other decks, but similar to that of the lightweight beams. The lightweight concrete panels had achieved a strength of approximately 7000 psi (48.3 MPa) when the beam was tested, with a modulus similar to that of the full-depth cast-in-place lightweight concrete deck.

The unit weights of the beams with various deck components were discussed previously in Section 3.2.1. The figure from that Section is reproduced here as Figure 4.3, with black indicating lightweight concrete.

76
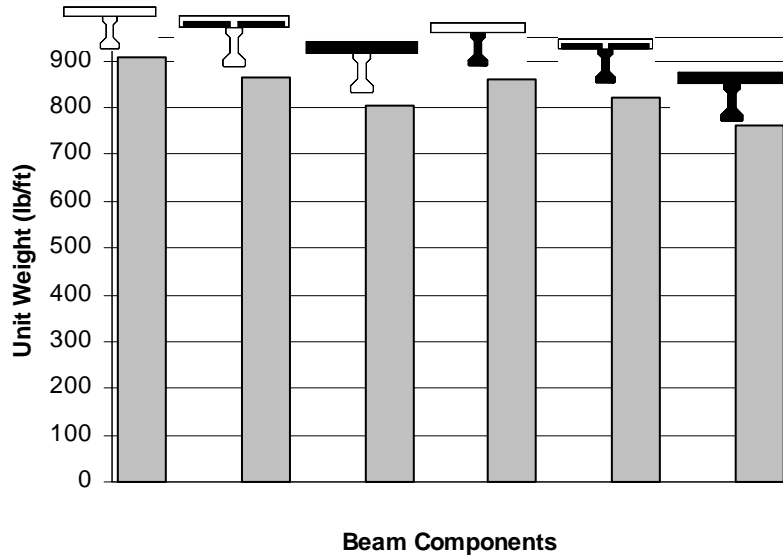
Figure 4.3 Unit Weight

The twelve tests took place at three different embedment lengths in order to experimentally determine the development length of the beams. These ranged from 80 to 60 in (2032 to1524 mm), with a similar length repeated between beams in order to allow correlation of the test data from the different beams. The normal weight beam was tested at the two bounds of embedment length testing, 80 and 60 in (2032 to 1524 mm), in order to bracket the testing of the lightweight beams.

4.2.2 Initial Stiffness

The initial stiffnesses of the beams during each test are presented in this subsection. The stiffnesses calculated from the geometry of the cross section and the modulus of elasticity of the concrete are shown in Table 4.2 and Figure 4.4, as well as the stiffnesses observed during the testing of the beams. The impact of the elastic

77

modulus of the concrete on the initial stiffness was discussed in Section 3.2.2. The composite beams tested had varying components of lightweight concrete. One was a normal weight beam with a normal weight deck. Of the five lightweight beams, the amount of lightweight concrete in the deck varied. This is indicated by the figures above each pair of columns in Figure 4.4, with lightweight concrete indicated by the black portions of the cross section.

Table 4.2 Initial Stiffness

Beam ID	Modulus of Elasticity (ksi)			Moment of Inertia (in^4) Transformed to E_{beam}	Calculated Stiffness ($k\text{-}in^2$)	Measured Stiffness ($k\text{-}in^2$)
	E_{beam}	E_{Deck}	E_{Panel}			
NW6000-1-N-80	5742	5335		102,202	5.87E+08	1.39E+09
NW6000-1-S-60	5335	5076		102,769	5.48E+08	1.23E+09
LW6000-1-N-80	3253	5335		120,272	3.91E+08	1.03E+09
LW6000-1-S-70	3253	5335		120,272	3.91E+08	1.07E+09
LW6000-2-N-70	3253	4486	2539	111,119	3.61E+08	1.60E+09
LW6000-2-S-60	3253	4486	2539	111,119	3.61E+08	1.14E+09
LW8000-1-N-80	2576	4803		125,979	3.25E+08	1.26E+09
LW8000-1-S-70	2576	4803		125,979	3.25E+08	1.22E+09
LW8000-2-N-70	3141	4453	2680	112,019	3.52E+08	---
LW8000-2-S-60	3141	4453	2680	112,019	3.52E+08	8.32E+08
LW8000-3-N-70	3104	2511		99,147	3.08E+08	1.03E+09
LW8000-3-S-60	3104	2511		99,147	3.08E+08	8.03E+08

Figure 4.4 Initial Stiffness

The results of the testing indicate that the expectation of slightly lower initial stiffness for increased percentage of lightweight components in the cross section was generally true. However, the relative effect was small when considering the magnitude of the values. Again, for the tests on LW8000-1, the lower modulus of elasticity colors the data, as discussed in Section 3.2.2. All of the beams had relatively similar initial stiffnesses, and show good correlation of the test data. The reduced stiffness of lightweight concrete should not be a significant problem on pretensioned girder applications.

4.2.3 Cracking and Ultimate Moment and Load

The cracking and ultimate moments are shown in Figure 4.5. The ultimate moments are relatively the same for all of the tests, as was expected due to the similarity in the beams being tested. The cracking moments show some significant

79

difference. This is likely largely due to the difficulty in observing the exact onset of flexural cracking in the beam during testing.
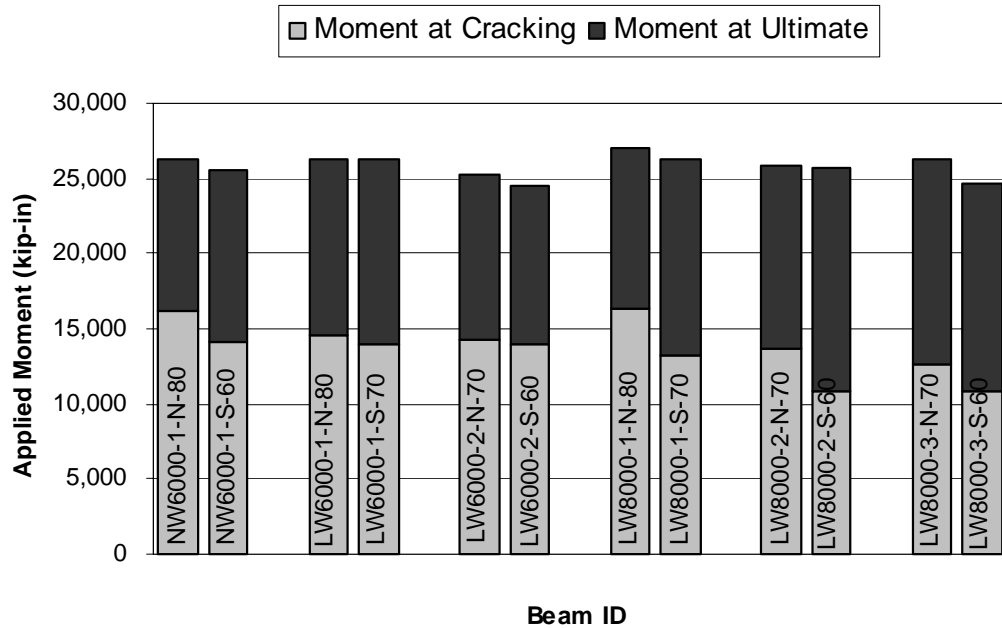
Figure 4.5 Cracking and Ultimate Moments

The cracking and ultimate loads are shown in Figure 4.6, and are grouped according to the embedment length tested. The cracking loads were similar within embedment length groups, except for the NW6000 beam that had a higher cracking moment due to its higher tensile strength than that of the lightweight beams. The ultimate loads are also shown in Figure 4.6. Within groups, the ultimate loads are similar, with some slightly higher than others due to the subjective decision as to when to stop the test and declare an ultimate condition.
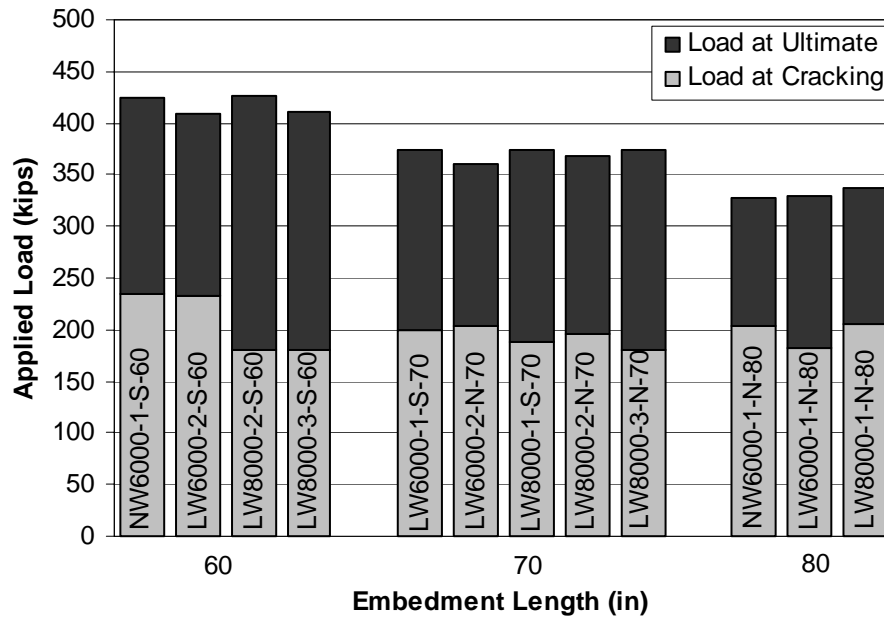
Figure 4.6 Cracking and Ultimate Loads

4.2.4 Strand Elongation

The elongation of the strands at ultimate is presented in this subsection. The strand elongation was calculated for the bottom layer of strands in the beams. The values were obtained assuming a linear strain distribution in the composite beams. The depth of the cracking in the deck was observed visually, and the maximum strains in the deck above the web due to the load were measured. The strain in the steel was then calculated from the deck strain and the geometry of the cross section. This was added to the strain already present in the strands due to prestressing and subsequent losses. From this final strain in the steel strands, the elongation was calculated. The results are given in Table 4.3 and shown in Figure 4.7. The data of

LW8000-2-N-70 is incomplete, due to problems with the strain gages during that
particular test.

Table 4.3 Strand Elongation

| Beam ID	L_e in (mm)	Depth of Cracking at Ultimate, in / (mm)	Concrete Strain at Top, microstrain	Strand Elongation (%)
NW6000-1-N	80 (2,032)	2.7 (68)	2,033	2.9
NW6000-1-S	60 (1,524)	3.0 (77)	2,688	3.3
LW6000-1-N	80 (2,032)	2.5 (64)	4,349	6.0
LW6000-1-S	70 (1,778)	2.8 (71)	3,266	4.2
LW6000-2-N	70 (1,778)	1.9 (48)	3,462	6.4
LW6000-2-S	60 (1,524)	1.4 (37)	4,015	9.6
LW8000-1-N	80 (2,032)	2.9 (74)	3,650	4.5
LW8000-1-S	70 (1,778)	2.5 (64)	2,732	4.0
LW8000-2-N	70 (1,778)	2.5 (64)	---	---
LW8000-2-S	60 (1,524)	2.5 (64)	3,061	4.4
LW8000-3-N	70 (1,778)	2 (51)	3,711	6.5
LW8000-3-S	60 (1,524)	2.5 (64)	3,646	5.1
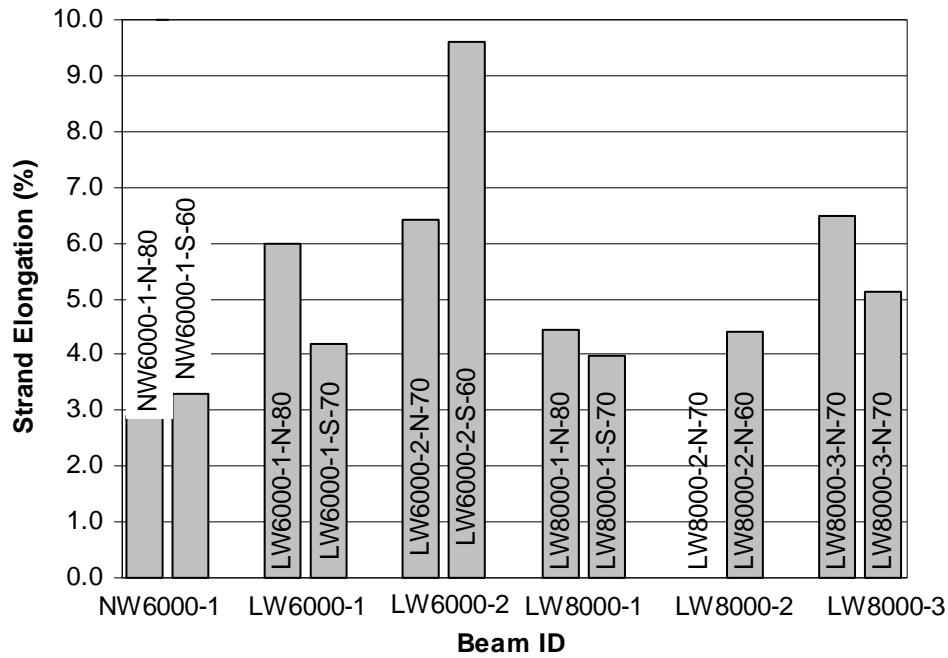
Figure 4.7 Strand Elongation

Yielding of the strands will occur at around 1% elongation, and the percentage strain in the strands at ultimate for each of the tests was substantially higher than that value. Between 1% and 4% elongation, the individual strand will undergo an increase in load of 2.3 kips. The large yielding of the strands at ultimate is an indication that the flexural ultimate load was actually reached, since after yielding of the strands, further increases in strain occur without significant increases in stress, or load level. Only one of the strands slipped during the testing of the beams, LW6000-2-S-60, and the likely cause of the slip was suggested by Kolozs to be form oil accidentally placed on the strand when the beam was cast. [10]

4.2.5 Maximum Strain and Displacement

The average measured strains and maximum deflections are given in Table 4.4. Due to shear lag across the deck, the average of the strain gage readings was used. The data of LW8000-2-N-70 is incomplete, due to problems with the strain gages during that particular test. The maximum deflections were taken at the midpoint of the constant moment region in the beam.

Table 4.4 Strains and Deflections

Beam	Le	Maximum Load (kips)	Average Strain (microstrain)	Maximum Deflection (in)
NW6000-1 N	80 in	328	1697	1.8
NW6000-1 S	60 in	425	2105	3.0
LW6000-1 N	80 in	329	2755	3.0
LW6000-1 S	70 in	375	2824	3.5
LW6000-2 N	70 in	360	2958	2.9
LW6000-2 S	60 in	409	2651	2.5
LW8000-1 N	80 in	335	2695	2.9
LW8000-1 S	70 in	375	1984	3.0
LW8000-2 N	70 in	365	---	3.0
LW8000-2 S	60 in	425	2208	2.9
LW8000-3 N	70 in	375	3400	4.0
LW8000-3 S	60 in	410	2590	2.5

Plots of the applied moment vs. average microstrain across the top of the deck for each test are shown in Figures 4.8 and 4.9, for both the author's and Kolozs' test data [10]. The curves show similar behavior from all six tests within a beam series, as well as those carried out by the author versus those carried out by Kolozs. Plots of the applied load vs. average microstrain across the top of the deck for each test are shown in Figures 4.10 and 4.11, for both the author's and Kolozs' test data [10]. The

curves for tests of the same embedment length show similar behavior, as do the tests carried out by the author versus those carried out by Kolozs. Individual plots of the load vs. microstrain readings for each test are displayed in Appendix D.
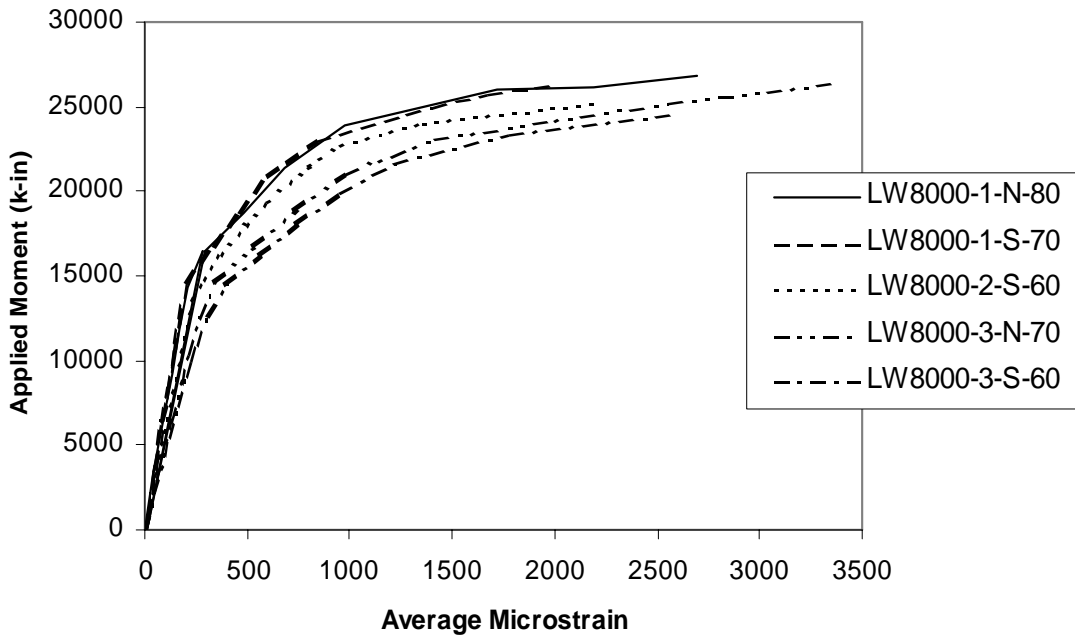
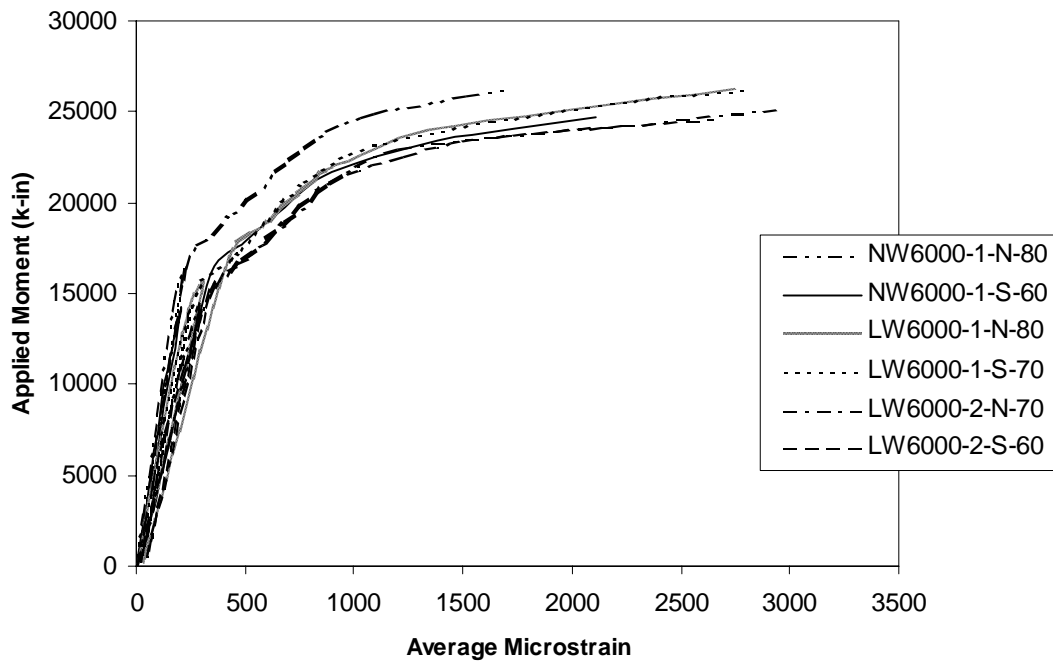**Figure 4.8 Applied Moment vs. Average Microstrain - Thatcher**

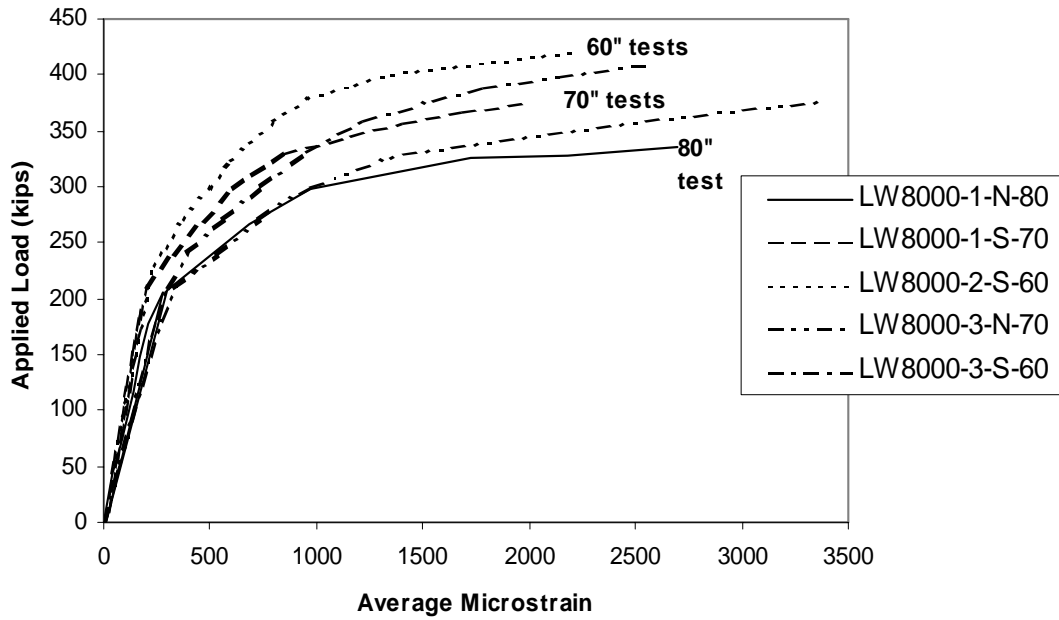**Figure 4.9 Applied Moment vs. Average Microstrain - Kolozs**

Figure 4.10 Applied Load vs. Average Microstrain - Thatcher
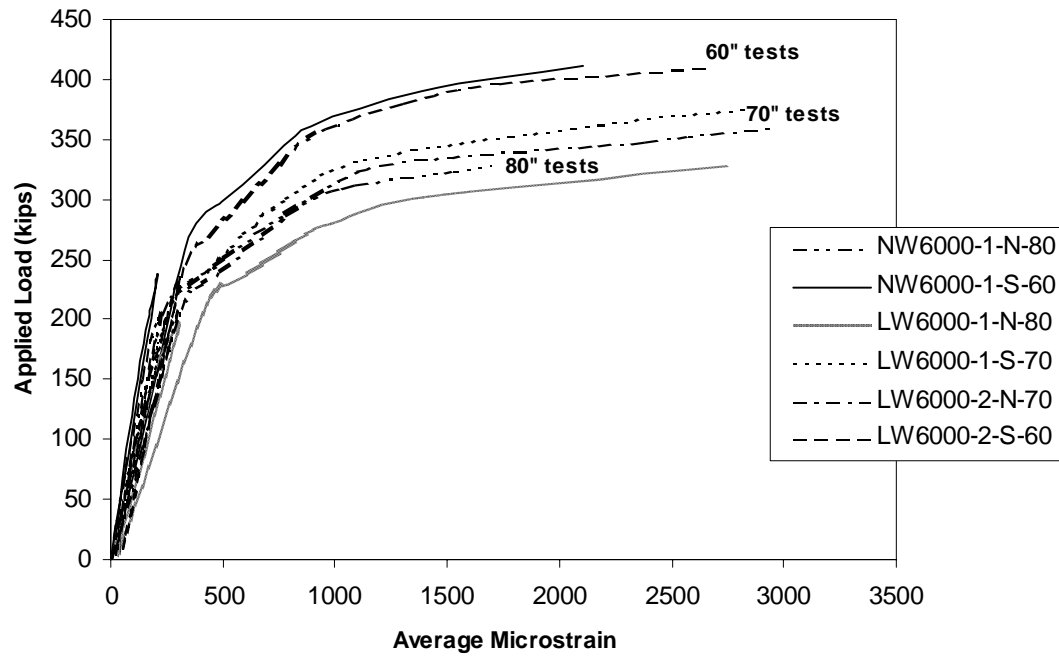
Figure 4.11 Applied Load vs. Average Microstrain - Kolozs

87

The ultimate deflections are shown in Figure 4.12. The deflections achieved were similar for all tests, since a deflection of approximately 3 in (76.2 mm) was used as one of the criteria for stopping the test procedure. The tests on LW6000-1-S-70 and LW8000-3-N-70 were pushed to a further limit to observe deck crushing and load pickup at high levels of strain. The initial test on NW6000-1-N-80 was stopped earlier due to inexperience and safety concerns, and the test on LW8000-3-S-60 was stopped due to high strains.

Figure 4.12 Ultimate Deflections

4.2.6 Crack Patterns

The crack patterns developed during the testing procedure were discussed in Section 3.2.7, and were similar for all twelve tests.

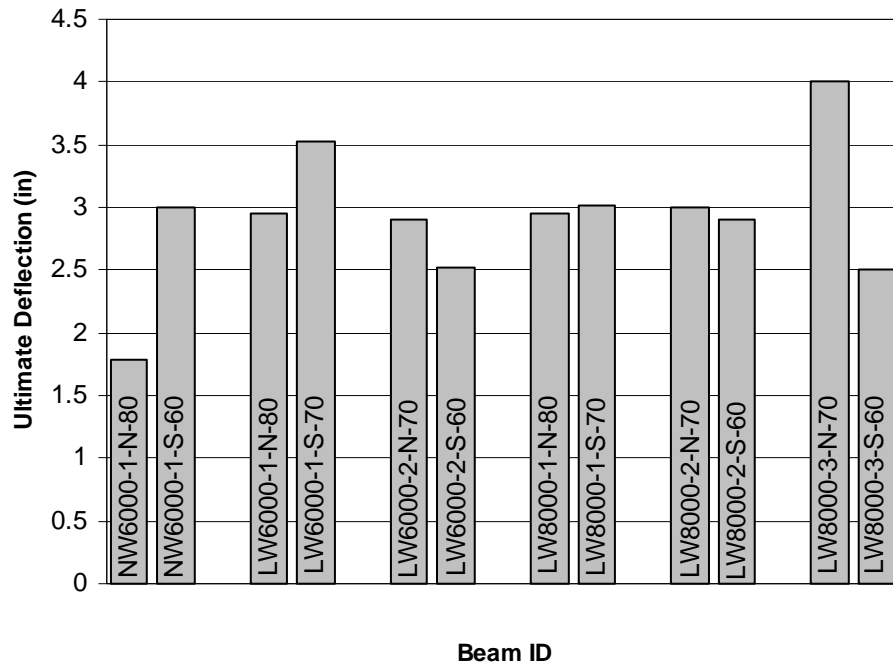### 4.2.7 Strand Slip

One strand slipped during the testing of the 6000 psi (41.4 MPa) beam series, and was discussed in Section 4.2.5. No strand slips occurred during the testing of the 8000 psi (55.2 MPa) beam series. For each of the tests excluding the slip case, the measured slip was less than 0.01 in (0.25 mm), which can be attributed to electronic noise in the data acquisition equipment. A slip of a strand would have indicated a bond failure, which would have established that the development length required was greater than the embedment length being tested. However, since none of the strands slipped, their full strength was developed. Therefore, the development length is some distance less than the minimum embedment length tested. The results are shown in Table 4.5.

Table 4.5 Strand Slip

Beam ID	Embedment Length, in / (mm)	Maximum Strand Slip, in / (mm)
NW6000-1-N-80	80 (2,032)	< 0.01 < (0.25)
NW6000-1-S-60	60 (1,524)	< 0.01 < (0.25)
LW6000-1-N-80	80 (2,032)	0.3 (7.62)
LW6000-1-S-70	70 (1,778)	< 0.01 < (0.25)
LW6000-2-N-70	70 (1,778)	< 0.01 < (0.25)
LW6000-2-S-60	60 (1,524)	< 0.01 < (0.25)
LW8000-1-N-80	80 (2,032)	< 0.01 < (0.25)
LW8000-1-S-70	70 (1,778)	< 0.01 < (0.25)
LW8000-2-N-70	70 (1,778)	< 0.01 (7.62)
LW8000-2-S-60	60 (1,524)	< 0.01 < (0.25)
LW8000-3-N-70	70 (1,778)	< 0.01 < (0.25)
LW8000-3-S-60	60 (1,524)	< 0.01 < (0.25)

4.2.8 Failure Types

Several types of failure were observed during the testing of the 6000 psi (41.4 MPa) and 8000 psi (55.2 MPa) beams, and are presented in this subsection. They are listed in Table 4.6. All of the beams were tested to some form of flexural failure; however, the exact manifestation of the failure varied for each beam and each test. The failure state was limited to a flexural one by the design of the beam, which

included heavy shear reinforcement to ensure such a failure, as discussed previously in Section 2.2.4. The criterion for a flexural failure varied somewhat for each test, but was generally one of high deflection or strain in the beam at ultimate load.

Table 4.6 Types of Failure

Beam ID	Type of Failure
NW6000-1-N-80	Flexural Failure
NW6000-1S-60	Flexural Failure, Deck Crack Initiation
LW6000-1-N-80	Flexural Failure, Deck Crack Initiation
LW6000-1-S-70	Flexural Failure, Strand Slip, Deck Crack
LW6000-2-N-70	Flexural Failure, Complete Deck Crack, V-Crack, Spalling at Support in Beam Flange
LW6000-2-S-60	Flexural Failure, Deck Cracking Initiation, V-Crack, Spalling at Support in Beam Flange
LW8000-1-N-80	Flexural Failure
LW8000-1-S-70	Flexural Failure
LW8000-2-N-70	Flexural Failure, V-Crack, Spalling at Support in Beam Flange
LW8000-2-S-60	Flexural Failure, Complete Deck Crack, V-Crack, Spalling at Support in Beam Flange
LW8000-3-N-70	Flexural Failure, Deck Cracking Initiation
LW8000-3-S-60	Flexural Failure, Complete Deck Crack, Spalling at Support in Beam Flange

The various modes of failure were discussed previously in Section 3.2.8. The modes of failure introduced during the testing of the 6000 psi (41.4 MPa) beams were similar to those of the 8000 psi (55.2 MPa) beams, as Table 4.5 shows.

4.2.9 Support Spalling

Five of the twelve tests had support spalling prior to ultimate. This condition was not considered to be an ultimate condition, since the ultimate load of the beam was not affected by the formation of the spall. The spalls were very similar in appearance in all five tests, and occurred on only one side of the beam in each case. They are shown in Figures 3.17, 3.18, and 3.19 in Section 3.2.9.

The load at which the spall occurred is shown in Figure 4.13 as a ratio of the spalling load relative to the cracking load. The first time the spall occurred, when testing LW6000-2-N-70, the test was stopped. On future tests, the loading was continued after the spall was noted and measured. For LW6000-2-S-60, the spall occurred at 97% of the ultimate load during the test. For LW8000-2-N-70 and LW8000-3-S-60, the spall occurred at 92% and 98%, respectively, of the ultimate load during the test. For LW8000-2-S-60, the spall occurred at 75% of the ultimate load during the test, but the ultimate load was not affected by the formation of the spall. Again, the occurrence of the spall in each of the cases was at a load level at least twice the service load level with dead equal to live, and at least three times the service load level with dead equal to twice live. An explanation of the formation of the support spalls was discussed in Section 3.3.2, and will be readdressed in Section 4.3.2.
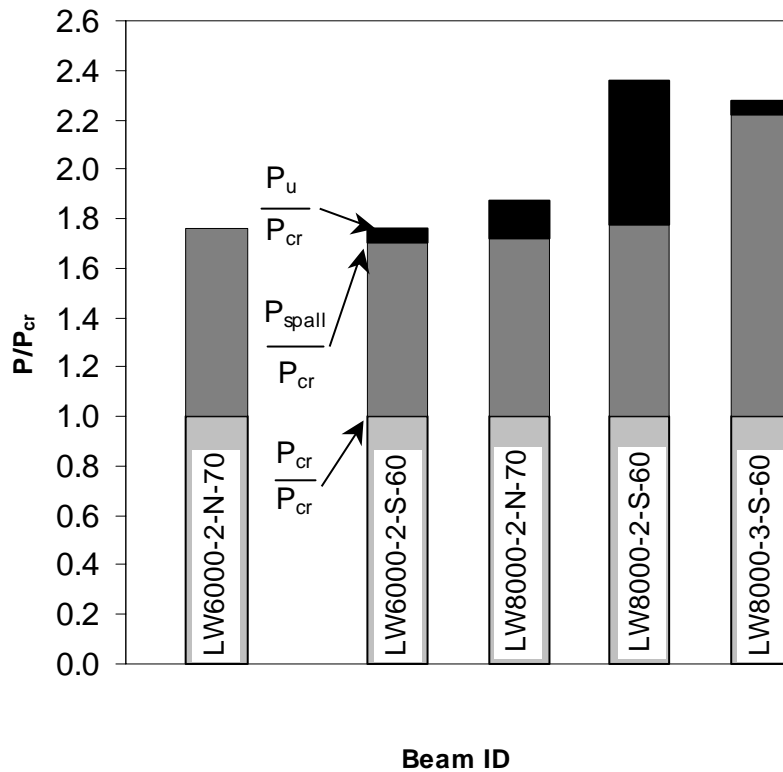
Figure 4.13 Support Spalling Loads

4.3 DISCUSSION

This section presents a discussion of the results of the 6000 psi (41.4 MPa) and 8000 psi (55.2 MPa) beam tests. The test results are discussed, a theory for the formation of the support spalls is reexamined, and behavior observed with the use of the lightweight panels is discussed.

4.3.1 Test Results

This subsection compares the results obtained from the testing of the 6000 psi (41.4 MPa) and 8000 psi (55.2 MPa) beams.

4.3.1.1 Moment Comparison

Two methods of calculating the theoretical moment capacity were used: the AASHTO STANDARD Method, the Whitney Stress Block method, and the Stress Block Factors Method [6]. A factor of $\phi = 1.0$ was used in each method. All of these methods are based on the assumption of strain compatibility and give virtually identical results for these beams. The results of these calculations are shown in Table 4.7, as well as the ultimate moment achieved by the beams during testing. This moment includes both the applied moment and the moment in the beam due to prestressing. The ultimate-to-calculated moment ratios are shown as well, and demonstrate substantial correlation between test groups.

Table 4.7 Moment Comparison

Beam ID	AASHTO Standard, k-in (kN-mm)	Whitney Stress Block, k-in (kN-mm)	Stress Block Factors, k-in (kN-mm)	Ultimate Moment, k-in (kN-mm)	Ultimate / Calculated
NW6000-1-N-80	14,788 (2,609)	14,850 (2,620)	14,870 (2,623)	16,500 (2,911)	1.11
NW6000-1-S-60	14,829 (2,616)	14,890 (2,627)	14,900 (2,628)	16,800 (2,964)	1.13
LW6000-1-N-80	14,773 (2,606)	14,830 (2,616)	14,850 (2,620)	16,500 (2,911)	1.11
LW6000-1-S-70	14,773 (2,606)	14,830 (2,616)	14,850 (2,620)	17,000 (2,999)	1.15
LW6000-2-N-70	14,654 (2,585)	14,860 (2,621)	14,870 (2,623)	16,300 (2,875)	1.10
LW6000-2-S-60	14,654 (2,585)	14,860 (2,621)	14,870 (2,623)	16,200 (2,858)	1.09
Averages	**14,745 (2,601)**	**14,853 (2,620)**	**14,868 (2,620)**	**16,550 (2,900)**	**1.12**
LW8000-1-N-80	14,743 (2,601)	14,800 (2,611)	14,820 (2,614)	17,900 (123,421)	1.21
LW8000-1-S-70	14,743 (2,601)	14,800 (2,611)	14,820 (2,614)	18,200 (125,489)	1.23
LW8000-2-N-70	14,758 (2,603)	14,810 (2,612)	14,830 (2,616)	17,900 (123,421)	1.21
LW8000-2-S-60	14,758 (2,603)	14,810 (2,612)	14,830 (2,616)	18,400 (126,868)	1.24
LW8000-3-N-70	14,964 (2,640)	15,050 (2,655)	15,060 (2,657)	18,100 (124,800)	1.20
LW8000-3-S-60	14,964 (2,640)	15,050 (2,655)	15,060 (2,657)	17,600 (121,352)	1.17
Averages	**14,822 (2,615)**	**14,887 (2,626)**	**14,903 (2,620)**	**18,017 (2,900)**	**1.21**

The ultimate moment achieved by the beams exceeded the theoretical calculated moment in the 6000 psi (41.4 MPa) tests by an average of 12%, and in the 8000 psi (55.2 MPa) tests by an average of 21%. These differences are due to the conservative nature of the design theory and possibly a higher ultimate stress in the strand than the reported 270 ksi. The difference between the two groups of tests is

due to the increased experience of the author when carrying out the tests to a further degree of ultimate before terminating the loading.

4.3.1.2 Displacement Comparison

This subsection compares the deflections of the beams during all twelve tests. The plots of applied moment versus deflection are shown in Figures 4.14 and 4.15., with all six tests plotted together in order to show direct comparisons. Data from the author's testing is presented in Figure 4.14, and data from the testing carried out by Kolozs is presented in Figure 4.15. The figures show that the applied moment vs. deflection for all of the tests was very similar, except for NW6000-1-N-80, which was stopped early for safety concerns due to being the first test, and LW8000-3-N-70, which was pushed further in order to observe additional crushing behavior in the deck.
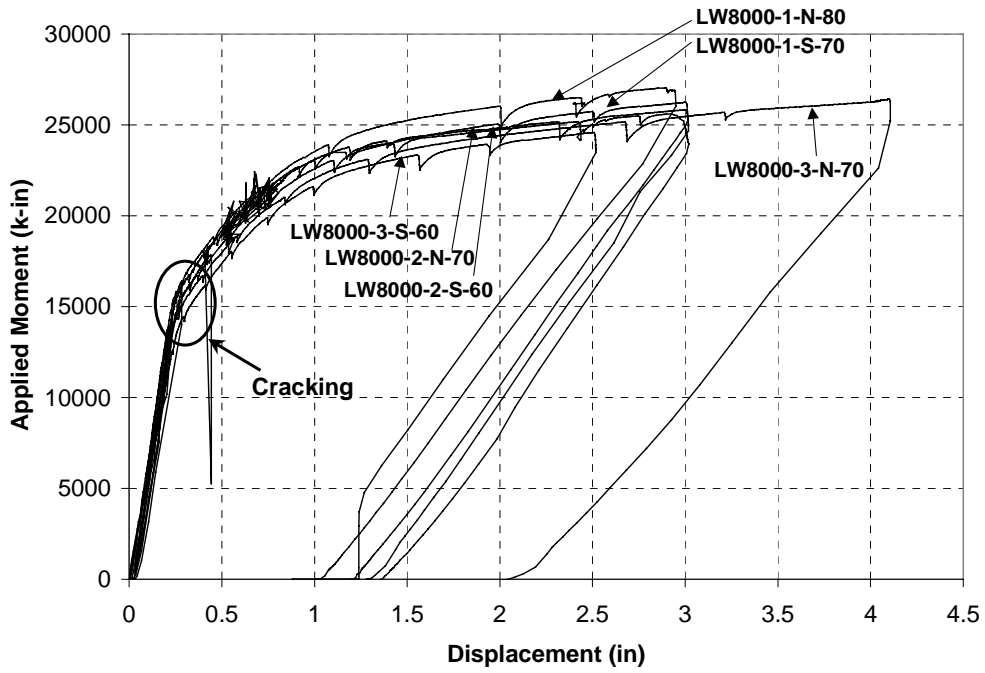
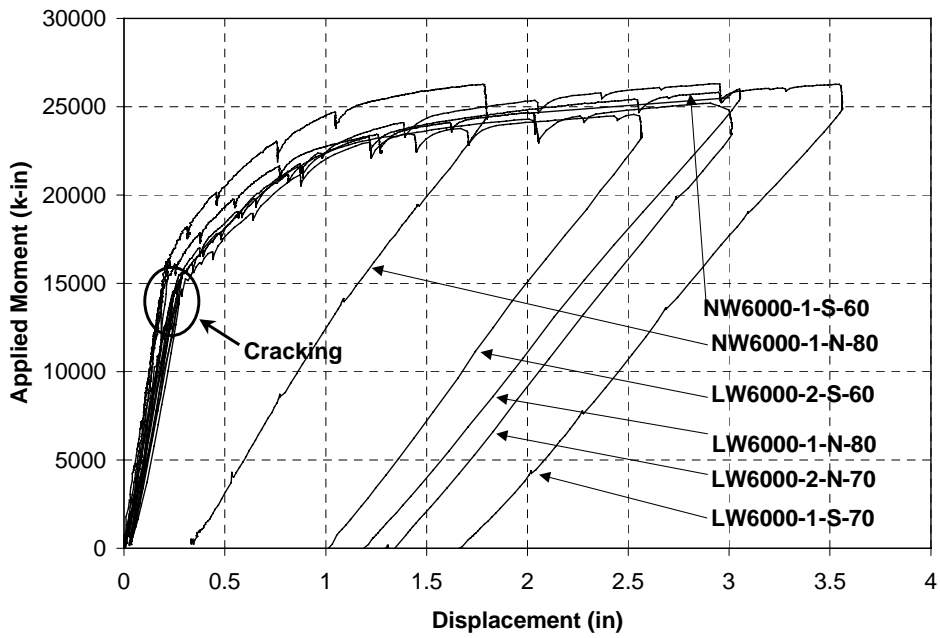**Figure 4.14 Displacement Comparison (Moment) - Thatcher**

Figure 4.15 Displacement Comparison (Moment) – Kolozs

97

The plots of applied load versus deflection are shown in Figure 4.16 and 4.17, with all the group tests plotted together in order to show direct comparisons. Individual plots of the load versus deflection for each test are displayed in Appendix C. Except for the difference in initial stiffness due to the differing compositions of the decks, the plots for tests of the same embedment length show similar behavior. The 80, 70, and 60 in (2032, 1778, and 1524 mm) tests all show similar behavior for the same embedment length tested.
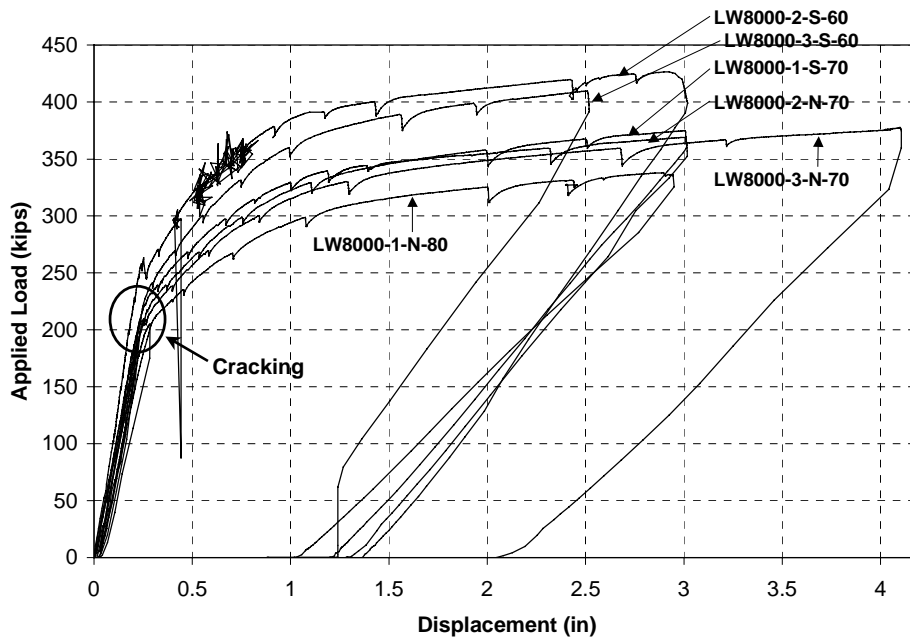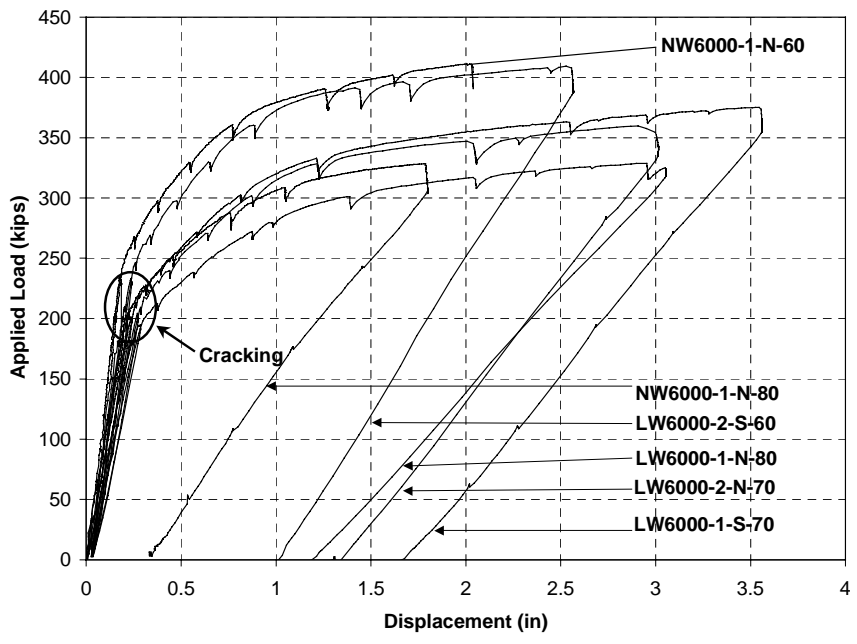
Figure 4.16 Displacement Comparison (Load) - Thatcher

Figure 4.17 Displacement Comparison (Load) - Kolozs

99

4.3.1.3 Development Length Comparison

This subsection compares the tested embedment lengths with the calculated development lengths of the beams. The development lengths were calculated using several different methods. The results from these calculations are shown in Table 4.8, as are the results of the development length testing. In all twelve tests, the calculated development length exceeded the actual development length of the beam. Again, the equation proposed by Mitchell [13] comes the closest to the actual range of the development length, which was experimentally determined to be less than 60 in (1524 mm).

Table 4.8 Development Length Comparison

Author	Development Length Equation	L_d NW6000 in / (mm)	L_d LW6000 in / (mm)	L_d LW8000 in / (mm)
ACI 318 / AASHTO [2,1]	$L_d = \left(f_{ps} - \frac{2}{3} f_{se} \right)$	82 (2,091)	86 (2,193)	86 (2,193)
Zia & Mostafa [18]	$L_d = L_t + 1.25(f_{pu} - f_{se})d_b$	88 (2,246)	92 (2,328)	92 (2,344)
Buckner (FHWA) [5]	$L_d = L_t + \lambda(f_{ps} - f_{se})d_b$	78 (1,984)	104 (2,630)	102 (2,601)
Mitchell [13]	$L_d = L_t + (f_{ps} - f_{se})d_b \sqrt{\dfrac{4.5}{f'_c}}$	69 (1,753)	67 (1,694)	68 (1,724)
Actual L_d	Determined from testing	< 60 < (1,524)	< 60 < (1,524)	< 60 < (1,524)

100

4.3.2 Support Spalling

This subsection discusses the support spalling that occurred during five of the test procedures. This topic was addressed in some detail in Section 3.3.2, and will be revisited here briefly. Again, the explanation for the formation of the support spalls is a topic for further study beyond this thesis. No direct correlation between lightweight concrete decks and the formation of the spalls could be drawn. A possible explanation for the formation of the spalls was presented by Kolozs [10], and is included in Section 3.3.2. A modification to the theory was introduced in Section 3.3.2. Examining the results from all of the tests did not provide any additional observations beyond those already discussed. Kolozs found no spalls in the testing of the normal weight beam, and this would be consistent with the theory previously discussed. Again, further study of this matter is required before a definitive answer can be provided, but the ultimate capacity of the composite beam was not affected by the local concrete spalling at the support.

4.3.3 Lightweight Deck Panels

The panels' use during construction, as well as their performance during testing, was discussed in Section 3.3.3. Kolozs' use of the panels during the 6000 psi (41.4 MPa) tests produced similar results in terms of ease of use and performance. Overall, the panels were found to be both useful and behaviorally satisfactory.

Chapter 5: Summary and Conclusions

5.1 INTRODUCTION

This chapter covers the summary and conclusions derived from the nominal 6000 psi and 8000 psi concrete strength beam test results. A summary of the results is presented, followed by conclusions drawn. Finally, recommendations are made in Section 5.3.2.

5.2 SUMMARY

The objective of Project 0-1852 is to examine the feasibility of using high performance lightweight concrete in prestressed bridge girders in Texas. The use of prestressed lightweight concrete panels as bridge deck formwork was also included in the project. This thesis draws conclusions from the results of the testing program carried out in Project 0-1852.

The manufacture of the test beams was discussed in Section 2.2. The beams were produced at Heldenfel's Prestressing Plant in San Marcos, Texas. The beams were precast pretensioned lightweight concrete with 12 – ½ in (12.7 mm) diameter, Grade 270 ksi (1,861 MPa), low-relaxation steel strands. After the forms were removed and the transfer length instrumentation was in place, the beams were brought to Ferguson Structural Engineering Laboratory of The University of Texas at Austin for testing. The setup of the testing program was outlined in Section 2.3, and the actual test procedure was presented in Section 2.4.

The project's four main aspects were the lightweight concrete, the transfer length of the beams, the development length of the beams, and the use of prestressed lightweight concrete panels. These four aspects are examined in greater detail in the follow subsections.

5.2.1 Lightweight Concrete

The concrete mixes used in the manufacture of the test beams were developed by Heffington and Kolozs, and reported by Heffington [8]. The normal weight concrete mix was designed to be of nominal 6000 psi compressive strength. The lightweight concrete mixes were designed to be of nominal 6000 psi compressive strength and nominal 8000 psi compressive strength, respectively. The unit weight of the resulting lightweight concrete from the mix was required to fall between 118-122 lb/ft^3 (1,864-1,928 kg/m^3). The properties of the mixes are shown in Table 5.1.

Table 5.1 Concrete Properties

Beam ID	Compressive Strength (f'$_c$), psi / (MPa)		Unit Weight lb/ft^3 / (kN/m^3)
	1-day	Long Term	
NW6000	3,490 (24.1)	5,500 (37.9)	149 (23.4)
LW6000	4,900 (33.8)	8,130 (56.1)	118 (18.5)
LW8000	5,560 (38.3)	7,850 (54.1)	122 (19.2)

The manufacture of the beams with lightweight concrete took place without special consideration by the plant workers. No significant problems were experienced that might not come about from the use of normal weight concrete.

103

5.2.2 Transfer Length

The transfer lengths of the beams were tested and examined by Kolozs [10], and were beyond the scope of this thesis. He found the transfer length for all beams to be less than that predicted by AASHTO and ACI equations.

5.2.3 Development Length

Testing the beams at a certain embedment length and observing the type of failure that occurred allowed the development length of the beams under consideration to be approximated. A flexural failure with no indication of bond failure at a particular embedment length indicated that the development length of the beam was less than that tested. A range of embedment length tests, from 80 in (2032 mm) down to 60 in (1524 mm), was performed in order to isolate the approximate development length of the beams.

The beams were instrumented in order to record various types of behavior during the testing process. Concrete strain, horizontal and vertical deflections at the supports, vertical deflections of the beam at the load points, strand slip, and applied load were all measured and recorded. The clearest measurement of bond failure would be from the potentiometers used to measure strand slip. Because the number of beam tests performed was limited the fact that no bond failures occurred at the shortest embedment length of 60 in (1524 mm) indicates the actual development length was some value less than 60 in (1524 mm).

The embedment length, maximum strand slip, development length upper bound, as well as the ultimate moment developed in the beams, are collectively reported in Table 5.2

Table 5.2 Development Length Summary

Beam ID	Embedment Length, in / (mm)	Maximum Strand Slip, in / (mm)	Development Length Upper Bound, in / (mm)	Ultimate Moment, k-in / (kN-mm)	Actual / Predicted Ultimate Moment
NW6000-1-N-80	80 (2,032)	< 0.01 < (0.25)	< 60 < (1,524)	16,500 (2,911)	1.11
NW6000-1-S-60	60 (1,524)	< 0.01 < (0.25)	< 60 < (1,524)	16,800 (2,964)	1.13
LW6000-1-N-80	80 (2,032)	0.3 (7.62)	< 60 < (1,524)	16,500 (2,911)	1.11
LW6000-1-S-70	70 (1,778)	< 0.01 < (0.25)	< 60 < (1,524)	17,000 (2,999)	1.15
LW6000-2-N-70	70 (1,778)	< 0.01 < (0.25)	< 60 < (1,524)	16,300 (2,875)	1.10
LW6000-2-S-60	60 (1,524)	< 0.01 < (0.25)	< 60 < (1,524)	16,200 (2,858)	1.09
LW8000-1-N-80	80 (2,032)	< 0.01 < (0.25)	< 60 < (1,524)	17,900 (123,421)	1.21
LW8000-1-S-70	70 (1,778)	< 0.01 < (0.25)	< 60 < (1,524)	18,200 (125,489)	1.23
LW8000-2-N-70	70 (1,778)	< 0.01 (7.62)	< 60 < (1,524)	17,900 (123,421)	1.21
LW8000-2-S-60	60 (1,524)	< 0.01 < (0.25)	< 60 < (1,524)	18,400 (126,868)	1.24
LW8000-3-N-70	70 (1,778)	< 0.01 < (0.25)	< 60 < (1,524)	18,100 (124,800)	1.20
LW8000-3-S-60	60 (1,524)	< 0.01 < (0.25)	< 60 < (1,524)	17,600 (121,352)	1.17

Average, All Tests | **1.16**

Standard Deviation, All Tests | **0.05**

5.2.4 Lightweight Panels

Prestressed lightweight concrete panels were added to the scope of the project. The panels are used as formwork for the deck, and comprise half of the depth of the deck. The panels were manufactured and placed without any difficulty, as discussed in Sections 2.2.5 and 3.3.3.

The behavior of the panels during testing was discussed in Sections 3.3.3 and 4.3.3. The use of the panels introduced a new form of crack propagation. V-cracks formed in the deck at the joints between the panels, but these cracks only occurred near failure of the composite beam and deck crushing. The support spalls that formed during testing of the beams with panels are not directly linked to panel use, and occurred only at loads near ultimate.

5.3 CONCLUSIONS

This section presents the conclusions drawn from the test results of the nominal 6000 psi and 8000 psi beam tests.

5.3.1 Development Length

The following are conclusions regarding the development length of the normal weight and lightweight concrete test beams:

1) The AASHTO/ACI development length equation is conservative for normal weight concrete.

2) The AASHTO/ACI development length equation is conservative for lightweight concrete.

3) The development length of the ½ in (12.7 mm) strand in the normal weight concrete beam in this study is less than 60 in (1524 mm).

4) The development length of the ½ in (12.7 mm) strand in the lightweight concrete beams in this study is less than 60 in (1524 mm).

5) The use of the prestressed lightweight concrete panels was simple and straightforward during the construction process.

6) The use of the prestressed lightweight concrete panels had no significant adverse effect on the behavior of the composite beams, and

did not affect the development length of the ½ in (12.7 mm) strand in the beams.

7)   The support spalling observed in some beams was not a critical failure condition.

5.3.2 Recommendations

The following are recommendations for the AASHTO Bridge Design Specification and for application of the results of this study:

1)   The development length models identified in this thesis and by Kolozs [10] all appear to be conservative for both normal weight and lightweight concrete. AASHTO should consider modifying its requirements to reflect this fact.

2)   If an economic analysis shows feasibility, lightweight concrete can be used in the design and construction of bridge girders in Texas. Such use could result in significant savings in the dead load of the structure.

3)   If an economic analysis shows feasibility, prestressed lightweight concrete deck panels can be used in the design and construction of bridge decks in Texas.

5.3.3 Future Study

The following areas are recommended for future study and clarification:

1)   Determination of the exact development length of the ½ in (12.7 mm) strand in the normal weight and lightweight concrete test beams and comparison to design equations.

2)   Determination of the exact cause of the support spalling failure that occurred during the testing procedure.

3)   Determination of the transfer length of the prestressed lightweight concrete panels.

4)   Study of the economic benefits of using lightweight concrete in bridge girders.

5)   Study of the economic benefits of using prestressed lightweight concrete panels in bridge deck construction.

Appendix A: Notation

a	Distance from first load point to location of actuator
d_b	Nominal diameter of prestressing strand
E_c	Modulus of elasticity of concrete
f'_c	Concrete compressive strength
f_{ps}	Stress in prestressing strands at nominal strength
f_{pu}	Ultimate tensile strength of prestressing strands
f_{se}	Effective stress in prestressing strands after losses
L_d	Development length of prestressing strands
L_e	Embedment length of prestressing strands
L_o	Distance to centerline of support bearing pad from end of beam
L_t	Transfer length of prestressing strand
M_u	Ultimate moment strength
P	Applied load
P_{cr}	Applied load at first flexural crack
P_{spall}	Applied load at support spalling
P_u	Applied load at ultimate moment strength
λ	Coefficient indicating bond stress distribution

Appendix B: English to SI Unit Conversion

English	Multiply by	= SI
1 psi	6,8948	Pa
1 ksi	6.8948	MPa
1 in	25.4	mm
1 in^2	6.4516	cm^2
1 lb	4.448	N
1 kip	4.448	kN
1 oz	28.349	g
1 kip-in	0.112997	kN-m
1 lb/ft^3	0.1571	kN/m^3

Appendix C: Load vs. Deflection Charts
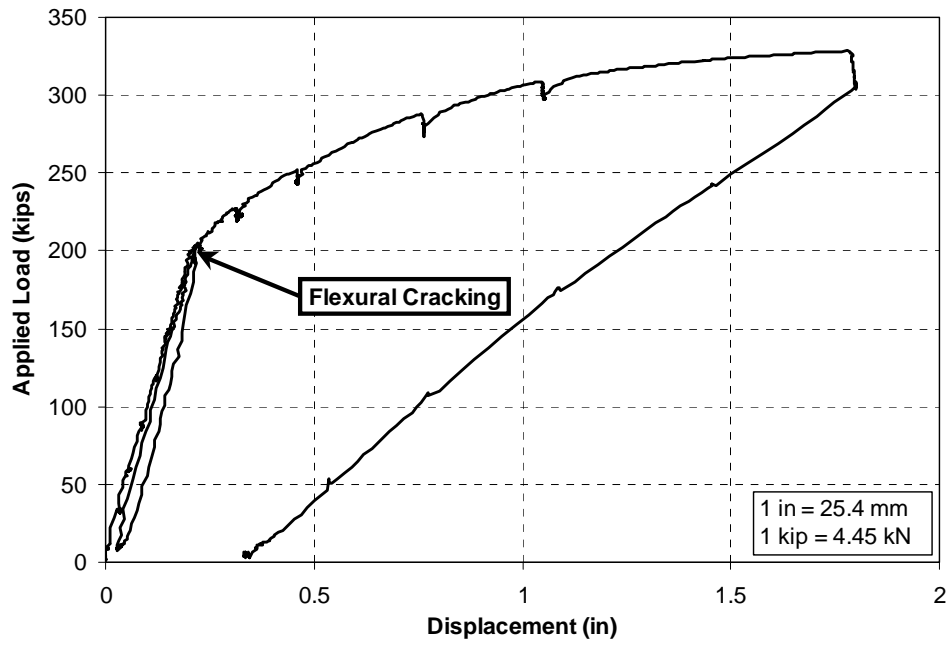
Figure C.1 Load vs. Deflection for NW6000-1-N-80
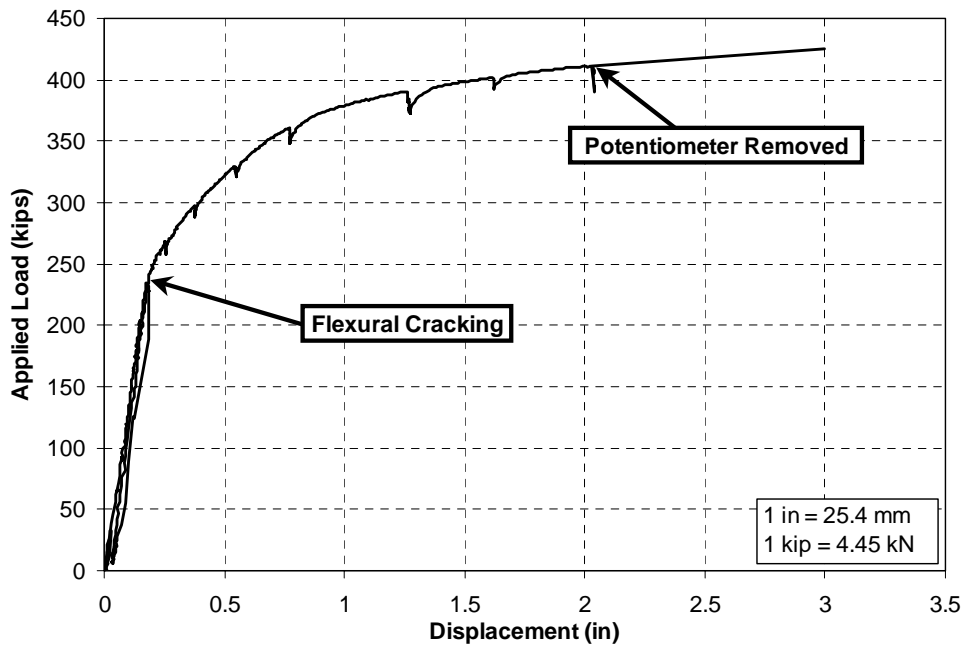
Figure C.2 Load vs. Deflection for NW6000-1-S-60

112
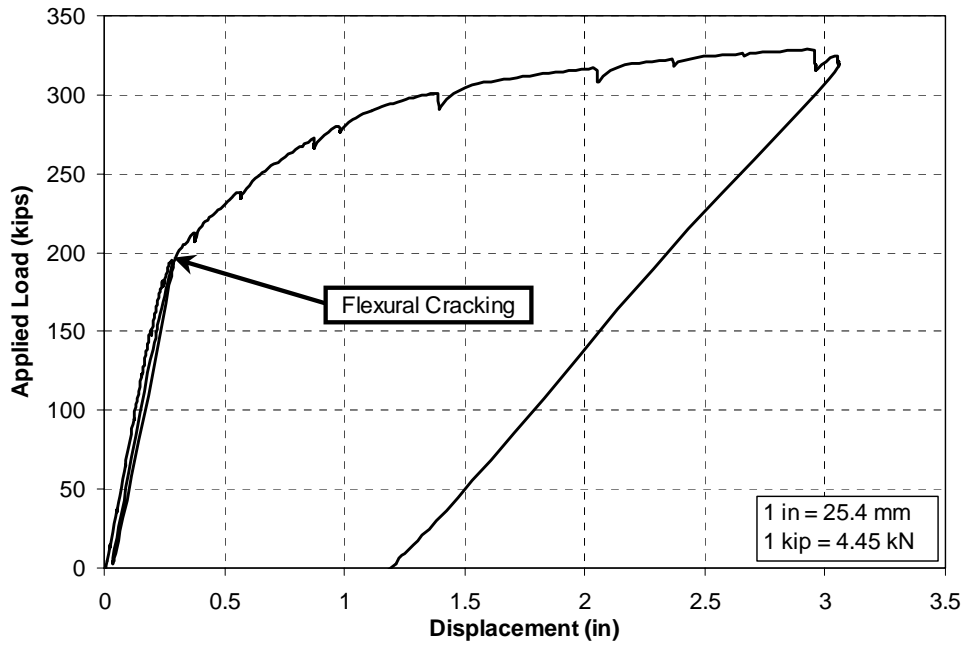
Figure C.3 Load vs. Deflection for LW6000-1-N-80
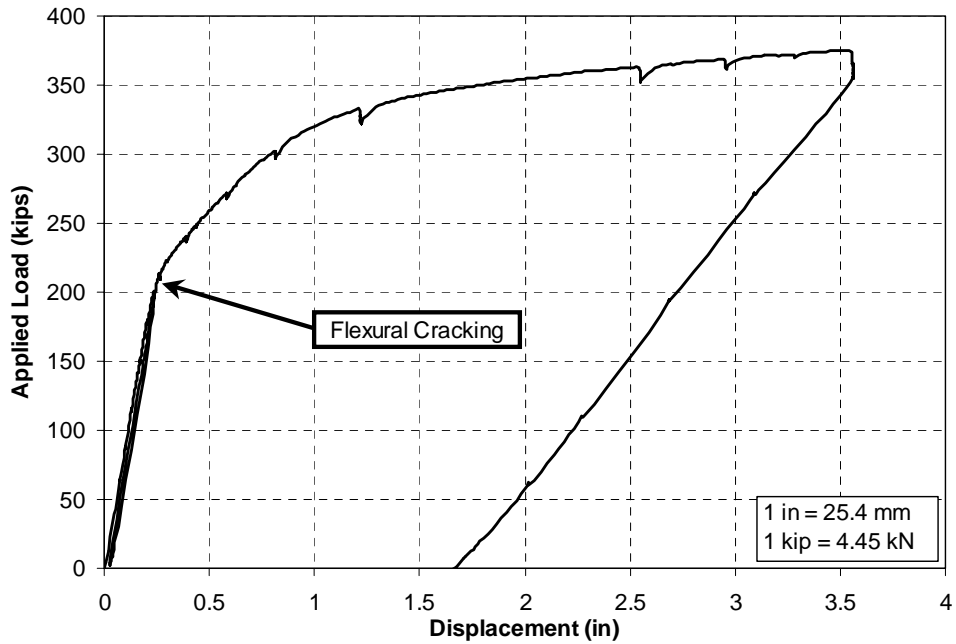
Figure C.4 Load vs. Deflection for LW6000-1-S-70

113
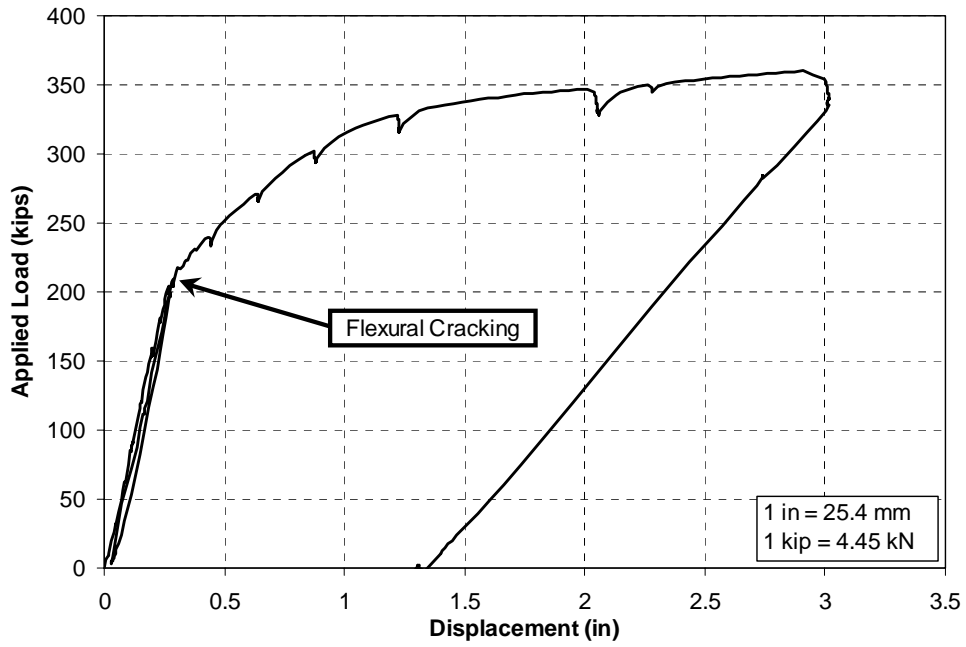
Figure C.5 Load vs. Deflection for LW6000-2-N-70
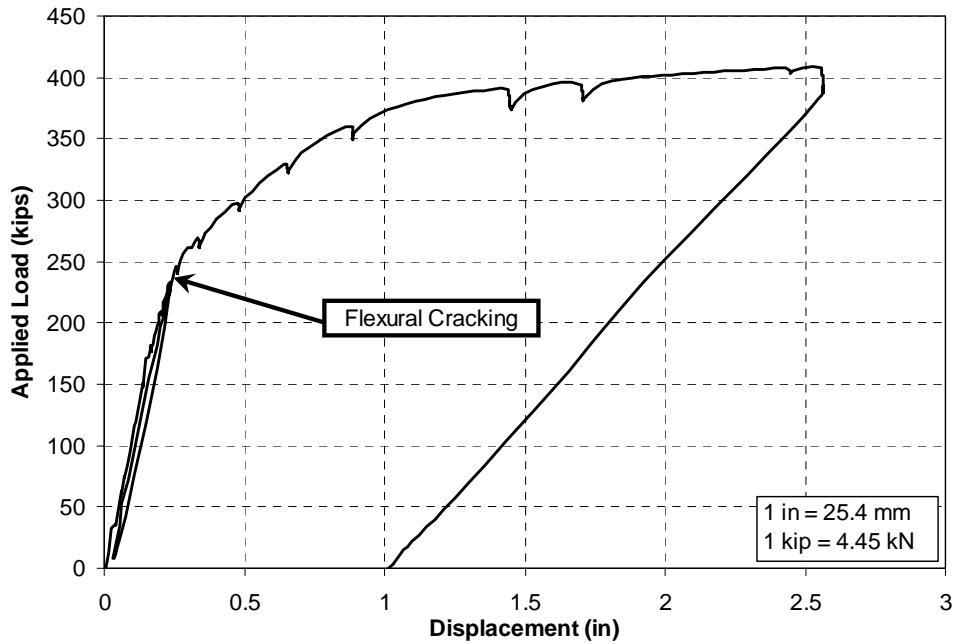
Figure C.6 Load vs. Deflection for LW6000-2-S-60

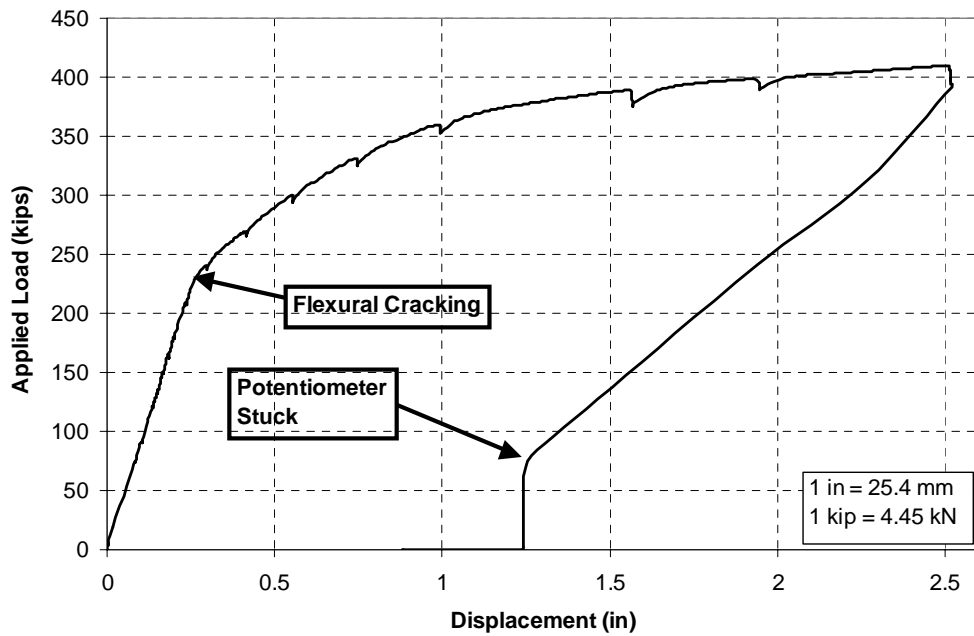114
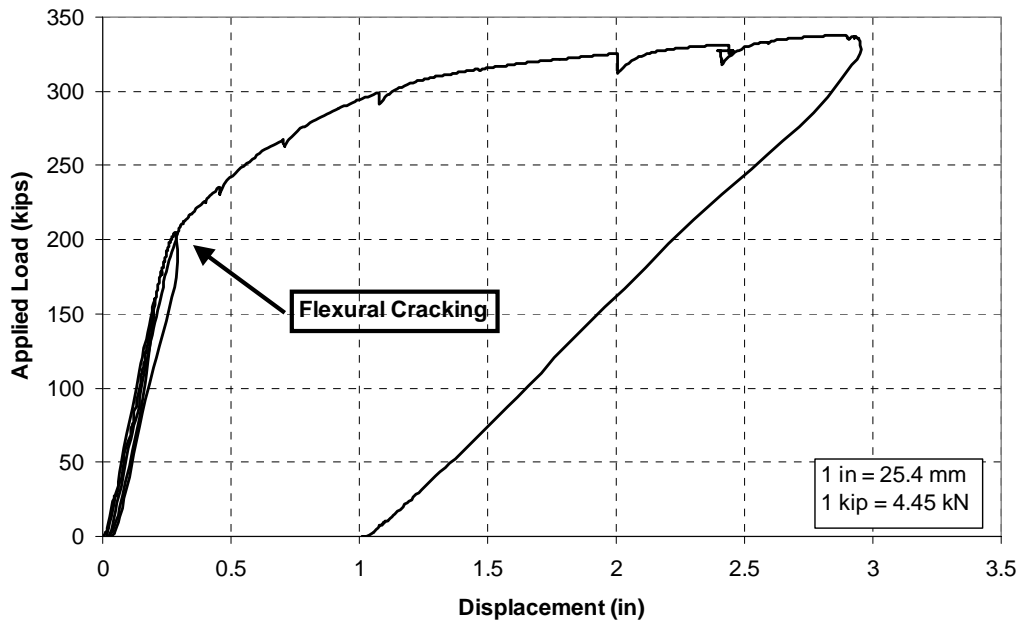
Figure C.7 Load vs. Deflection for LW8000-1-N-80
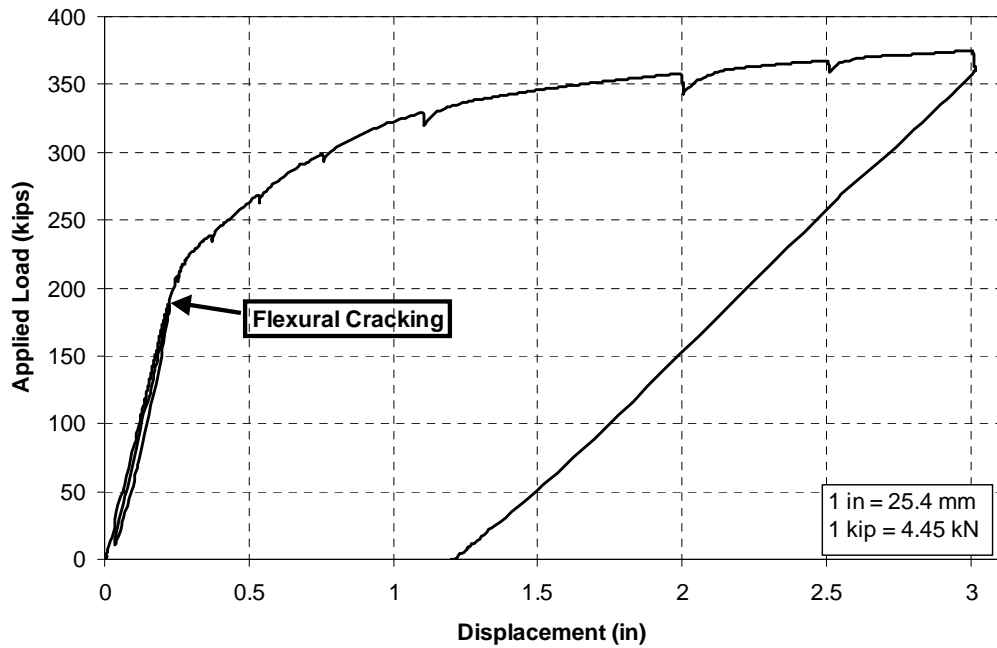
Figure C.8 Load vs. Deflection for LW8000-1-S-70

115
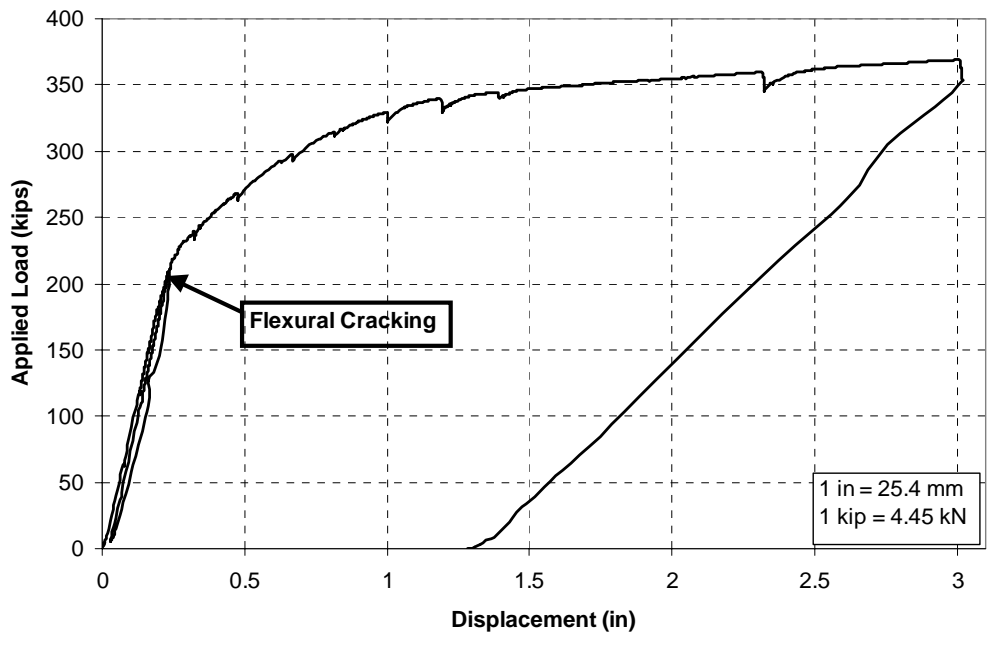
Figure C.9 Load vs. Deflection for LW8000-2-N-70
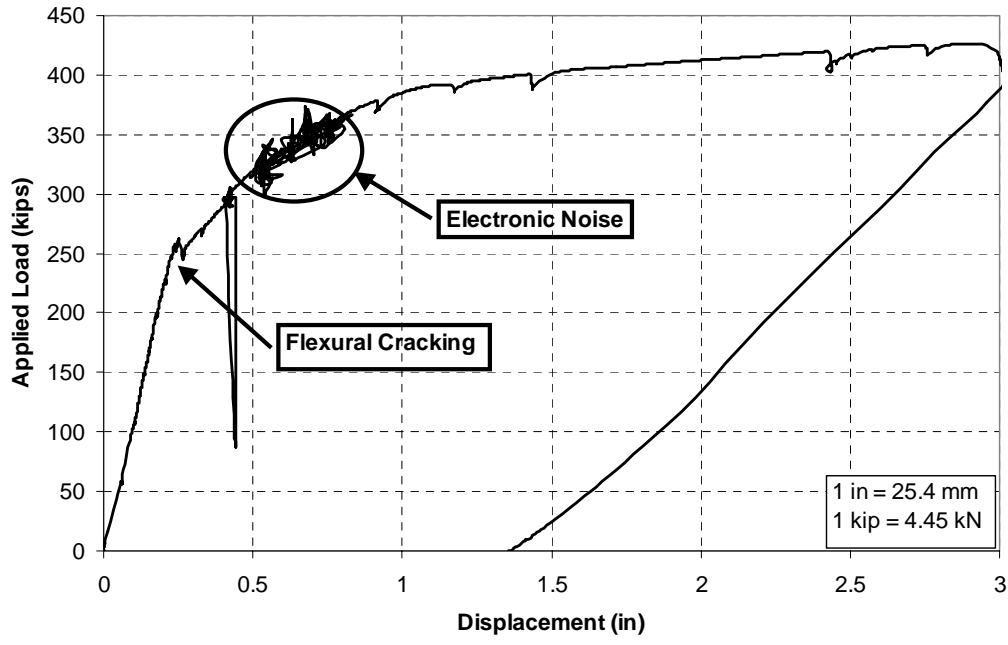
Figure C.10 Load vs. Deflection for LW8000-2-S-60

116
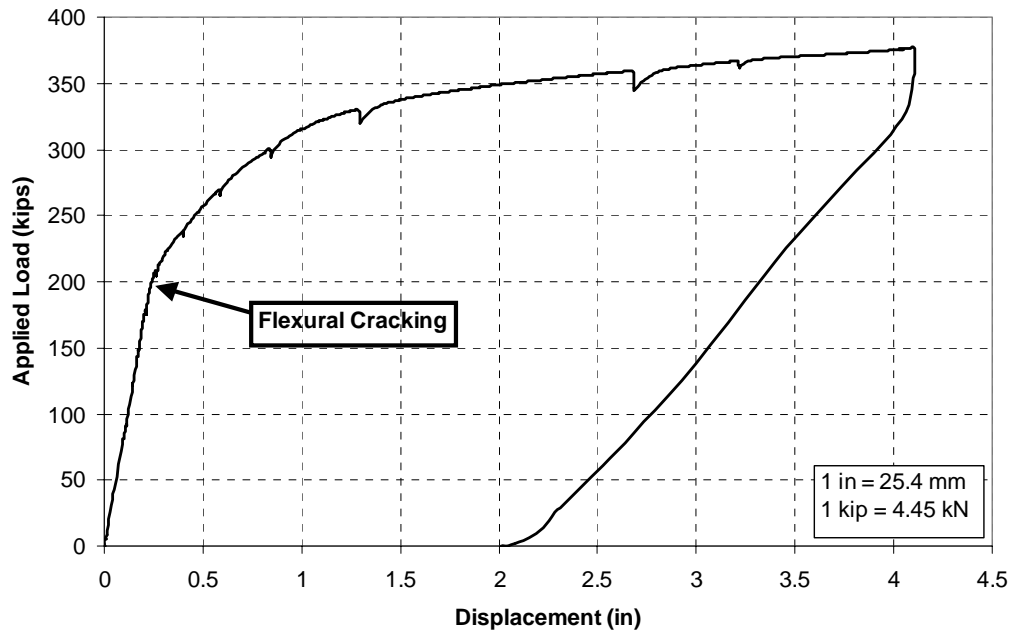
Figure C.11 Load vs. Deflection for LW8000-3-N-70

Figure C.12 Load vs. Deflection for LW8000-3-S-60

117

Appendix D: Strain Gauge Data from Deck
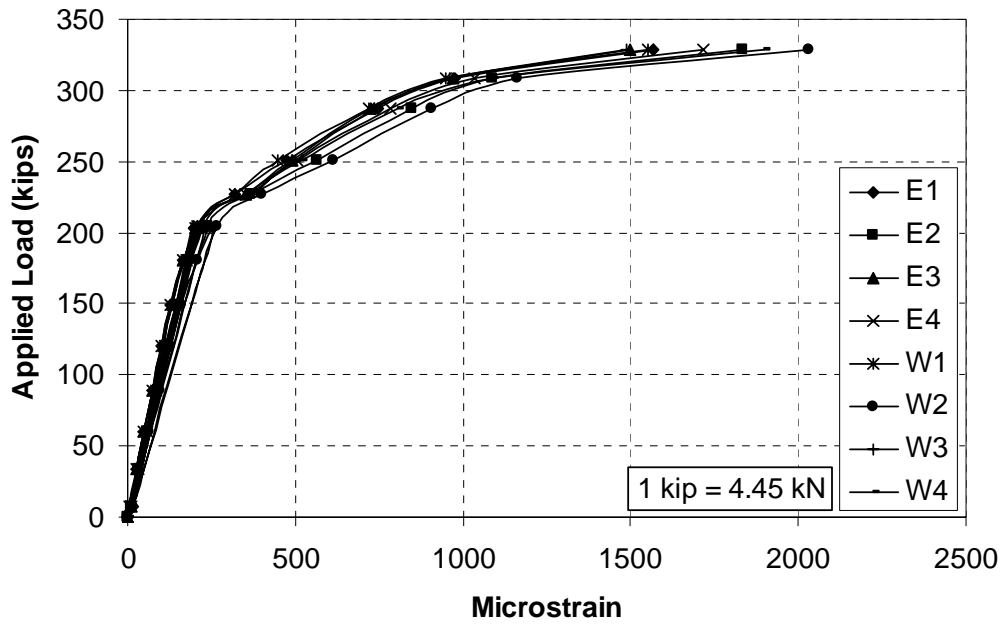
Figure D.1 Microstrain vs. Applied Load for NW6000-1-N-80
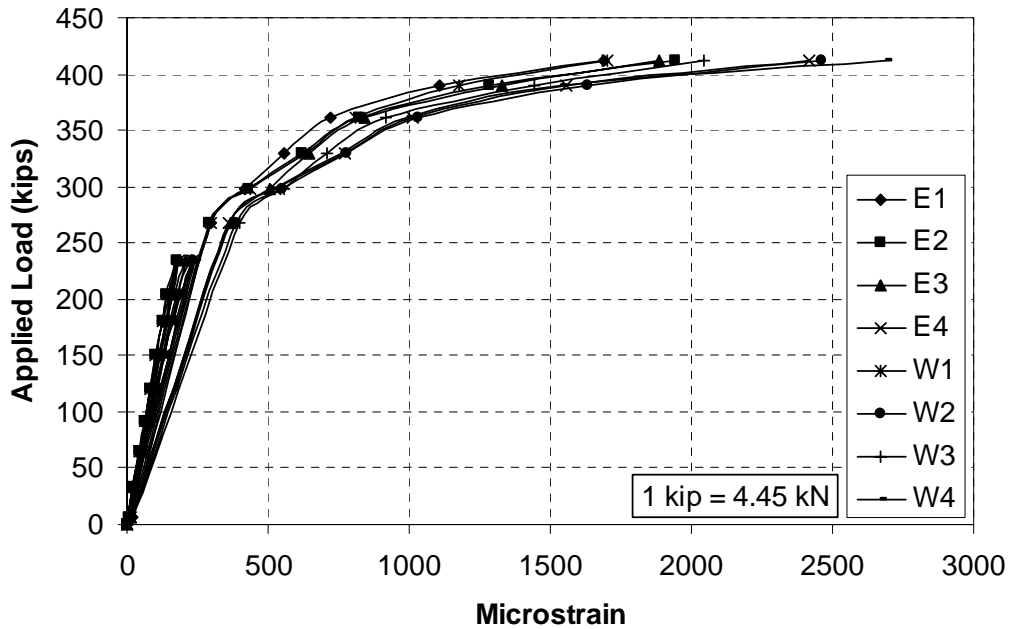
Figure D.2 Microstrain vs. Applied Load for NW6000-1-S-70

119
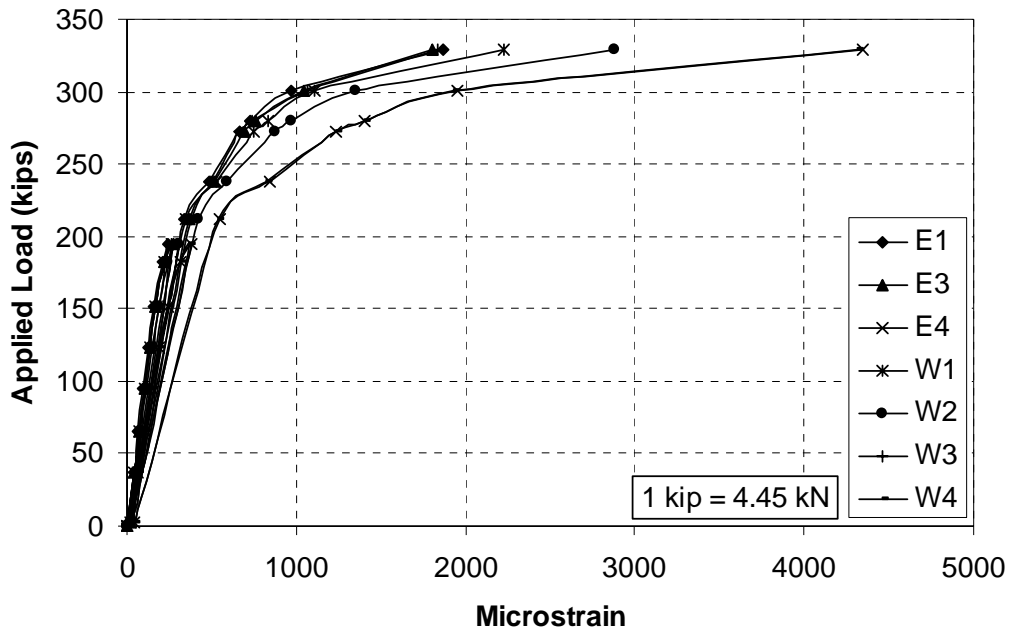
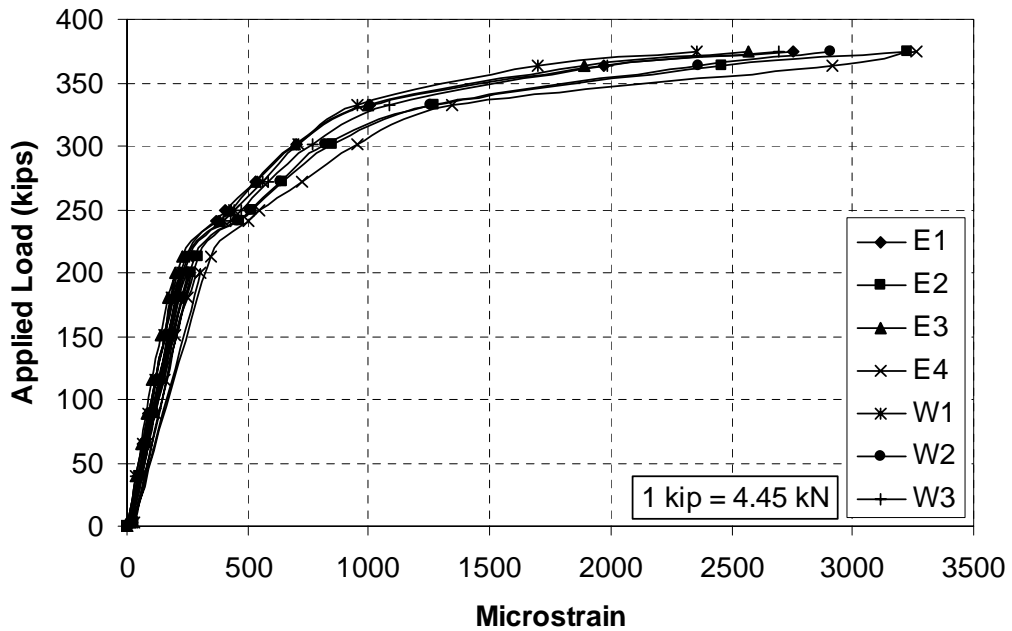**Figure D.3 Microstrain vs. Applied Load for LW6000-1-N-80**

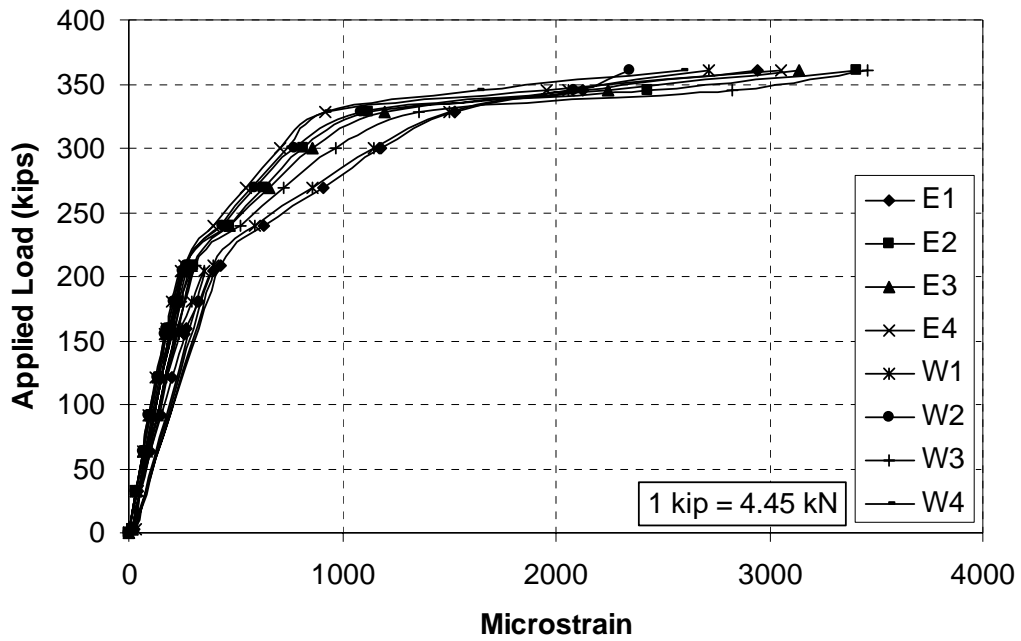**Figure D.4 Microstrain vs. Applied Load for LW6000-1-S-70**

120

Figure D.5 Microstrain vs. Applied Load for LW6000-2-N-70
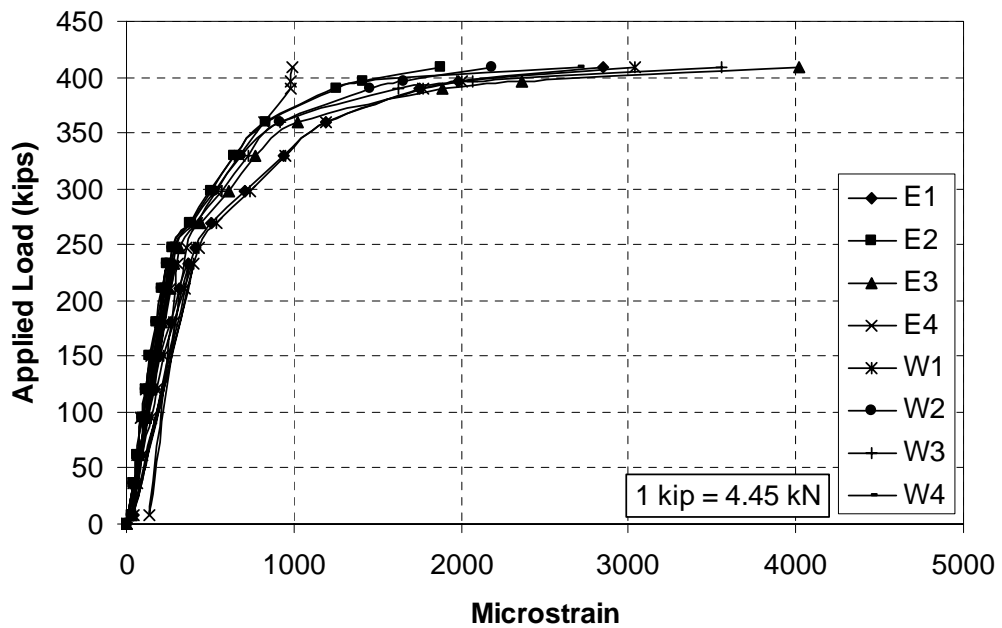

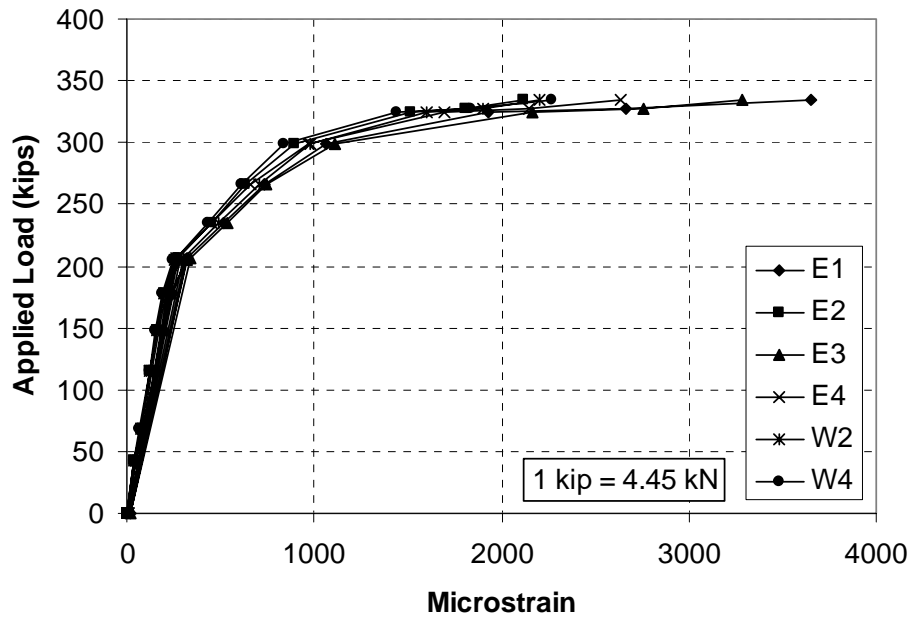**Figure D.6 Microstrain vs. Applied Load for LW6000-2-S-60**

121

Figure D.7 Microstrain vs. Applied Load for LW8000-1-N-80
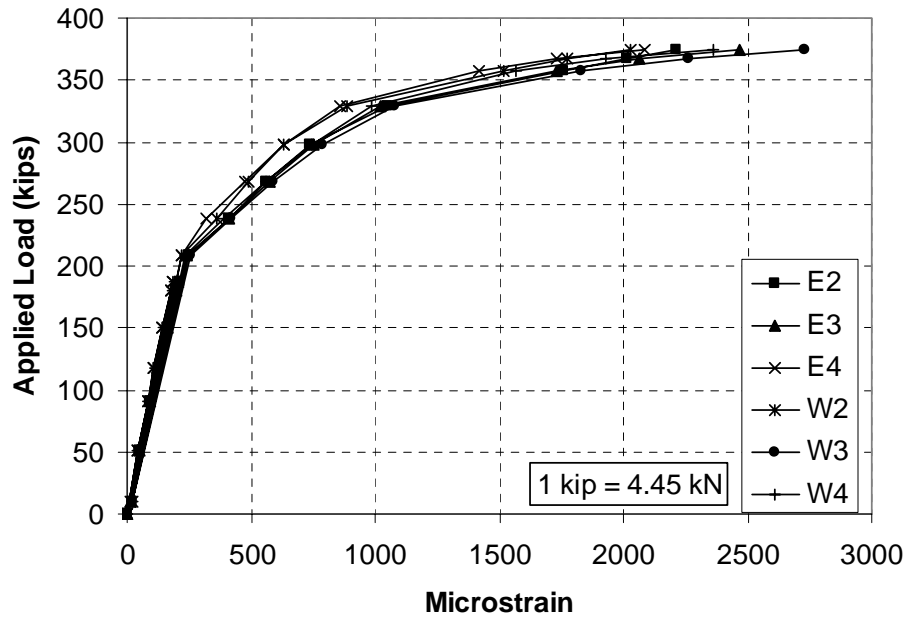

Figure D.8 Microstrain vs. Applied Load for LW8000-1-S-70

122

No Strain Gage Data for LW8000-2-N-70

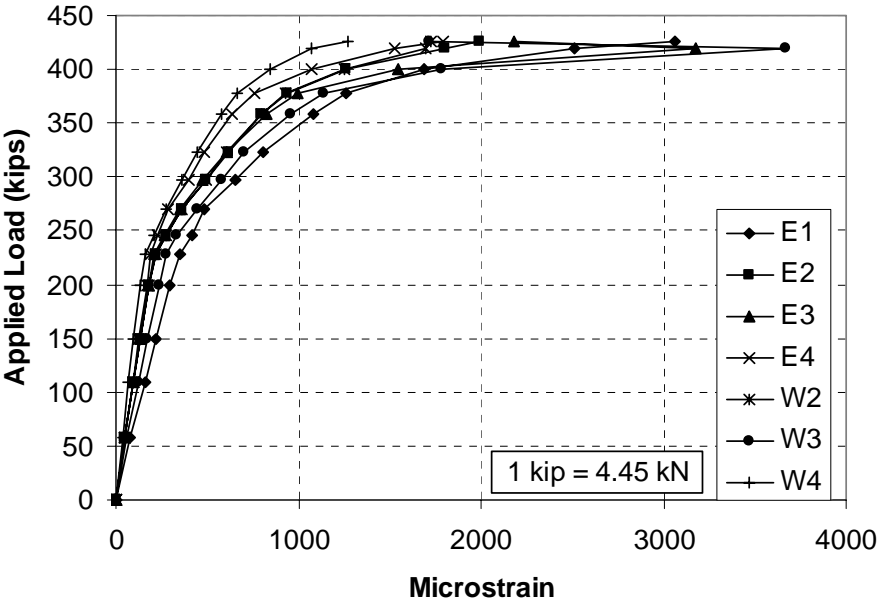**Figure D.9 Microstrain vs. Applied Load for LW8000-2-N-70**

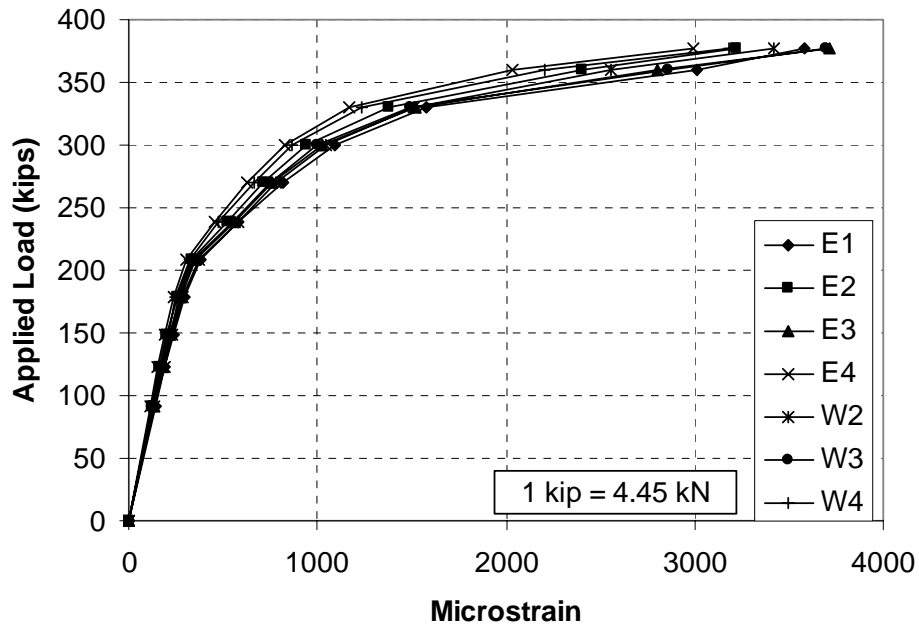**Figure D.10 Microstrain vs. Applied Load for LW8000-2-S-60**

Figure D.11 Microstrain vs. Applied Load for LW8000-3-N-70
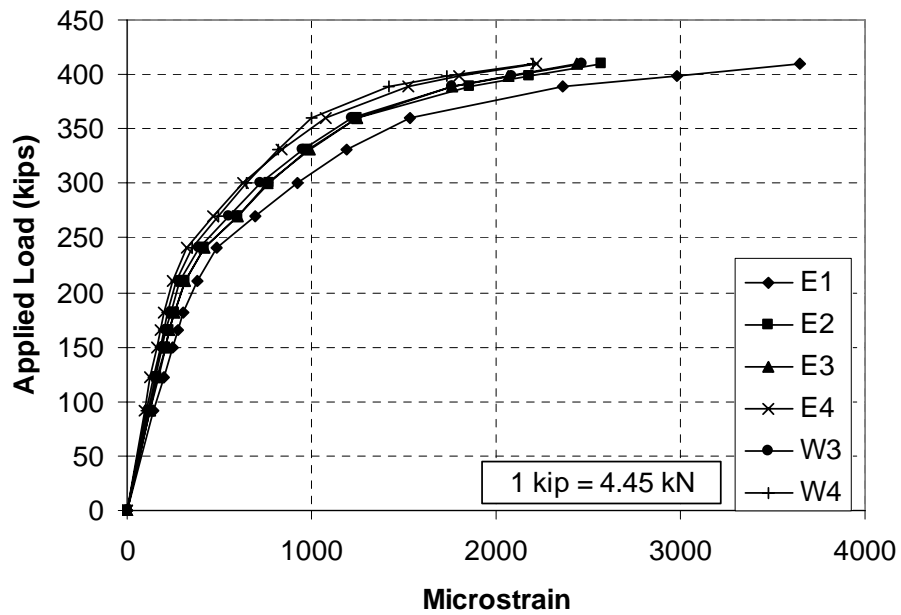

Figure D.12 Microstrain vs. Applied Load for LW8000-3-S-60

124

References

1. AASHTO. 1998. *AASHTO LRFD bridge design specifications: Customary U.S. units*. 2nd ed., Washington, D.C.: American Association of State highway and Transportation Officials (AASHTO).

2. ACI Committee 318. 1999. *Building code requirements for structural concrete (318-99) and commentary (318R-99)*. Farmington Hills, Michigan: American Concrete Institute (ACI).

3. Barnoff, R. M., Orndorff, J. A. Jr., Harbaugh, R. B. Jr., and Rainey, D. E., "Full scale test of prestressed bridge with precast deck planks," *PCI Journal* (Sept.-Oct 1977): 66-82.

4. Bridges, C. P., and Fish, R. C. 1996. Design of structural lightweight concrete for the Folsom Bridge. Caltrans: International Symposium on Lightweight Concrete Bridges.

5. Buckner, C.D. An Analysis of Transfer and Development Lengths for Pretensioned Concrete Structures. Report No. FHWA-RD-94-049. McLean, Virginia: Federal Highway Administration (1994).

6. Collins, M. P., and Mitchell, D. 1991. *Prestressed concrete structures*. Englewood Cliffs, NJ: Prentice-Hall, Inc.

7. Hanson, N. W., and Kaar, P. H., "Flexural bond tests of pretensioned prestressed beams," *ACI Journal, Proceedings* 55, no. 7 (1959): 783-802.

8. Heffington, J. A. 2000. Development of High Performance Lightweight Concrete Mixes for Prestressed Bridge Girders. Thesis, The University of Texas at Austin.

9. Jobson, H. L. 1997. Transfer and development length of fully bonded 15.2 mm (0.6 in) diameter prestressing strand in standard AASHTO Type I concrete beams. Thesis, The University of Texas at Austin.

10. Kolozs, R. T. 2000. Transfer and Development Lenfths of Fully Bonded 1/2 –Inch Prestressing Strand in Standard AASHTO Type I Pretensioned High Performance Lightweight Concrete (HPLC) Beams. Thesis, The University of Texas at Austin.

11. Lin, T. Y., and N. H Burns. 1981. *Design of prestressed concrete structures*. Third Edition, New York, NY: John Wiley & Sons.

12. MacGregor, J. G. 1988. *Reinforced Concrete: Mechanics and Design*. Third Edition, Upper Saddle River, NJ: Prentice Hall.

13. Mitchell, D., Cook, W.D., Khan, A. A., and Tham, T. "Influence of high strength concrete on transfer and development length of prestressing strand," *PCI Journal* 38, no. 3 (1993): 52-66.

14. Nilson, A. H. 1978. *Design of prestressed concrete*. 2nd Edition, New York, NY: John Wiley & Sons.

15. PCI. 1999. *PCI design handbook: precast and pretensioned concrete*. 5th ed., Chicago: Precast/Prestressed Concrete Institute.

16. Poston, R. W., Carrasquillo, R.L., and Breen, J.E, "Durability of Post-Tensionded Bridge Decks," *ACI Materials Journal* 84, no.4 (July-August 1987): 315-326.

17. Somayaji, S. 1995. *Civil Engineering Materials*. Engelwood Cliffs, NJ: Prentice Hall.

18. Zia, P. and Mostafa, T., "Development length of prestressing strands," *PCI Journal* 22, no. 5 (1997): 54-65.

Vita

Daniel Benish Thatcher was born in Lansing, MI, to Richard John and Julie Ann Thatcher. His family moved to Bloomington, IN, when he was nine, where he attended Bloomington High School South and graduated Valedictorian in June of 1994. He attended Purdue University on a merit scholarship in pursuit of a degree in Civil Engineering. While at Purdue, he participated in the Cooperative Education Program, working for Wiss, Janney, Elstner, Assoc., Inc. (WJE) in Northbrook, IL for five semesters during his undergraduate work. In 1996, he made the best decision of his life by marrying the lovely Karen (Kerry) Kathleen Allee, daughter of James Nelson and Ida Jo Allee. Kerry joyfully joined Dan in his travels back and forth between Chicago and West Lafayette, IN.

Upon receiving his B.S. from Purdue in May of 1999, Dan interned with Arsee Engineers, Inc. of Noblesville, IN. In August of 1999, he and his wife moved to Austin, TX where he began his graduate work at the University of Texas at Austin on a University Fellowship and Research Assistantship. After the exciting news that Dan and Kerry were expecting their first child in October of 2000, he accelerated his activities and completed his degree requirements in time to return to their native state of Indiana for the birth of their child.

Mr. Thatcher began work for HNTB Corporation in September of 2000.

Permanent address: 1311 Elliston Dr
                    Bloomington, IN 47401

This thesis was typed by the author.